Coupling of Adenine Nucleotide Binding and Hydrolysis to Single- and Double-Stranded DNA Binding Determines the Topoisomerase Activity of Reverse Gyrase from *Thermotoga maritima*

INAUGURALDISSERTATION

zur

Erlangung der Würde eines Doktors der Philosophie

vorgelegt der

Philosophisch-Naturwissenschaftlichen Fakultät

der Universität Basel

von

Stefan Patrick Jungblut

aus

Biberach an der Riß, Deutschland

Basel, 2009

Genehmigt von der Philosophisch-Naturwissenschaftlichen Fakultät

auf Antrag von

Prof. Dr. Dagmar Klostermeier
Prof. Dr. Joachim Seelig

Basel, den 24. März 2009

Prof. Dr. Eberhard Parlow
(Dekan)

“Turpe est aliud loqui, aliud sentire.”

It is dishonourable to speak one thing, and to think another - *Seneca the Younger*

To those who believe in me.

And for myself.

In loving memory of Lina

Table of Contents

1. Introduction

1.1 Structure and Topology of DNA

Nucleic acids are the basis for all life. The two most important groups of nucleic acids only differ in the type of pentose sugar contained in the nucleotide building blocks of these biopolymers. Ribonucleic acid (RNA) is hypothesised to be the origin of life due to its ability to store both information and exhibit catalytic activity[1-3]. Deoxyribonucleic acid (DNA) is chemically more stable than RNA and is the ultimate molecule for genetic data storage. The discovery of the double helical structure of DNA in 1953 was the beginning of modern molecular biology[4].

In bacteria, genetic information is stored in circular molecules that consist of double-stranded DNA (dsDNA). In addition to their bacterial chromosome of several million base pairs (bp), bacteria often contain plasmids that are only several thousand bp in size. Cellular processes like DNA duplication or transcription of genetic data require dsDNA strand separation introducing tension in the rest of the molecule. Thus, strand separation is mechanically demanding (Figure 1).

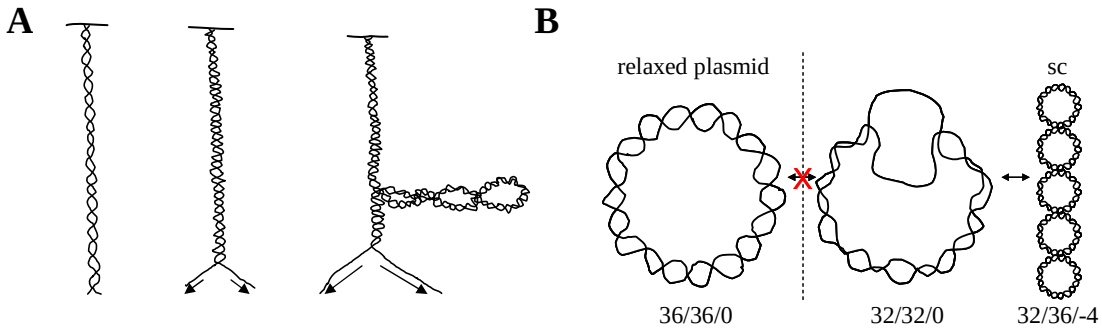

Figure 1. Consequences of strand separation of dsDNA. (A) Progressive unwinding of a double strand with one fixed end (top) introduces supercoils behind the unwound region. (B) Relaxed and partially unwound plasmid are not freely interconvertible without strand cleavage (indicated by the red cross). These forms are topoisomers of each other. However, the partially unwound plasmid is equivalent to a supercoiled form (sc). The numbers indicate the *linking number* (L)/*twist* (T)/*writhe* (W) of the depicted plasmid, explained below. Thus, decreasing the *linking number* of a relaxed plasmid by 4 (left) to partially unwind it requires strand cleavage and is equivalent to the introduction of 4 negative supercoils (right). Pictures are modified after[5,6].

Thinking of dsDNA as two strings wound around each other and fixed at one end, it is easy to illustrate the telephone cord problem arising upon unwinding[5] (Figure 1A). In plasmids, unwinding stress has to be eased to achieve strand separation (Figure 1B). The degree of tension and twisting in plasmids is expressed mathematically:

$$L = T + W$$

The *linking number* L is the number of helical turns of one strand around the helical axis. Slightly different, the *twist* T denotes the number of helical turns of both strands around each other. The *writhe* W (also supercoiling number) is a measure of how twisted the helical axis itself is and can be negative (right-handed supercoils) or positive (left-handed supercoils).

Plasmids differing in the *linking number* are topological isomers or topoisomers, i.e. a regionally unwound plasmid and a negatively supercoiled plasmid are isomers. Plasmids with identical *linking number* can be interconverted without strand cleavage (Figure 1B). However, changing the *linking number* of a plasmid requires strand cleavage. A decrease in the *linking number* facilitates plasmid unwinding, which is required for many cellular processes, while an increase impedes strand separation rendering plasmids more resistant to heat. Alteration of the plasmid *linking number* can be achieved by changing the *writhe*, which corresponds to plasmid supercoiling or relaxation depending on an increases or decrease of the absolute value of the *writhe*. Plasmid relaxation and supercoiling in cells is managed by DNA topoisomerases.

1.2 DNA-Topoisomerases

Topoisomerases are involved in almost every cellular action that requires DNA reorganisation and alter DNA topology during replication, recombination, chromosomal segregation and DNA transcription[7]. The general mechanism includes strand cleavage, passage or rotation of the non-cleaved strand and final religation. During strand cleavage, covalently bound intermediates are formed by nucleophilic attack of an activated tyrosine to the phosphate backbone of dsDNA. Type I and II topoisomerases cleave one or two DNA strands, respectively. Furthermore, type IA and type II topoisomerases covalently bind to the 5'-end of the cleaved strand(s), while type IB topoisomerases bind to the 3'-end. Strand passage through the resulting gap or strand rotation alters the *linking number* of the plasmid, where one DNA strand (type I) or a whole dsDNA region (type II) is transported. Finally, the cleaved strand(s) is religated[8].

Topoisomerases are found in eukaryotes and prokaryotes and are able to alter the *linking number* of plasmid DNA. The monomeric type I topoisomerases are a structurally very heterogeneous group and exhibit various cellular functions[9]. Earlier studies were aimed at elucidating structure-function relations like the molecular requirements for DNA binding and cleavage, but the exact DNA relaxation mechanism remains unknown[10,11]. Together,

type I and type II topoisomerases control the level of supercoiling in organisms by introducing DNA supercoils, relaxing supercoiled DNA and resolving catenation of plasmids after replication[7-9]. Furthermore, topoisomerases II function as dimers. Eukaryotic topoisomerase II from *Saccharomyces cerevisiae* is a homodimer with strong homology to the *Escherichia coli* enzyme, which is a type A_2B_2 heterotetramer. Bacterial topoisomerases II are called gyrases and are able to negatively supercoil plasmids in an ATP-dependent manner[7,8]. The subunit Gyr A bears a DNA cleavage and religation activity separated from the ATPase activity of Gyr B. *E. coli* gyrase reconstitutes fully functional *in vitro* from the two subunits[12].

The first deduction of the ATP-dependent topoisomerase II mechanism stems from *S. cerevisiae* topoisomerase IIA. Here, dsDNA is cleaved and covalently bound with two active tyrosines. ATP hydrolysis is required to move a distant dsDNA region, held by subdomains, through the resulting gap[13-15]. A similar mechanism has been demonstrated for the non-analogous *E. coli* gyrase, where different subunits carry out the strand migration functions[16]. A striking new study provides structural evidence for a 150° DNA bending by the *S. cerevisiae* enzyme, facilitating positioning of the active tyrosines[17]. Concomitant large conformational changes have been directly observed with single molecule Förster resonance energy transfer (smFRET)[18]. A similar mechanism in a different architectural background has been proposed for heterotetrameric topoisomerase VI, an archeal topoisomerase IIB[19]. Finally, a lot of effort is put into understanding why ATP hydrolysis by topoisomerases II is required for plasmid relaxation, which is an energetic downhill reaction[20], and to determine DNA sequence requirements for strand cleavage[21].

Helicases are another important class of enzymes required for nucleic acid-related reorganisations during replication, recombination, repair and expression[22]. Helicases unwind either dsDNA or dsRNA in an ATP-dependent manner[22-24]. The largest family of RNA helicases is the so called DEAD-box family that shares a common helicase core. This core consists of two RecA-like domains that are connected by a flexible linker and contain all motifs required for ATP binding and hydrolysis, as well as RNA binding and unwinding[24]. Substrate specifity is often mediated by heterogeneous flanking domains. For example, the *Bacillus subtilis* RNA helicase YxiN has a C-terminal domain for specific binding to ribosomal RNA[25,26]. Mechanistically, coupling of ATP hydrolysis and binding of nucleic acid substrates to conformational changes in YxiN has been studied on the single molecular level using FRET[26].

1.3 Reverse Gyrase

A special topoisomerase was discovered in 1984 in *Sulfolobus acidocaldarius* bearing the unique ability to positively supercoil plasmid DNA in an ATP-dependent manner[27]. First believed to be a topoisomerase II[27], today we know that reverse gyrase is a hyperthermophilic topoisomerase IA with a helicase-like domain and a topoisomerase domain[28]. Reverse gyrase is thought to represent general adaptation to life at high temperatures as it is the only enzyme class unique to hyperthermophilic archea and bacteria[29]. Indeed, the presence of positive superhelical turns inhibits strand separation and segregation in plasmid DNA[30]. However, appearance of reverse gyrase is not a strict requirement for hyperthermophiles. This was shown for *Thermococcus kodakaraensis*, where disruption of the reverse gyrase gene leads to reduced growth but is not lethal[31]. More additional functions of reverse gyrase have been discovered that demonstrate a close relationship of the enzyme's occurrence for life at high temperatures. There is evidence that reverse gyrase is recruited to the DNA after UV treatment[32], where it may exert a reported DNA chaperone activity that is independent of positive plasmid supercoiling[33]. Reverse gyrase acts as a communicator of DNA damage by cooperatively recruiting proteins to nicked DNA sites[30]. Direct interaction with a single strand DNA binding protein of the replication machinery has been shown[34]. Also, reverse gyrase harbours a DNA renaturase activity for annealing circles of single stranded DNA (ssDNA) in addition to its unique positive supercoiling activity[35]. In summary, various protein functions are related to reverse gyrase, but its true cellular role remains unknown.

Unfortunately, structural data for closer elucidation of the catalytic activity of reverse gyrase is rare. Reverse gyrase is described as a monomeric enzyme with a helicase-like domain and a topoisomerase domain throughout published literature[36]. There is only one example for a homodimeric reverse gyrase in *Methanopyrus kandleri*[37,38], which will not be further discussed. Electron microscopy of monomeric reverse gyrase from *Sulfolobus tokodaii* indicates a hole in the enzyme with a diameter of 10-20 Å suitable for dsDNA binding[39]. The only available crystal structure of reverse gyrase is from *Archeoglobus fulgidus*[40] and confirms the finding of a 10-20 Å hole in the enzyme (Figure 2).

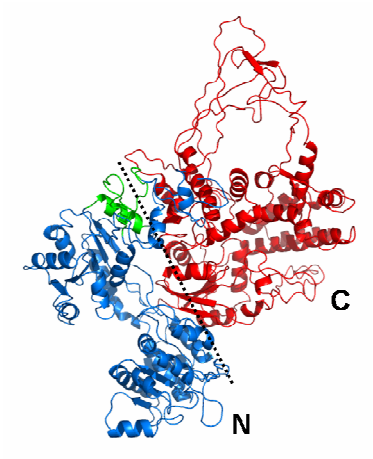

Figure 2. Homology model of *Thermotoga maritima* reverse gyrase based on the crystal structure of the *A. fulgidus* enzyme[40]. The structure reveals a padlock-shape of $50 \cdot 70 \cdot 130$ Å^3. The ATPase is contained in the N-terminal helicase-like domain (blue). The C-terminal part of the helicase-like domain is interrupted by the latch region (green), which was suggested to bind DNA and to trigger opening of the topoisomerase IA domain (red) like a lid. The opening in the topoisomerase domain has a diameter of 16 Å. The two putative zinc finger domains are not resolved in the structure due to insufficient electron density, indicating flexibility of these regions. They should be positioned in the region of the C- and N-terminus[40].

Functionally, reverse gyrase belongs to the type IA topoisomerases as described above[30]. Thus, its positive supercoiling mechanism must be different from the negative supercoiling mechanism of gyrase, for example (see Chapter 1.2). Figure 3 presents a hypothetical catalytic cycle of reverse gyrase based on the crystal structure of the *A. fulgidus* enzyme[40] described in Figure 2.

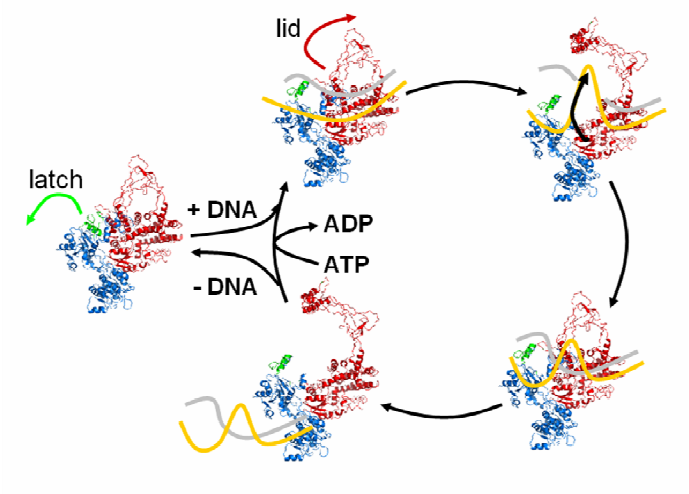

Figure 3. Catalytic cycle and hypothetical mechanism of positive plasmid supercoiling by reverse gyrase in the presence of ATP. Large conformational changes are predicted for different enzyme regions. The reaction cycle is modified after[37] showing a homology model for *T. maritima* reverse gyrase based on the structure from the *A. fulgidus* enzyme. The single steps are explained in the text.

The postulated reaction mechanism is based on the required steps for topoisomerase activity and takes possible binding sites for DNA into account[40]. In the first step, ATP binds to the helicase-like domain (blue) and dsDNA (yellow and grey lines) binds to the topoisomerase domain (red). After cleavage of a single DNA strand (grey line) by the catalytically active tyrosine (not shown), the latch domain (green) swings and releases the lid domain. The still intact single strand (yellow line) can now pass through the ssDNA gap, which is subsequently religated upon topoisomerase domain closure. Finally, the supercoiling product and ADP are released[40]. It remains unknown at which point of the cycle ATP is hydrolysed and how many positive supercoiling cycles a dsDNA substrate has to undergo before it is released.

The role of some structural elements of reverse gyrase has been examined in deletion studies. For example, the latch region has been identified as a DNA binding element and communicator between the helicase-like domain and the topoisomerase domain of reverse gyrase[41,42]. Mutation of the N-terminal putative zinc finger leads to reduced positive supercoiling activity, indicating a role for DNA binding[43]. Additionally, mutations in motifs of the helicase-like domain were reported to inhibit plasmid supercoiling, leaving DNA binding and cleavage abilities unaffected[43]. Gradually, evidence is being provided that the helicase-like domain couples ATP hydrolysis to the topoisomerase activity of reverse gyrase[43-45]. However, the functional description of reverse gyrase properties is very diverse, and in part, contradictory results are gained from reverse gyrases from different organisms with respect to nucleotide utilisation for positive supercoiling[41,46].

Reverse Gyrase from *Thermotoga maritima*

The gene structure and the primary sequence of *T. maritima* reverse gyrase have been known for 10 years[47]. The enzyme is a monomer consisting of 1104 amino acids[47] and has a molecular weight of 128'275 Daltons, a calculated molar extinction coefficient of 111'470 M^{-1} cm^{-1} and a calculated pI of 8.5. As a topoisomerase IA, it bears the N-terminal helicase-like domain and the C-terminal topoisomerase domain along with the latch region and two putative zinc fingers containing four native cysteines each[43]. The contribution of the structural modules for inter-domain communication during positive supercoiling have begun to be investigated in mutation studies of *T. maritima* reverse gyrase[48]. However, adenine nucleotide binding and hydrolysis by reverse gyrase from *T. maritima* have not been systematically characterised and DNA substrate binding has not been investigated. The molecular basis for the unique positive supercoiling activity of reverse gyrase and the underlying mechanism, remain unknown.

It will be interesting to investigate coupling between adenine nucleotide hydrolysis and DNA binding to topoisomerase activity of *T. maritima* reverse gyrase in greater detail and to more profoundly determine structure-function correlations of the helicase-like domain, the latch region, the topoisomerase domain and the two putative zinc fingers.

1.4 Specific Methods

Supercoiling Activity Visualised by Multi-dimensional Agarose Gel Assays

Negatively supercoiled pUC18 plasmid is used as starting substrate to monitor relaxation or positive supercoiling by reverse gyrase in dependence of adenine nucleotides. In the presence of ATP, the plasmid will first be relaxed and subsequently positively supercoiled. DNA topoisomers with different *linking number* generated after a certain time are separated by agarose gel electrophoresis, due to compacted size of species with higher supercoiling degree. Plasmids only differing in the sign of their *writhe* (or supercoiling sign) are separated in a second gel dimension upon addition of the DNA intercalator chloroquine[49,50] (Figure 4). Nominally, the anti-malaria agent chloroquine introduces more positive supercoils into plasmid DNA[51]. Hence, formerly negatively supercoiled plasmids are partially relaxed, and thus, slower than the even more compacted positive supercoiled species[5,50,51]. A schematic depiction of two-dimensional gel analysis of DNA topoisomers is given in Figure 5.

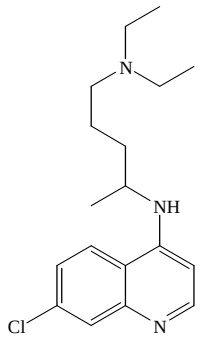

Figure 4. Chloroquine.

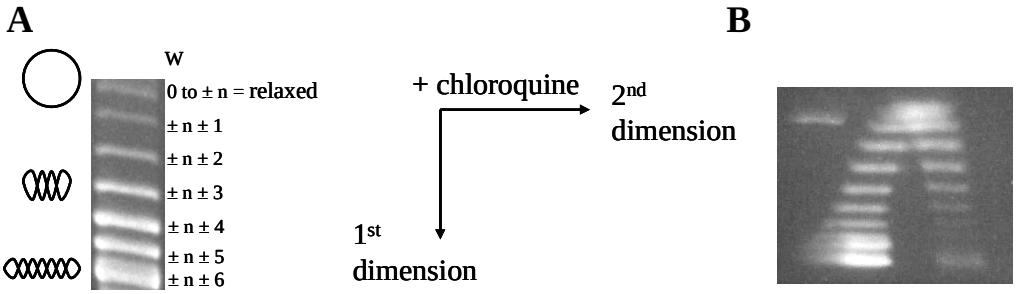

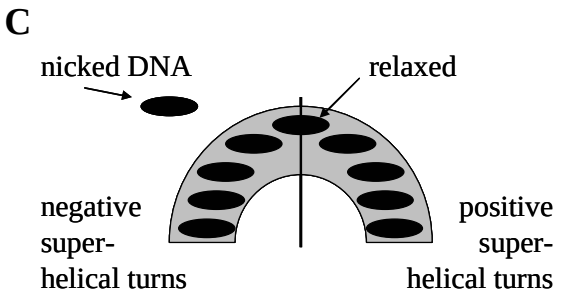

Figure 5. Principal of two-dimensional gel analysis for separation of DNA topoisomers. 15 nM pUC18 were incubated with 1 µM reverse gyrase in 50 mM Tris/HCl (pH 7.5), 150 mM NaCl, 10 mM $MgCl_2$, 100 µM $Zn(OAc)_2$, 2 mM β-ME, 2 mM ATP, 10% (w/v) PEG 8000 at 75°C for 10 minutes. (A) Plasmids with different *linking number* are separated in the first dimension. (B) Plasmids are separated by sign of the *writhe* in the second dimension. (C) Schematic depiction modified after[42].

The typical arch pattern of DNA topoisomers obtained by two dimensional gel analysis shows negatively or positively supercoiled plasmid species at the bottom left or right corner and relaxed plasmid at the arch top (Figure 5). An alternative method for the

analysis of the supercoiling degree of plasmids uses only one-dimensional gel analysis. Here, plasmid band patterns of identical samples are compared in the presence of different concentrations of chloroquine[52]. This method was not applied for the PhD thesis at hand.

Single Molecule Förster Resonance Energy Transfer

A method to determine inter- and intramolecular distances is Förster resonance energy transfer (FRET)[53]. FRET could be used to observe conformational changes in reverse gyrase during the nucleotide and supercoiling cycle. The method is based on non-radiative energy transfer from an excited donor chromophore to an acceptor chromophore. The emitted fluorescence from the acceptor is red-shifted compared to the donor emission. The underlying dipole-dipole coupling is dependent on the inverse sixth power of the distance. The transfer efficiency (E_{FRET}) is described by:

$$E_{FRET} = \frac{r_0^6}{r^6 + r_0^6} \qquad (1),$$

where r is the distance under question in nm. The Förster distance r_0 for a specific fluorescence donor-acceptor couple is the distance where E_{FRET} is 50% (Figure 6).

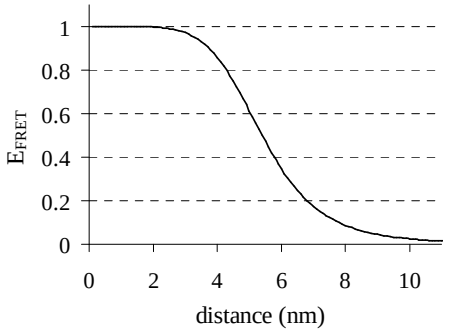

Figure 6. The distance dependency of E_{FRET} is shown for a donor-acceptor pair with a r_0 of 5.4 nm. At this distance, E_{FRET} is 50%. Distance changes can be reliably measured between 10% and 90% E_{FRET}.

Exact knowledge of the r_0 value is necessary to use FRET as a molecular ruler[53,54]. Several abilities of the chosen chromophores influence the value for r_0:

$$r_0 = \sqrt[6]{8.785 \cdot 10^{-5} \frac{\kappa^2 \cdot \phi_D \cdot J_{DA}}{n^4}} \qquad (2).$$

κ^2 is the orientation factor for the transition dipoles of the donor and acceptor chromophore and lies between 0 and 4 when the dipoles are orthogonal or parallel to each other. κ^2 is usually set to 2/3 assuming that the chromophores can freely rotate and have no fixed orientation. Φ_D is the quantum yield of donor in the absence of acceptor[55]. The refractive

index n of the solvent is 1.33 in aqueous solutions. J_{DA} is the spectral overlap integral of the donor's emission with the acceptor's absorbance:

$$J_{DA} = \int F_D(\lambda) \cdot \varepsilon_A(\lambda) \cdot \lambda^4 d\lambda \qquad (3).$$

F_D is the integrated area of the donor emission spectrum normalised to 1. $\varepsilon_A(\lambda)$ is the absorbance spectrum of the acceptor normalised to the molar extinction in dependence of the wavelength. High E_{FRET} values are only achieved, if the emission spectrum of the donor agrees well with the absorbance spectrum of the acceptor. The most commonly used fluorescent dyes are derivatives of fluoresceine (Figure 7).

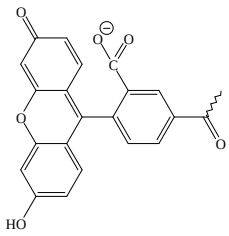

Figure 7. Fluoresceine.

FRET can be used to measure distance changes between 2 nm and 10 nm. Thus, it is a suitable method to observe conformational changes during topoisomerase activity of reverse gyrase. However, ensemble FRET measurements only reflect the average distance of fluorescent dyes attached to a protein. The solution to this problem is the application of FRET on the single molecule level[56]. A typical setup for smFRET is depicted in Figure 8.

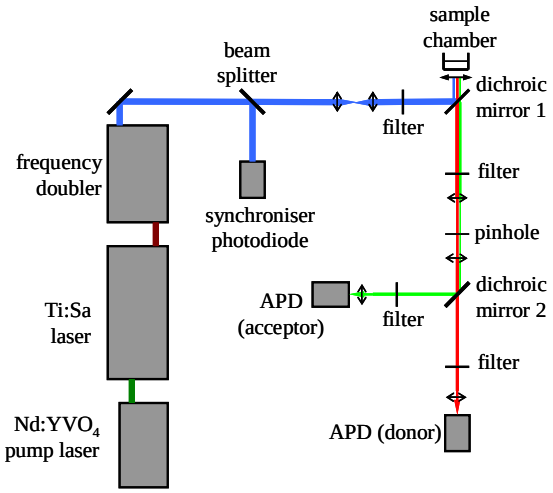

Figure 8. Confocal setup for smFRET. A neodymium: yttrium-vanadate laser pumps a titanium:sapphire solid-state laser, which emits pulsed light of 950 nm wavelength. Light of 475 nm is generated by a frequency doubler. Part of the light is diverted to a synchroniser photodiode as time reference. Laser divergence generated by the frequency doubler is corrected by two lenses ⇕ with identical focal length. The laser beam is lead through a bandpass filter, reflects from the first dichroic mirror and is focused into the sample chamber. Emitted fluorescence passes through the first dichroic mirror and is focussed again with a 3:1 telescope and a pinhole. Emission is split into donor and acceptor fractions at the second dichroic mirror and detected in separate avalanche photo diodes (APD).

The setup focuses the excitation laser beam of 475 nm with a confocal microscope on a femtolitre volume in a sample chamber (for details see Figure 8). The donor and acceptor fluorescence are separately detected with avalanche photodiodes (APD)[57]. The advantage of smFRET is the exact distance information of many single protein molecules in the focus one at a time, giving distance populations and distance changes rather then an average over all measured distances[56,57].

1.5 Literature

(1) Crick F. H., Central Dogma of Molecular Biology, *Nature.*, **1970**, *227*, 561-563.

(2) Cech T. R., A Model for the RNA-catalyzed replication of RNA, *PNAS*, **1986**, *83*, 4360-4363.

(3) Gilbert W., The RNA World, *Nature*, **1986**, *319*, 618.

(4) Watson J. D., Crick F. H., A Structure for Deoxyribose Nucleic Acid, *Nature*, **1953**, *171*, 737-738.

(5) Bates A. D., Maxwell A., DNA Topology, *Oxford University Press*, **2005**.

(6) Internet source: www.vetmed.iastate.edu/faculty_staff/users/phillips/Micro402/03-chromsome/supercoilnos.jpg

(7) Wang J. C., Cellular Roles of DNA Topoisomerases: A Molecular Perspective, *Nature Rev.*, **2002**, *3*, 430-440.

(8) Champoux J. J., DNA Topoisomerases: Structure, Function, and Mechanism, *Annu. Rev. Biochem.*, **2001**, *70*, 369-413.

(9) Schoeffler A. J., Berger J. M., DNA topoisomerases: harnessing and constraining energy to govern chromosome topology, *Quart. Rev. Biophys.*, **2008**, *41*, 41-101.

(10) Stewart L., Ireton G. C., Parker L. H., Madden K. R., Champoux J. J., Biochemical and Biophysical Analyses of Recombinant Forms of Human Topoisomerase I, *J. Biol. Chem.*, **1996**, *271*, 7593-7601.

(11) Hansen G., Harrenga A., Wieland B., Schomburg D., Reinemer P., Crystal Structure of Full Length Topoisomerase I from *Thermotoga maritima*, *J. Mol. Biol.*, **2006**, *358*, 1328-1340.

(12) Higgins N.P., Peebles C. L., Sugino A., Cozzarelli N. R., Purification of subunits of *Escherichia coli* DNA gyrase and reconstitution of enzymatic activity, *Proc. Natl. Acad. Sci.*, **1978**, *75*, 1773-1777.

(13) Roca J., Wang J. C., The capture of a DNA double helix by an ATP-dependent protein clamp: a key step in DNA transport by a type II DNA topoisomerases, *Cell*, **1992**, *71*, 833-840.

(14) Roca J., Wang J. C., DNA transport by a type II DNA topoisomerase: evidence in favour of two-gate mechanism, *Cell*, **1994**, *77*, 609-616.

(15) Roca J., Berger J. M.,Harrison S. C., Wang J. C., DNA transport by a type II topoisomerase: Direct evidence for a two-gate mechanism, *Proc. Natl. Acad. Sci.*, **1996**, *93*, 4057-4062.

(16) Williams N. L., Maxwell A., Probing the Two-Gate Mechanism of DNA Gyrase Using Cystein Cross-Linking, *Biochemistry*,**1999**, *38*, 13502-13511.

(17) Dong K. C., Berger J. M., Structural basis for gate-DNA recognition and bending by type IIA topoisomerases, *Nature*, **2007**, *450*, 1201-1206.

(18) Collins T. R., Hammes G.G., Hsieh T-S., Analysis of the eukaryotic topoisomerase II DNA gate: a single-molecule FRET and structural perspective, *NAR*, **2009**, *ahead of print*, 1-9.

(19) Corbett K. D., Benedetti P., Berger J. M., Holoenzyme assembly and ATP-mediated conformational dynamics of topoisomerase VI, *Nat. Struct. Mol. Biol.*, **2007**, *14*, 611-619.

(20) Bates A. D., Maxwell A., Energy Coupling in Type II Topoisomerases: Why Do They Hydrolyze ATP?, *Biochemistry*, **2007**, *46*, 7929-7941.

(21) Mueller-Planitz F., Herschlag D., DNA topoisomerase II selects DNA cleavage sites based on reactivity rather than binding affinity, *NAR*, **2007**, *35*, 3764-3764.

(22) Gorbalenya A. E., Koonin E. V., Helicases: amino acid sequence comparisons and structure-function relationships, *Curr. Opin. Struct. Biol.*, **1993**, *3*, 419-429.

(23) Tuteja N., Tuteja R., Unraveling DNA helicases. Motif, structure, mechanism and function, *Eur. J. Biochem.*, **2004**, *271*, 1849-1863.

(24) Cordin O., Banroques J., Tanner N. K., Linder P., The DEAD-box protein family of RNA helicases, Gene, **2006**, *367*, 17-37.

(25) Kossen K., Karginov F. V., Uhlenbeck O. C., The carboxyterminal domain of the DExDH protein YxiN is sufficient to confer specificity for 23S rRNA, *J. Mol. Biol.*, **2002**, *324*, 625-636.

(26) Theissen B., Karow A. R., Köhler J., Gubaev A., Klostermeier D., Cooperative binding of ATP and RNA induces a closed conformation in a DEAD box RNA helicase, *PNAS*, **2008**, *105*, 548-553.

(27) Kikuchi A., Asai K., Reverse gyrase - a topoisomerase which introduces positive superhelical turns into DNS, *Nature*, **1984**, *309*, 677-681.

(28) Nadal M., Reverse gyrase: An insight into the role of DNA-topoisomerases , *J. Biochimie*, **2007**, *89*, 447-455.

(29) Forterre P., A Hot Story from comparative genomics: reverse gyrase is the only hyperthermophile-specific protein, *Trends in Genetics*, **2002**, *18*, 236-238.

(30) Déclais A.-C., Bouthier de la Tour C., Duguet M., Reverse gyrases from bacteria and archaea, *Methods Enzymol.*, **2001**, *334*, 146-162.

(31) Atomi H., Matsumi R., Imanaka T., Reverse Gyrase Is Not a Prerequisite for Hyperthermophilic Life, *J. Bact.*, **2004**, *186*, 4829-4833.

(32) Napoli A., Valenti A., Salerno V., Nadal M., Garnier F., Rossi M., Ciaramella M., Reverse Gyrase Recruitment to DNA after UV Light Irradiation in *Sulfolobus solfataricus*, *J. Biol. Chem.*, **2004**, *32*, 33192-33198.

(33) Kampmann M., Stock D., Reverse gyrase has heat-protective DNA chaperone activity independent of supercoiling, *Nucl. Acids Res.*, **2004**, *32*, 3537-3545.

(34) Napoli A., Valenti A., Salerno V., Nadal M., Garnier F., Rossi M., Ciaramella M., Functional interaction of reverse gyrase with single-strand binding protein of the archaeon *Sulfolobus*, *Nucl. Acids. Res.*, **2005**, *33*, 564-576.

(35) Hsieh T-S., Plank J. L., Reverse Gyrase Functions as a DNA Renaturase, *J. Biol. Chem.*, **2006**, *281*, 5640-5647.

(36) Confalonieri F., Elie C., Nadal M., Bouthier de la Tour C., Forterre P., Duguet M., Reverse Gyrase: A helicase-like domain and a type I topoisomerase in the same polypeptide, *Proc. Natl. Acad. Sci.*, **1993**, *90*, 4753-4757.

(37) Kozyavkin S. A., Krah R., Gellert M., Stetter K. O., Lake J. A., Slesarev A. I., A Reverse Gyrase with an Unusual Structure, *J. Biol. Chem.*, **1994**, *269*, 11081-11089.

(38) Krah R., Kozyavkin S. A., Gellert M., A two-subunit type I DNA topoisomerase (reverse gyrase) from an extreme thermophile, *Proc. Natl. Acad. Sci.*, **1996**, *93*, 106-110.

(39) Matoba K., Mayanagi K., Nakasu S., Kikuchi A., Morikawa K., Three-dimensional electron microscopy of the reverse gyrase from *Sulfolobus tokodaii*, *Biochem. Biophys. Res. Comm.*, **2002**, *297*, 749-755.

(40) Rodríguez A. C., Stock D., Crystal structure of reverse gyrase: insights into the positive supercoiling of DNA, *EMBO Journal*, **2002**, *21*, 418-426.

(41) Rodríguez A. C., Studies of a Positive Supercoiling Machine, *J. Biol. Chem.*, **2002**, *277*, 29865-29873.

(42) Rodríguez A. C., Investigating the Role of the Latch in the Positive Supercoiling Mechanism of Reverse Gyrase, *Biochemistry*, **2003**, *42*, 5993-6004.

(43) Bouthier de la Tour C., Amrani L., Cossard R., Neuman K. C., Serre M.C., Duguet M., Mutational Analysis of the Helicase-like Domain of Thermotoga maritima Reverse Gyrase, *J. Biol. Chem.*, **2008**, *283*, 27395-27402.

(44) Jungblut S. P., Klostermeier D., Adenosine 5′-O-(3-thio)triphosphate (ATPγS) Promotes Positive Supercoiling of DNA by *T. maritima* Reverse Gyrase, *J. Mol. Biol.*, **2007**, *371*, 197-209.

(45) del Toro Duany Y., Jungblut S. P., Schmidt A. S., Klostermeier D., The reverse gyrase helicase-like domain is a nucleotide-dependent switch that is attenuated by the topoisomerase domain, *Nucleic Acids Research*, **2008**, *36*, 5882-5895.

(46) Shibata T., Nakasu S., Yasui K., Kikuchi A., Intrinsic DNA-dependent ATPase Activity of Reverse Gyrase, *J. Biol. Chem.*, 1987, *262*, 10419-10421.

(47) Bouthier de la Tour C., Portemer C., Kaltoum H., Duguet M., Reverse Gyrase from the Hyperthermophilic Bacterium *Thermotoga maritima*: Properties and Gene Structure, *J. Bact.*, **1998**, *180*, 274-281.

(48) Valenti A., Perugino G., D'Amaro A., Cacace A., Napoli A., Rossi M., Ciaramella M., Dissection of reverse gyrase activities: insight into the evolution of a thermostable molecular machine, *NAR*, **2008**, *36*, 4587-4597.

(49) Pfüller R., Hammerschmidt W., Plasmid-Like Replicative Intermediates of the Eppstein-Barr Virus Lytic Origin of DNA Replication, *J. Virol.*, **1996**, *70*, 3423-3431.

(50) Changela A., Perry K., Taneja B., Mondragón A., DNA manipulators: caught in the act, *Curr. Opin. Struct. Biol.*, **2003**, *13*, 15-22.

(51) Lee C.-H., Mizusawa H., Kakefuda T., Unwinding of double-stranded DNA helix by dehydration, *Proc. Natl. Acad. Sci.*, **1981**, *78*, 2838 -2842.

(52) Hsieh T-S., Capp C., Nucleotide- and stoichiometry-dependent DNA supercoiling by reverse gyrase, *J. Biol. Chem.*, **2005**, *280*, 20467-20475.

(53) Förster T., Transfer mechanisms of electronic excitation, *Far. Soc.*, **1959**, *27*, 7-17.

(54) Parker C. A., .Rees W. T., Correction of fluorescence spectra and measurement of fluorescence quantum efficiency, *Analyst*, **1960**, *85*, 587-600.

(55) Magde D., Wong R., Seybold P. G., Fluorescence Quantum Yields and Their Relation to Lifetimes of Rhodamine 6G and Fluorescein in Nine Solvents: Improved Absolute Standards for Quantum Yields, *Photochem. Photobiol.*, **2002**, *75*, 327-334.

(56) Wang D., Geva E., Protein Structure and Dynamics from Single-Molecule Fluorescence Resonance Energy Transfer, *J. Phys. Chem.*, **2005**, *109*, 1626-1634.

(57) Mukhopadhyay., Deniz A. A., Fluorescence from Diffusing Single Molecules Illuminates Biomolecular Structure and Dynamics, *J. Fluoresc.*, **2007**, *17*, 775-783.

2. Aims of Research

The mechanism of the ATP-dependent introduction of positive supercoils into plasmids by the topoisomerase IA reverse gyrase has only been investigated superficially. Reverse gyrase from the eubacterium *Thermotoga maritima* is an ideal test subject and is not fully characterised. The aim of this PhD thesis was to further our understanding of adenine nucleotide binding and hydrolysis, DNA substrate binding and their importance for plasmid relaxation and positive supercoiling by reverse gyrase from *T. maritima*. Furthermore, the project was designed to get insight into the supercoiling and nucleotide cycle by observing the molecular machine reverse gyrase on a molecular level.

The first task was to improve the existing purification protocol to yield monomeric reverse gyrase. Subsequently, the dependency of plasmid relaxation and positive supercoiling by reverse gyrase on the presence of various ADP- and ATP-analogues was systematically investigated. As the literature suggests multiple necessary DNA binding sites for reverse gyrase topoisomerase activity, binding of artificial single- and double-stranded DNA substrates by reverse gyrase *T. maritima* was tested. Conformational changes in the helicase-like domain and the topoisomerase domain during supercoiling activity of reverse gyrase are predicted throughout literature, but have not been demonstrated. Therefore, we planned to apply smFRET as a molecular ruler to observe potential conformational changes. In the case of reverse gyrase from *T. maritima*, this could be very demanding, as eight native cysteines in two putative zinc fingers may interfere with direct fluorescent labelling of specifically introduced cysteines. Also, a mutation study of the putative zinc fingers was aimed at elucidating their role for topoisomerase activity of reverse gyrase.

3. Relaxation and Supercoiling Activity of *T. maritima* Reverse Gyrase

3.1 Introduction

The unique ATP-dependent positive supercoiling activity of reverse gyrase distinguishes it from all other topoisomerases[1,2]. In the presence of ADP, the enzyme relaxes both positively and negatively supercoiled plasmid DNA[3,4]. Different ATP analogues also promote these converse activities[4-6].

The topoisomerase activity of reverse gyrase is only available at high temperatures for this typical hyperthermophilic enzyme[7]. Buffer conditions such as pH, Na^+/Mg^{2+} content or presence of polyethylene glycol (PEG) influence the velocity of supercoiling[8]. For reverse gyrase from *Thermotoga maritima*, the supercoiling and relaxation conditions are not optimised until now[9]. Elucidation of such optimal conditions is important for the design of future experiments. Two-dimensional gel electrophoresis separates topoisomers according to the number and sign of supercoils, allowing for the distinction of reaction products after a certain time and under varying conditions (Chapter 1.4).

In this way, topoisomerase activity of wild type reverse gyrase and mutants can be compared. For example, pairs of cysteines introduced at flexible domain positions allow for labelling with fluorescent dyes, and thus, application to smFRET measurements. Corresponding cystein mutants of reverse gyrase have to be tested for wild type activity. Additionally, it is necessary to examine DNA cleavage-deficient and ATPase-deficient mutants to further understand the mechanism of positive supercoiling in *T. maritima* reverse gyrase.

3.2 Material and Methods

Purification of Reverse Gyrase

The reverse gyrase gene from *T. maritima* was amplified from genomic DNA with PCR and cloned into the pET28a vector (Novagen) as previously described[4]. The protein was produced in an in-house constructed bacterial strain, namely *E. coli* BL21 Star (DE3) (Invitrogen) containing the RIL plasmid (Stratagene)[4], using auto-inducing medium[10]. The purification protocol includes cell disruption in a microfluidizer followed by hydrophobic interaction-, cation exchange-, affinity- and size exclusion chromatography as published[4].

Negatively Supercoiled Plasmid

pUC18 (2686 bp) or pETM30 plasmids (6346 bp, EMBL) were amplified in *E. coli* XL1 blue (Stratagene) and purified with kits from Promega (Pure Yield^{TM}) and Qiagen (Midiprep System) following the manufacturer's instructions.

Relaxed Plasmid

Negatively supercoiled pUC18 was relaxed with *wheat germ* topoisomerase I (Promega) according to the manufacturer's instructions. Relaxation of 30 µg pUC18 plasmid DNA was carried out for 2 h at 37°C with 90 U *wheat germ* topoisomerase I instead of 30 U. The reaction was stopped by adding 0.1% SDS (final concentration).

Denatured topoisomerase I and SDS were removed with a modified phenol/chloroform extraction protocol. Samples were extracted twice with equal volumes of chilled phenol/chloroform/isoamyl alcohol (25:24:1, Merck). After vortexing for 1 minute, phases were separated in a table top centrifuge at maximum speed (13 krpm) for 10 minutes at 4°C. An equal volume of chilled isopropanol was added to the supernatant and the mixture was inverted gently for 1 minute. After 20 minutes of centrifugation, the resulting DNA pellet was washed twice with cold 70% ethanol, vacuum-dried for 40 minutes and resuspended in water.

Relaxation and Supercoiling of Plasmid DNA with Reverse Gyrase

Conditions for relaxation of 15 nM pUC18 were 1 µM reverse gyrase in 50 mM Tris/HCl (pH 7.5), 150 mM NaCl, 10 mM $MgCl_2$, 100 µM $Zn(OAc)_2$, 2 mM β-ME, 10% (w/v) PEG 8000 at 75°C. Plasmid relaxation was started upon addition of 2 mM ADP. Positive plasmid supercoiling was achieved using ATP, respectively. Adenine nucleotides and analogues were purchased from Pharma Waldhof or Jena Bioscience. Reactions were placed on ice and incubated with 1 U μl^{-1} Proteinase K (Qiagen) for 10 minutes before stopping buffer with 10 mM EDTA and 1% SDS was added. The degree of relaxed plasmid was analysed on a 1.2% (w/v) agarose gel run at 11 V cm^{-1}. Positively and negatively supercoiled plasmids were separated *via* two-dimensional electrophoresis in 2% agarose gels with 10 mg ml^{-1} chloroquine in the second dimension (see Chapter 1.4).

3.3 Results

Optimal Conditions for Plasmid Supercoiling by Reverse Gyrase

To determine optimal conditions for topoisomerase activity of reverse gyrase, the pH, the concentrations of NaCl, $MgCl_2$, PEG 8000, the plasmid and the reaction temperature were varied. Starting conditions for relaxation and supercoiling of plasmids were 1 μM reverse gyrase, 50 mM Tris/HCl (pH 7.5), 150 mM NaCl, 10 mM $MgCl_2$, 100 μM $Zn(OAc)_2$, 2 mM β-ME, 2 mM ATP, 15 nM pUC18, 10% (w/v) PEG 8000, 75°C[8,9].

Influence of pH

For reverse gyrase wild type with a calculated pI of 8.5, a pH region from 5.7 to 7.5 was screened. Reaction products were analysed with gel electrophoresis (Figure 1).

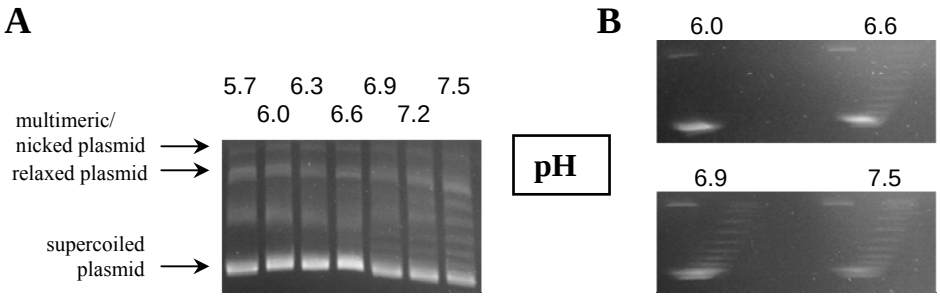

Figure 1. One- (A) and two-dimensional (B) agarose gel analysis of a pH-dependent supercoiling reaction with reverse gyrase. The typical relative position of multimeric/nicked, relaxed and supercoiled pUC18 is depicted in the left panel. Conditions were 1 μM reverse gyrase, 50 mM Tris/HCl (**pH varied**), 150 mM NaCl, 10 mM $MgCl_2$, 100 μM $Zn(OAc)_2$, 2 mM β-ME, 2 mM ATP, 15 nM pUC18, 10% (w/v) PEG 8000, 75°C, 30 minutes. Reverse gyrase activity has an optimum at pH 7.5.

After 30 minutes, no supercoiling is observed for values under pH 6.3. Topoisomers of pUC18 appear from pH 6.6-6.9. Two-dimensional gel electrophoresis separates negatively and positively supercoiled species visible for pH 6.9 and pH 7.5 (Figure 1B). Due to a pI of 8.5 for *T. maritima* reverse gyrase, values higher than pH 7.5 were not tested. At this pH value supercoiling activity is maximal.

NaCl-concentration

Many topoisomerases are inhibited by high salt concentrations interfering with protein-DNA interaction[11]. Thus, it is important to optimise the NaCl conditions for supercoiling activity of reverse gyrase. Figure 2 shows the optimisation.

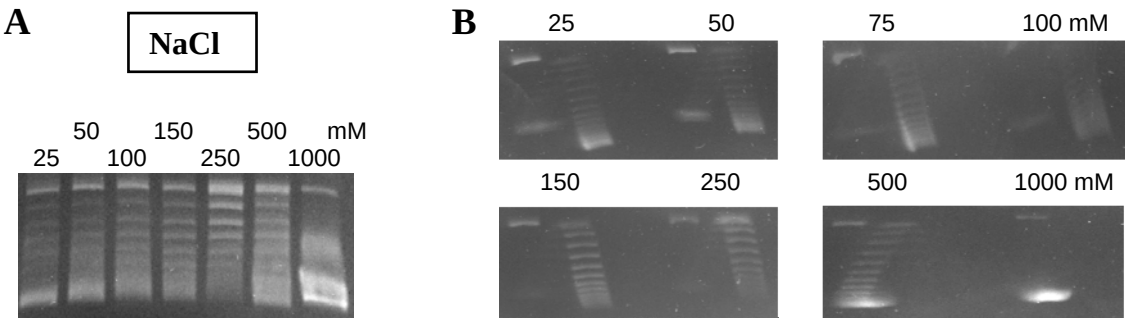

Figure 2. One- (A) and two-dimensional (B) agarose gel analysis of a supercoiling reaction. 1 µM reverse gyrase, 50 mM Tris/HCl (pH 7.5), **NaCl varied**, 10 mM $MgCl_2$, 100 µM $Zn(OAc)_2$, 2 mM β-ME, 2 mM ATP, 15 nM pUC18, 10% (w/v) PEG 8000, 75°C, 45 minutes. 150 mM NaCl were chosen as the standard concentration.

The gel in Figure 2A shows increasing relaxation of plasmid up to 250 mM NaCl. Positively supercoiled topoisomers are generated at these concentrations (Figure 2B). Above 250 mM NaCl, only negative supercoiled or relaxed species are present. At 25 mM NaCl, approximately 50% positive supercoiled plasmid is generated while negatively supercoiled topoisomers also remain. 150 mM NaCl give the same degree of positive supercoiling leaving no negatively supercoiled topoisomers. Hence, the standard NaCl content was set to 150 mM. Lower concentrations were not chosen due to precipitation of the protein, even at moderate temperatures (data not shown).

K^+-glutamate

Contrary to reverse gyrase, topoisomerase VI activity is inhibited in the presence of NaCl. As an alternative co-solute, K^+-glutamate (KGlu) is commonly used[12]. The stimulating effect of this salt on reverse gyrase topoisomerase activity was tested (Figure 3).

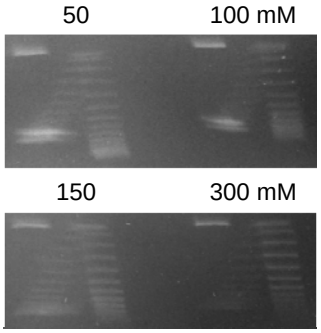

Figure 3. Two-dimensional agarose gel analysis of a supercoiling reaction containing 1 µM reverse gyrase, 50 mM Tris/HCl (pH 7.5), **KGlu varied**, 10 mM $MgCl_2$, 100 µM $Zn(OAc)_2$, 2 mM β-ME, 2 mM ATP, 15 nM pUC18, 10% (w/v) PEG 8000 at 75°C for 30 minutes. NaCl from the reverse gyrase storing buffer was exchanged with KGlu in a dialysis. The optimal KGlu concentration in the absence of NaCl lies at 100 mM.

KGlu also stimulates positive supercoiling of plasmid DNA with an optimum at 100 mM KGlu. However, negatively supercoiled plasmid is still present indicating that the reaction is not very effective. Comparison of Figures 2 and 3 shows that 150 mM NaCl promote the

positive supercoiling activity of reverse gyrase more efficiently. Therefore, NaCl was chosen as the standard salt.

$MgCl_2$-dependency

Bivalent cations like Mg^{2+} bridge adjacent phosphate groups of nucleic acids. Enzymes employ this to interact with DNA indirectly[11] or to coordinate phosphate groups of nucleotides by also binding Mg^{2+} ions. The latter is common for ATPases such as reverse gyrase[9]. Optimal concentrations for the *T. maritima* enzyme are unknown and were therefore tested (Figure 4).

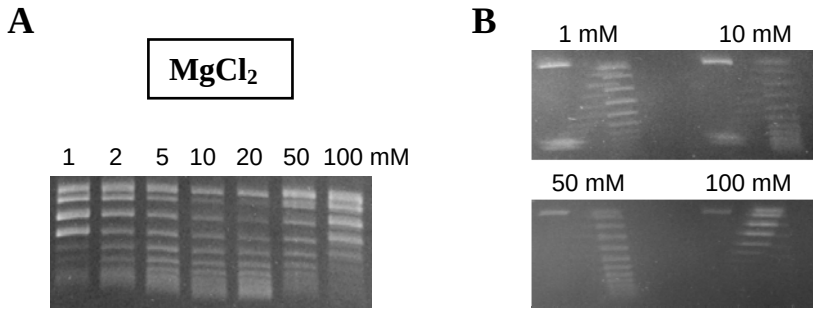

Figure 4. One- (A) and two-dimensional (B) agarose gel electrophoresis of a $MgCl_2$-dependent supercoiling reaction. Conditions were 1 µM reverse gyrase, 50 mM Tris/HCl (pH 7.5), 150 mM NaCl, **$MgCl_2$ varied**, 100 µM $Zn(OAc)_2$, 2 mM β-ME, 2 mM ATP, 15 nM pUC18, 10% (w/v) PEG 8000, 75°C, 30 minutes. 10 mM is the optimal $MgCl_2$ concentration.

The topoisomerase pattern alternates between relaxed plasmid and supercoiled species from 1 mM to 100 mM $MgCl_2$ (Figure 4A). Two-dimensional gel electrophoresis identifies maximum positive supercoiling at 10 mM $MgCl_2$ (Figure 4B).

Stabilisation by PEG 8000

Polyethylene glycol is a hydrophilic polymer frequently used to increase protein solubility and DNA-protein interaction[13]. Interestingly, it also enhances the supercoiling activity of reverse gyrase[8]. Therefore the optimal PEG 8000 concentration for the *T. maritima* enzyme was screened (Figure 5).

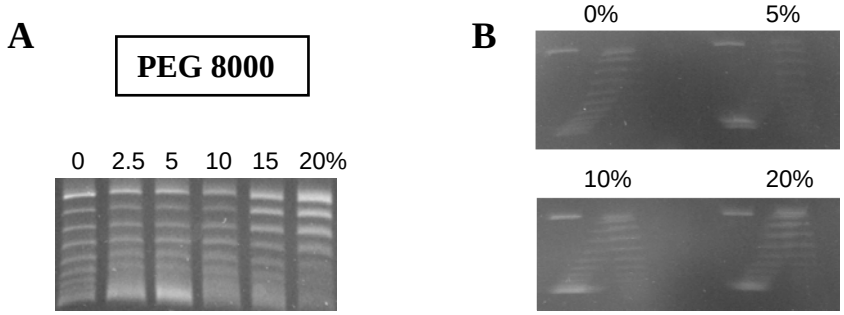

Figure 5. One- (A) and two-dimensional (B) agarose gel analysis. Supercoiling samples contained 1 µM reverse gyrase, 50 mM Tris/HCl (pH 7.5), 150 mM NaCl, 10 mM $MgCl_2$, 100 µM $Zn(OAc)_2$, 2 mM β-ME, 2 mM ATP, 15 nM pUC18, **variable PEG 8000** and were incubated at 75°C for 30 minutes. 10% (w/v) PEG 8000 stimulates topoisomerase activity of *T. maritima* reverse gyrase most effectively.

The highest positive supercoiling degree of pUC18 is achieved at 10% (w/v) PEG 8000 for *T. maritima* reverse gyrase.

Length and purity of substrate plasmid

It is unclear, if the number of topoisomers between supercoiled and relaxed pUC18 species corresponds to the number of visible gel bands. Therefore, comparing the number of topoisomers during the supercoiling of a larger plasmid could elucidate additional steps of this reaction. Also, plasmid purity is essential for proper supercoiling activity. Two different purification methods for pUC18 and pETM30 as an alternative plasmid were tested (Figure 6).

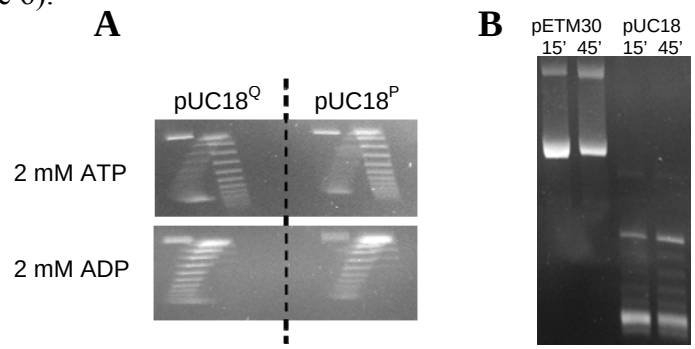

Figure 6. Different plasmids used as supercoiling substrate. Samples contained 1 µM reverse gyrase, 50 mM Tris/HCl (pH 7.5), 150 mM NaCl, 10 mM $MgCl_2$, 100 µM $Zn(OAc)_2$, 2 mM β-ME, 2 mM nucleotide, 15 nM **plasmid** as indicated, 10% (w/v) PEG 8000 and were incubated at 75°C for 45 minutes. (A) pCU18 purified after Qiagen or Promega are equal substrates for reverse gyrase topoisomerase activity. Introduction of positive supercoils in the presence of ADP is due to contamination with ATP[4]. (B) pETM30 is not a substrate for reverse gyrase.

There is no difference in the topoisomerase activity of reverse gyrase with pUC18 as a substrate purified with Qiagen or Promega kits (Figure 6A). Surprisingly, reverse gyrase does not accept pETM30 as a supercoiling substrate under the conditions used (Figure 6B).

Temperature-dependency

Reverse gyrases from different organisms have different temperature optima[5-7]. Determination of the optimal supercoiling temperature for reverse gyrase from *T. maritima* is shown in Figure 7.

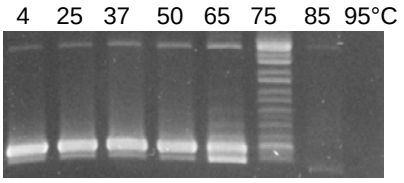

Figure 7. Topoisomerase activity of reverse gyrase at different **temperatures** analysed on an agarose gel. Conditions were 1 µM reverse gyrase, 50 mM Tris/HCl (pH 7.5), 150 mM NaCl, 10 mM $MgCl_2$, 100 µM $Zn(OAc)_2$, 2 mM β-ME, 2 mM ATP, 15 nM pUC18, 10% (w/v) PEG 8000, 45 minutes. The optimal supercoiling temperature is 75°C.

Reverse gyrase generates no additional topoisomers at temperatures below 50°C. Few reaction products are visible at 65°C. The optimal reaction temperature for positive supercoiling is 75°C, where many topoisomers are present. No activity is observed at 85°C and above. The fact that the overall intensity of plasmid bands is strongly decreased indicates degradation of plasmid DNA in the presence of reverse gyrase at these temperatures. pUC18 plasmid alone is stable at 95°C for 45 minutes (data not shown).

Time course of plasmid supercoiling

The topoisomerase activity of reverse gyrase unites both relaxation and positive supercoiling of plasmid DNA. Time resolved supercoiling gives insight into the coordination of underlying reactions and their relative velocities (Figure 8).

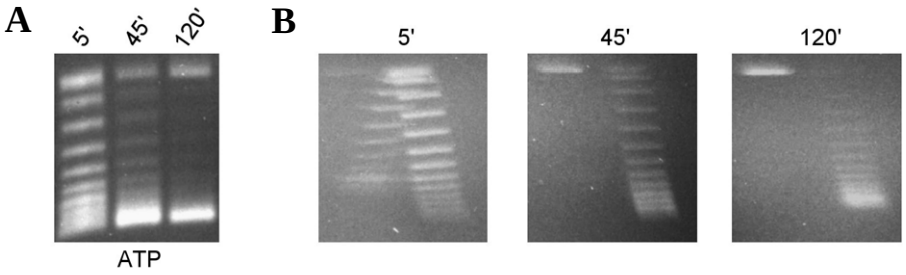

Figure 8. One- (A) and two-dimensional (B) agarose gels (pictures taken from[4]). A **time-course** was recorded with 1 µM reverse gyrase, 50 mM Tris/HCl (pH 7.5), 150 mM NaCl, 10 mM $MgCl_2$, 100 µM $Zn(OAc)_2$, 2 mM β-ME, 2 mM ATP, 15 nM pUC18, 10% (w/v) PEG 8000, 75°C. The reaction is complete after 120 minutes.

pUC18 plasmid is relaxed and subsequently positively supercoiled. Relaxation occurs rapidly in about 5 minutes. Only positively supercoiled topoisomers are present after 45 minutes. Positive supercoiling is complete after 2 h.

Separation of negative and positive supercoils can also be observed on one-dimensional gels. Double bands appear at high resolution, which is often not achieved (cp. Figure 7).

The paired bands correspond to topoisomers with the same number of supercoils but with opposite sign. The positive form precedes the negatively supercoiled form in both gel dimensions (see 5'-frame in Figure 8,). This behaviour is clearer in the second dimension, due to the intercalation of chloroquine (Chapter 1.4).

Relaxation of plasmid DNA

All reverse gyrases can introduce positive supercoils into negatively supercoiled plasmid in the presence of ATP or relax the plasmid in the presence of ADP[4] (Chapter 1.3). Relaxation was monitored in the presence of ADP at different temperatures (Figure 9).

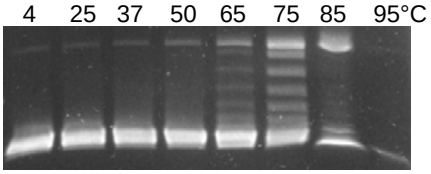

Figure 9. Plasmid relaxation at different **temperatures** analysed by agarose gel electrophoresis. Conditions were 1 μM reverse gyrase, 50 mM Tris/HCl (pH 7.5), 150 mM NaCl, 10 mM $MgCl_2$, 100 μM $Zn(OAc)_2$, 2 mM β-ME, 2 mM **ADP**, 15 nM pUC18, 10% (w/v) PEG 8000, 45 minutes. The optimal temperature for plasmid relaxation is 75°C.

Similar to the temperature-dependent positive supercoiling reaction, no reaction activity is observed below 50°C. Plasmid relaxation does not start until 65°C and is most effectively promoted at 75°C. At temperatures of 85°C and higher, no relaxation occurs and the plasmid is degraded, as judged from the decrease in band intensity. No positive supercoils are introduced into plasmid DNA in the presence of ADP (Figure 10).

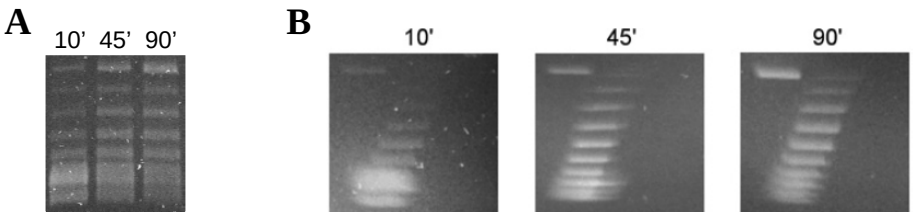

Figure 10. One- (A) and two-dimensional (B) agarose gels (panel B taken from[4]). **Time-course** recorded for 1 μM reverse gyrase, 50 mM Tris/HCl (pH 7.5), 150 mM NaCl, 10 mM $MgCl_2$, 100 μM $Zn(OAc)_2$, 2 mM β-ME, 1 mM **ADP**, 15 nM pUC18, 10% (w/v) PEG 8000, 75°C. Relaxation is advanced but not complete after 45 minutes.

As a result of the optimisation described above, the standard conditions for all supercoiling reactions in this thesis were 1 μM reverse gyrase, 50 mM Tris/HCl (pH 7.5), 150 mM NaCl, 10 mM $MgCl_2$, 100 μM $Zn(OAc)_2$, 2 mM β-ME, 2 mM ATP, 15 nM pUC18, 10% (w/v) PEG 8000 at 75°C.

Relaxed Plasmid as a Substrate for Reverse Gyrase

Negatively supercoiled plasmid was used as a substrate for reverse gyrase in the above sections. Providing relaxed plasmid as starting material is important to further elucidate supercoiling activity of *T. maritima* reverse gyrase[3]. Negatively supercoiled pUC18 purified with kits from Qiagen and Promega was relaxed with *wheat germ* topoisomerase I (Figure 11).

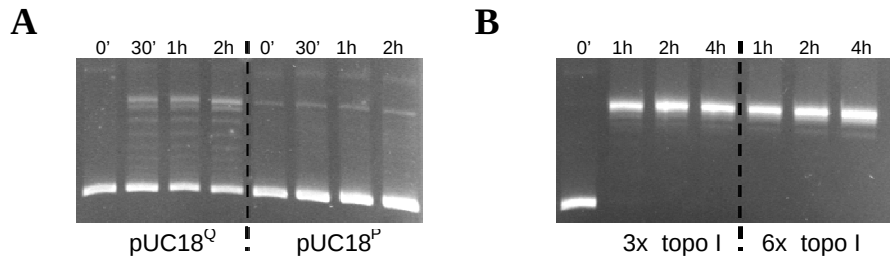

Figure 11. (A) Relaxation of pUC18 (purified with Qiagen or Promega kits) with *wheat germ* topoisomerase I (Promega) following manufacturer's instructions. (A) Promega-purified pCU18 is not a substrate for topoisomerase I. (B) Using 3-fold topoisomerase I compared to manufacturer's instructions on Qiagen-purified pUC18 yields relaxed plasmid after 2h.

pUC18 plasmid purified with the Promega kit is not relaxed by topoisomerase I. The Qiagen-purified plasmid is only partially relaxed (Figure 11A). Homogeneous relaxation of pUC18 (Qiagen) is achieved after 2 h with 3-fold increased topoisomerase I concentrations compared to the manufacturer's instructions (Figure 11B). Such relaxed pUC18 plasmid was tested as a substrate for reverse gyrase in the presence of ATP analogues[4] (Figure 12).

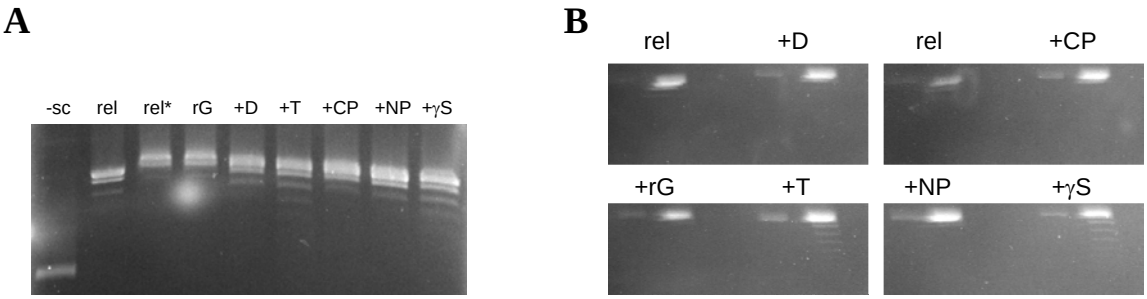

Figure 12. Positive supercoiling of relaxed pUC18 analysed by one- (A) and two-dimensional (B) agarose gel electrophoresis. Conditions were 1 µM reverse gyrase (rG), 50 mM Tris/HCl (pH 7.5), 150 mM NaCl, 10 mM $MgCl_2$, 100 µM $Zn(OAc)_2$, 2 mM β-ME, 2 mM adenine nucleotide, 15 nM **relaxed pUC18**, 10% (w/v) PEG 8000, 75°C, 30 minutes. Positive supercoils are introduced in the presence of ATP (T) and ATPγS (γS). Abbreviations: negatively supercoiled pUC18 (-sc), relaxed pUC18 before/after phenol-extraction (rel/rel*), ADP (D), ADPCP (CP), ADPNP (NP).

ATP and ATPγS[4] are hydrolysed by reverse gyrase and promote positive supercoiling of relaxed pUC18 at 75°C. The supercoiling state of relaxed plasmid is not changed in the presence of the non-hydrolysable nucleotides ADPCP, ADPNP and ADP.

3.4 Discussion

Positive supercoiling of plasmid DNA by reverse gyrase is unique to this enzyme class. The optimal temperature for both relaxation and supercoiling of plasmid DNA by *T. maritima* reverse gyrase is 75°C. Obviously, these converse topoisomerase activities require similar domain flexibility for the two potentially different underlying enzyme mechanisms. At temperatures of 85°C and above, plasmid DNA is degraded in the presence of both reverse gyrase and ADP or ATP. This may be due to an accumulation of cleaved plasmid supercoiling intermediate with reverse gyrase prone to heat-degradation. Plasmid DNA alone is stable in the presence and absence of ADP and ATP.

Like all reverse gyrases studied so far, the *T. maritima* enzyme positively supercoils plasmid DNA in the presence of ATP at 75°C. This is true starting from both negatively supercoiled and relaxed plasmids[4]. Furthermore, plasmid relaxation occurs starting from negatively supercoiled plasmid in an ADP-dependent manner. Plasmid relaxation is notably faster in the presence of ATP. This might be due to simultaneous relaxation of plasmid DNA accompanied by positive supercoiling. No change in plasmid topology is observed during incubation of relaxed plasmid with reverse gyrase in the presence of non-hydrolysable ATP analogues ADPCP, ADPNP and ADP. Unfortunately, intermediate supercoiling steps remain unknown. Using a larger plasmid like pETM30 instead of pUC18 should elucidate intermediate steps, as a higher number of supercoils can be introduced. However, pETM30 is not a supercoiling substrate for reverse gyrase under the conditions applied. Possibly, plasmid relaxation and positive supercoiling by reverse gyrase might simply be slower with the pETM30 plasmid.

Finally, the single reaction steps for plasmid relaxation and positive supercoiling remain elusive, but it is evident that reverse gyrase topoisomerase activity is dependent on many factors. In this work, we optimised the pH value, the concentrations of NaCl, $MgCl_2$, PEG 8000, and the reaction temperature for topoisomerase activity of *T. maritima* reverse gyrase. Optimal conditions were 1 μM reverse gyrase, 50 mM Tris/HCl (pH 7.5), 150 mM NaCl, 10 mM $MgCl_2$, 100 μM $Zn(OAc)_2$, 2 mM β-ME, 2 mM ATP, 15 nM pUC18, 10% (w/v) PEG 8000 at 75°C.

3.5 Literature

(1) Kikuchi A., Asai K., Reverse gyrase - a topoisomerase which introduces positive superhelical turns into DNA, *Nature*, **1984**, *309*, 677-681.

(2) Champoux J. J., DNA Topoisomerases: Structure, Function, and Mechanism, *Annu. Rev. Biochem.*, **2001**, *70*, 369-413.

(3) Hsieh T-S., Plank J. L., Reverse Gyrase Functions as a DNA Renaturase, *J. Biol. Chem.*, **2006**, *281*, 5640-5647.

(4) Jungblut S. P., Klostermeier D., Adenosine 5′-O-(3-thio)triphosphate (ATPγS) Promotes Positive Supercoiling of DNA by *T. maritima* Reverse Gyrase, *J. Mol. Biol.*, **2007**, *371*, 197-209.

(5) Rodríguez A. C., Studies of a Positive Supercoiling Machine, *J. Biol. Chem.*, **2002**, *277*, 29865-29873.

(6) Hsieh T. S., Capp C., Nucleotide- and stoichiometry-dependent DNA supercoiling by reverse gyrase, *J. Biol. Chem.*, **2005**, *280*, 20467-20475.

(7) Forterre P., A Hot Story from comparative genomics: reverse gyrase is the only hyperthermophile-specific protein, *Trends in Genetics*, **2002**, *18*, 236-238.

(8) Forterre P., Mirambeau G., Jaxel C., Nadal M., Duguet M., High positive supercoiling in vitro catalyzed by an ATP and polyethylene glycol-stimulated topoisomerase from *Sulfolobus acidocaldarius*, *EMBO*, **1985**, *4*, 2123-2128.

(9) Bouthier de la Tour C., Portemer C., Kaltoum H., Duguet M., Reverse Gyrase from the Hyperthermophilic Bacterium *Thermotoga maritima*: Properties and Gene Structure, *J. Bact.*, **1998**, *180*, 274-281.

(10) Studier F.W, Protein production by auto-induction in high density shaking cultures, *Protein Expr. Purif.*, **2005**, *41*, 207-234.

(11) Stewart L., Ireton G. C., Parker L. H., Madden K. R., Champoux J. J., Biochemical and Biophysical Analyses of Recombinant Forms of Human Topoisomerase I, *J. Biol. Chem.*, **1996**, *271,* 7593-7601.

(12) Corbett K. D., Benedetti P., Berger J. M., Holoenzyme assembly and ATP-mediated conformational dynamics of topoisomerase VI, *Nat. Struct. Mol. Biol.*, **2007**, *14*, 611-619.

(13) Miller K. G., Liu L. F., Englund P. T., A homogeneous type II DNA topoisomerase from HeLa cell nuclei, *J. Biol. Chem.*, **1981**, *256*, 9334-9339.

4. Adenosine 5′-O-(3-thio)triphosphate (ATPγS) Promotes Positive Supercoiling of DNA by *T. maritima* Reverse Gyrase

Journal of Molecular Biology, 2007

Vol. *371*, 197-209

Stefan P. Jungblut and Dagmar Klostermeier

University of Basel, Biozentrum, Department of Biophysical Chemistry,
Klingelbergstrasse 70, CH-4056 Basel, Switzerland
Tel: +41 61 267 2381, Fax: +41 61 267 2189, E-mail: dagmar.klostermeier@unibas.ch

4.1 Summary

Reverse gyrase is a topoisomerase with a singular ATP-dependent positive supercoiling activity known only in hyperthermophilic bacteria and archea. In the presence of ADP, reverse gyrase relaxes negatively supercoiled plasmid DNA. Reverse gyrases consist of an N-terminal helicase-like domain with an intrinsic ATPase activity and a C-terminally fused topoisomerase IA. The data published about nucleotide utilisation of reverse gyrase during topoisomerase activity are mainly qualitative and are very diverse for different reverse gyrases from different organisms. The publication featured in this chapter presents a detailed study of *Thermotoga maritima* reverse gyrase nucleotide requirements for positive plasmid supercoiling and plasmid relaxation. In this study, we provide dissociation constants for the binding of ADP, ATPγS and ADPNP to reverse gyrase wild type and a mutant lacking the intrinsic ATPase activity.

Although positive supercoiling by different reverse gyrases is observed from 50°C, we found that reverse gyrase from *T. maritima* hydrolyses ATP at 37°C. Our finding that ATP hydrolysis is stimulated by pUC18 plasmid at 37°C may indicate a functional communication between the reverse gyrase domains already in the absence of supercoiling activity. The optimal temperature for ATP-dependent plasmid supercoiling by *T. maritima* reverse gyrase is 75°C, where plasmid relaxation is promoted with ADP and ADPNP, a non-hydrolysable ATP analogue. ATPγS, commonly used as a non-cleavable ATP analogue, is surprisingly hydrolysed at 37°C by reverse gyrase in the presence of pUC18. Furthermore, ATPγS is hydrolysed by reverse gyrase from *T. maritima* at 75°C, which is increased by a remarkable 15-fold in the presence of pUC18. Strikingly, we found that hydrolysis of ATPγS promotes positive supercoiling to a similar extent as ATP. Our findings were confirmed using an ATPase-deficient mutant of reverse gyrase, where hydrolysis of ATP and ATPγS is 20-fold reduced compared to the wild type enzyme. The ATPase-deficient mutant also shows reduced positive supercoiling with ATP and only plasmid relaxation is achieved in the presence of ATPγS. Thus, reduced hydrolysis capability accounts for reduced positive supercoiling ability.

Finally, both ATP and ATPγS hydrolysis energy must be transferred from the helicase-like domain to the topoisomerase domain of reverse gyrase. A model for inter-domain communication is presented, where nucleotide hydrolysis and affiliated positive plasmid supercoiling is triggered by cooperative binding of pUC18 and ATP/ATPγS.

4.2 Published Article

doi:10.1016/j.jmb.2007.05.031 *J. Mol. Biol.* (2007) **371**, 197–209

JMB

Available online at www.sciencedirect.com

ScienceDirect

ELSEVIER

Adenosine 5′-O-(3-thio)triphosphate (ATPγS) Promotes Positive Supercoiling of DNA by *T. maritima* Reverse Gyrase

Stefan P. Jungblut and Dagmar Klostermeier*

University of Basel, Biozentrum
Dept. of Biophysical Chemistry
Klingelbergstrasse 70
CH-4056 Basel, Switzerland

Reverse gyrases are topoisomerases that catalyze ATP-dependent positive supercoiling of circular covalently closed DNA. They consist of an N-terminal helicase-like domain, fused to a C-terminal topoisomerase I-like domain. Most of our knowledge on reverse gyrase-mediated positive DNA supercoiling is based on studies of archaeal enzymes. To identify general and individual properties of reverse gyrases, we set out to characterize the reverse gyrase from a hyperthermophilic eubacterium. *Thermotoga maritima* reverse gyrase relaxes negatively supercoiled DNA in the presence of ADP or the non-hydrolyzable ATP-analog ADPNP. Nucleotide binding is necessary, but not sufficient for the relaxation reaction. In the presence of ATP, positive supercoils are introduced at temperatures above 50 °C. However, ATP hydrolysis is stimulated by DNA already at 37 °C, suggesting that reverse gyrase is not frozen at this temperature, but capable of undergoing inter-domain communication. Positive supercoiling by reverse gyrase is strictly coupled to ATP hydrolysis. At the physiological temperature of 75 °C, reverse gyrase binds and hydrolyzes ATPγS. Surprisingly, ATPγS hydrolysis is stimulated by DNA, and efficiently promotes positive DNA supercoiling, demonstrating that inter-domain communication during positive supercoiling is fully functional with both ATP and ATPγS. These findings support a model for communication between helicase-like and topoisomerase domains in reverse gyrase, in which an ATP and DNA-induced closure of the cleft in the helicase-like domain initiates a cycle of conformational changes that leads to positive DNA supercoiling.

Keywords: reverse gyrase; non-hydrolyzable ATP analog; topoisomerase; nucleotide-driven conformational changes

*Corresponding author

Introduction

Reverse gyrase was discovered in 1984 as a special topoisomerase that catalyzes the ATP-dependent introduction of positive supercoils into the DNA of the hyperthermophilic archaeon *Sulfolobus acidocaldarius*.[1] Since then, it has been identified in various hyperthermophilic and thermophilic archaea and bacteria,[2,3] and is the only protein unique to hyperthermophilic organisms.[4] The *in vivo* function of reverse gyrase is not clear. Initially, positive supercoiling was proposed to protect DNA from damage at high temperatures. However, DNA isolated from the hyperthermophilic eubacterium *Thermotoga maritima* is negatively supercoiled, showing that reverse gyrase activity is over-compensated by DNA gyrase-mediated negative supercoiling. Also, reverse gyrase is not strictly required for hyperthermophilic life.[5] More recently, a heat-protective DNA chaperone activity of reverse gyrase has been reported that does not require positive supercoiling,[6] and a DNA renaturase activity[7] has been demon-

Abbreviations used: ATPγS, adenosine-5′-O-(3-thio) triphosphate; ADPNP, 5′-adenylyl-β,γ-imidodiphosphate; BME, β-mercaptoethanol; mant, 2(3)-*O*-(*N*-methyl-anthraniloyl); SF 2, helicase superfamily 2.

E-mail address of the corresponding author: dagmar.klostermeier@unibas.ch

strated. These results indicate that reverse gyrases may protect the DNA of hyperthermophiles from damage at high temperatures *via* a variety of activities.

Reverse gyrases consist of an N-terminal helicase-like domain, fused to a C-terminal topoisomerase domain.[8] Only limited structural information on reverse gyrases is available. In the structure of reverse gyrase from *Archaeoglobus fulgidus*, the C-terminal domain adopts the same torus-shaped structure as DNA topoisomerase I.[9] ATP binding and hydrolysis occurs in the helicase-like domain that contains a Walker A and a modified Walker B motif, while the catalytic tyrosine that catalyzes the transesterification of the DNA is located in the C-terminal domain. DNA binding most likely involves the helicase-like and the topoisomerase domains,[9,10] and an intimate communication between the two domains is required for positive supercoiling.[11]

There are diverse results on the nucleotide requirement for supercoiling by reverse gyrases. The *S. acidocaldarius* reverse gyrase strictly requires ATP for positive supercoiling, while in the presence of GTP, CTP, or UTP, negatively supercoiled DNA is relaxed.[12] In contrast, positive supercoiling by *A. fulgidus* reverse gyrase is powered by all four NTPs, but the optimum nucleotide concentration is tenfold lower for ATP than for GTP, CTP, or UTP.[13] In the presence of the non-hydrolyzable nucleotide analog 5′-adenylyl-β,γ-imidodiphosphate (ADPNP), the introduction of negative supercoils,[13,14] or the relaxation of negative supercoils[13] have been observed. In the presence of ADP, mostly relaxed supercoiled DNA is generated, but the formation of slightly positively supercoiled DNA has also been reported.[14] These controversial findings clearly indicate that more biochemical information is necessary to arrive at a detailed understanding of the nucleotide requirements for reverse gyrases.

Our current knowledge on reverse gyrase activity is predominantly derived from studies of the archaeal enzymes from *S. acidocaldarius*.[1,8,11,12,15] or *A. fulgidus*.[6,7,9,13,14,16] To identify general and individual properties of reverse gyrases, we characterized the reverse gyrase from the hyperthermophilic eubacterium *T. maritima* with respect to nucleotide binding and hydrolysis, and DNA supercoiling using the adenine nucleotides ADP, ATP, and the non-hydrolyzable ATP analogs adenosine-5′-O-(3-thio)triphosphate (ATPγS) and ADPNP. We find that ATPγS is efficiently hydrolyzed by reverse gyrase. Surprisingly, the hydrolysis rate is increased 15-fold in the presence of DNA, and ATPγS promotes positive supercoiling by reverse gyrase with a similar efficiency to ATP. Thus, the energy of ATPγS hydrolysis is converted into conformational changes that drive the catalytic cycle. While several other enzymes are known to accept this "non-hydrolyzable" analog as a substrate, this is the first case of ATPγS acting as a truly functional ATP analog in the complex reaction of DNA supercoiling.

Results

Purification of recombinant reverse gyrase

T. maritima reverse gyrase was produced recombinantly in *Escherichia coli*. Incubation of the crude extract at 65 °C for 10 min led to a precipitation of reverse gyrase, and the enzyme was therefore purified from the crude extract after a four-column protocol (Figure 1(a)). Reverse gyrase eluted as a monomer from a calibrated size-exclusion column. From 4 l of cell culture, 3 mg of >95% pure reverse gyrase were obtained. To exclude possible contaminations with endogenous *E. coli* topoisomerases, purified reverse gyrase was incubated with negatively supercoiled plasmid DNA in the absence and presence of ATP at 37 °C. After 45 min, no relaxation was observed (data not shown), confirming that the recombinant protein is highly pure.

The reverse gyrase absorption spectrum (Figure 1(b)) exhibits a distinct maximum at 280 nm, and the A_{280}/A_{260} ratio of 1.95 shows that the purified reverse gyrase is nucleotide and nucleic acid-free, which is a pre-requisite to study binding and

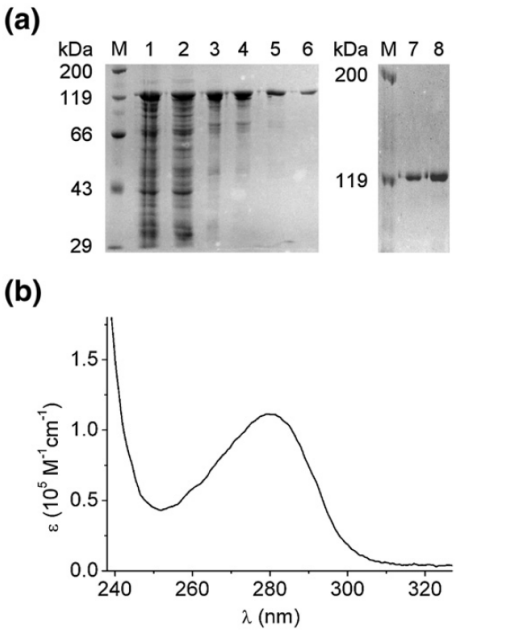

Figure 1. Purification of reverse gyrase. (a) SDS-PAGE of reverse gyrase purification steps (left panel, 10% acrylamide; right panel, 5% acrylamide). M, protein marker; lane 1, crude extract; lane 2, after polyethyleneimine treatment; lane 3, after phenyl Sepharose column; lane 4, after SP Sepharose; lane 5, after blue Sepharose; lane 6, after size-exclusion chromatography; lane 7, purified wild-type; lane 8, purified K106Q mutant. Purified reverse gyrases contain no contaminants in the 80–200 kDa range. (b) Absorption spectrum of purified reverse gyrase in 50 mM Tris-HCl (pH 7.5), 1 M NaCl, 10 mM $MgCl_2$, 100 μM $Zn(OAc)_2$, 2 mM BME. The absorbance maximum at 280 nm and the A_{280}/A_{260} ratio of 1.95 indicate that the protein is free of nucleotides or nucleic acids.

hydrolysis of different nucleotides, and their effect on reverse gyrase supercoiling activity.

Nucleotide binding

No quantitative data on nucleotide binding to reverse gyrases is found in the literature. We therefore first determined the dissociation constants for the reverse gyrase adenine nucleotide complexes in equilibrium fluorescence titrations at 37 °C (Figure 2). The fluorescence of the ADP analog mantADP increases 1.4-fold upon binding to *T. maritima* reverse gyrase. From the titration, a K_d value of 1.0(±0.1) μM for the mantADP/reverse gyrase complex was determined (Figure 2(a)). MantADP was completely displaced by ADP, which confirms that mantADP binds specifically and reversibly to the nucleotide binding site of reverse gyrase. The K_d value of the ADP complex was determined in a competitive titration of the reverse gyrase/mantADP complex with ADP (Figure 2(b)). With 1.6(±0.2) μM, it is very similar to the value for the mantADP complex. Hence, mantADP is a suitable analog for nucleotide binding studies with reverse gyrase. As the K_d value for the ATP/reverse gyrase complex could not be determined because of hydrolysis (see below), we titrated the mantADP/reverse gyrase complex with the non-hydrolyzable ATP analogs ATPγS and ADPNP to obtain estimates for the ATP complex. None of these nucleotides is hydrolyzed by reverse gyrase at 37 °C (see below). The corresponding K_d values are 14.3(±1.5) μM (ATPγS), and 43.2(±2.0) μM (ADPNP), respectively (Figure 2(b), Table 1). Reverse gyrase binds ADP ~20-fold more tightly than the ATP analogs, indicating that the binding energy from interactions with the γ-phosphate is converted into conformational changes.

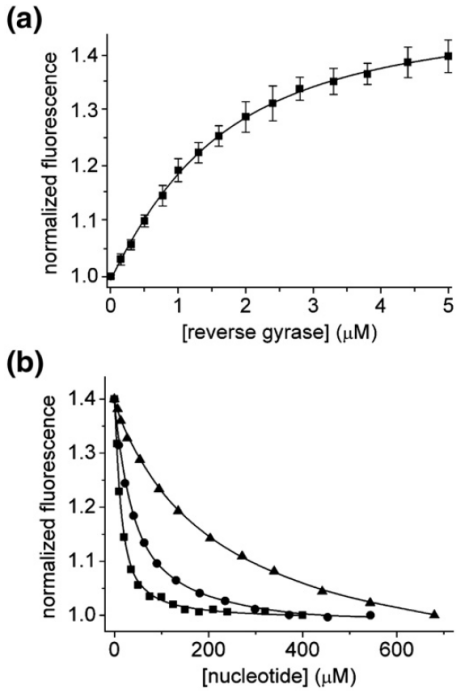

Figure 2. Nucleotide binding to reverse gyrase. Titrations were performed in 50 mM Tris-HCl (pH 7.5), 0.15 M NaCl, 10 mM $MgCl_2$, 100 μM $Zn(OAc)_2$, 2 mM BME. (a) Fluorescence equilibrium titration of 1 μM mantADP with reverse gyrase. The K_d value for the mantADP/reverse gyrase complex is 1.0(±0.1) μM. (b) Competitive titrations with ADP (squares), ATPγS (circles), and ADPNP (triangles). The K_d values are 1.6(±0.2) μM (ADP), 14.3(±1.5) μM (ATPγS), and 43.2(±2.0) μM (ADPNP).

Table 1. Nucleotide binding to reverse gyrase

	K_d (μM)	
Nucleotide	Wild-type	K106Q
ATP	n.d.	239(±33)
ADP	1.6(±0.2)	118(±11)
ATPγS	14.3(±1.5)	178(±60)
ADPNP	43.2(±2.0)	360(±49)

Relaxation of negatively supercoiled plasmid and positive supercoiling

As a critical test for functional integrity, we next examined supercoiling by recombinant *T. maritima* reverse gyrase. At the physiological temperature of 75 °C, negatively supercoiled pUC18 plasmid was incubated with reverse gyrase in the absence of nucleotide, and in the presence of ATP, ADP, ADPNP, or ATPγS. First, we tested the recombinant enzyme for ATP-dependent positive supercoiling of DNA (Figure 3), which is the hallmark reaction of reverse gyrases. In the presence of ATP, one-dimensional gel electrophoresis shows a rapid relaxation of negatively supercoiled pUC18, followed by slower supercoiling (Figure 3(a)). Analysis of the changes in topoisomer distribution with time by two-dimensional gel electrophoresis corroborates that the plasmid DNA is relaxed first, leading to a distribution of negatively supercoiled species in the left branch. The appearance of topoisomers in the right branch at longer reaction times confirms subsequent positive supercoiling. The supercoiling reaction is already highly efficient in the presence of ATP concentrations as low as 2 μM (Figure 3(c)). Importantly, reverse gyrase promotes ATP-dependent positive supercoiling down to a protein:DNA ratio of 0.07 (Figure 3(b)), confirming that the enzyme undergoes multiple supercoiling cycles and acts as a true catalyst.

Variation of the reaction temperature from 4–85 °C revealed no positive supercoiling below 50 °C (data not shown), consistent with previous findings with other reverse gyrases.[17–19] The temperature optimum of *T. maritima* reverse gyrase is at 75 °C, which was therefore used as the standard temperature for all supercoiling reactions.

In the absence of nucleotide (Figure 4(a)), the topology of the negatively supercoiled plasmid is not altered by reverse gyrase. Even in the presence of a 330-fold molar excess of reverse gyrase over

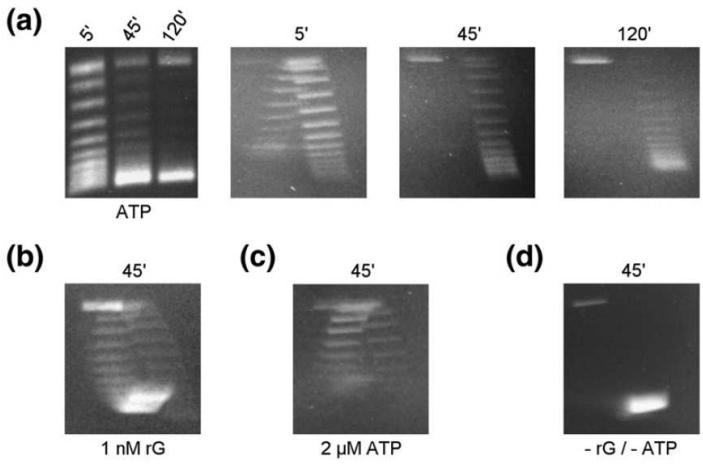

Figure 3. Positive supercoiling activity of reverse gyrase in the presence of ATP. Supercoiling reactions were performed with 1 μM reverse gyrase, 25 ng μl ^{1} pUC18, and 2 mM ((a) and (b)) or 2 μM (c) ATP in 50 mM Tris-HCl (pH 7.5), 0.15 M NaCl, 10 mM $MgCl_2$, 100 μM $Zn(OAc)_2$, 2 mM BME, 10% PEG 8000 at 75 °C. (a) ATP promotes positive supercoiling of DNA by reverse gyrase. The left panel shows a 1D gel of the supercoiling reaction stopped after 5, 45, and 120 min, the right panels show the corresponding 2D gels for selected time points. After a rapid redistribution of different topoisomers within 5 min, the right branch in the 2D gels, corresponding to positively supercoiled species, becomes populated. This shows that negatively supercoiled DNA is rapidly relaxed and then positively supercoiled by reverse gyrase in the presence of ATP. (b) Reverse gyrase (rG) is active in catalytic amounts (1 nM) at a protein:DNA ratio of 0.07. (c) ATP concentrations as low as 2 μM are sufficient to promote the introduction of positive supercoils by reverse gyrase. (d) In the absence of reverse gyrase and nucleotide, the plasmid is mostly negatively supercoiled after 45 min at 75 °C, with only a small nicked fraction.

DNA substrate and after extended incubation time (210 min) very few relaxed forms are detected, confirming that *T. maritima* reverse gyrase shows hardly any relaxation activity in the absence of nucleotides. This is in contrast to observations with other reverse gyrases for which relaxation has been observed in the absence of nucleotides.[13,14]

In the presence of ADP, reverse gyrase catalyzes a slow distribution to different topoisomers (Figure 4(b)). In two-dimensional gels, only the left branch corresponding to negatively supercoiled topoisomers is observed at 1 mM ADP, demonstrating that ADP only supports relaxation of negatively supercoiled plasmid, but not positive supercoiling. In addition, the relaxation reaction appears much slower than observed initially in the presence of ATP. Interestingly, at 2 mM ADP, limited positive supercoiling is observed. While formation of slightly positively supercoiled DNA in the presence of ADP has been reported,[14] reverse gyrase promotes positive supercoiling even at very low concentrations of ATP (see Figure 3(c)). Analysis of our ADP solution for traces of ATP by HPLC detected 0.1–0.3% ATP, which corresponds to 2–6 μM ATP in the supercoiling reaction with 2 mM ADP. This low ATP concentration is already sufficient to support positive supercoiling (Figure 3(c)), consistent with the trace amounts of ATP in our ADP solutions being responsible for the limited positive supercoiling observed. Taken together, our results demonstrate that ADP only allows for relaxation of negative supercoils, whereas the introduction of positive supercoils requires ATP.

To distinguish which reverse gyrase activities require only binding of nucleotide, and which activities depend on nucleotide hydrolysis, we investigated the ability of non-hydrolyzable ATP analogs to support supercoiling by reverse gyrase. In the presence of ADPNP, the formation of less supercoiled species is observed (Figure 4(c)), demonstrating that ADPNP allows for slow relaxation of negatively supercoiled DNA by reverse gyrase to a similar extent as ADP. In contrast, in supercoiling reactions with ATPγS a rapid relaxation of negatively supercoiled DNA, followed by a re-population of supercoiled species was observed (Figure 4(d)), very similar to the reaction with ATP. Two-dimensional gels clearly show a population of topoisomers in the right branch, corresponding to positively supercoiled species. Analysis of ATPγS by reversed phase HPLC excluded a contamination by ATP and confirmed that the positive supercoiling observed is indeed caused by ATPγS. Surprisingly, ATPγS promotes positive DNA supercoiling to a similar degree as ATP at 75 °C, and only about two to threefold more slowly.

Nucleotide hydrolysis and effects of DNA on hydrolysis: coupling

Two possible explanations exist for the observation of positive DNA supercoiling in the presence of ATPγS, but only relaxation in the presence of ADPNP. ADPNP could mimic the ADP state of reverse gyrase, while ATPγS mimics the ATP state, and ATPγS binding is sufficient to promote supercoiling. Alternatively, ATPγS, but not ADPNP, could be hydrolyzed, and ATPγS hydrolysis drives positive supercoiling.

To establish a link between supercoiling and nucleotide hydrolysis by reverse gyrase, we first studied ATP and ATPγS hydrolysis under steady-state conditions using a coupled spectrophotometric assay at 37 °C (Figure 5(a)). Reverse gyrase ATPase activity shows a hyperbolic dependence on ATP concentration, consistent with Michaelis-Menten behavior. The $K_{M,ATP}$ value is 44(±6) μM, and the turnover number k_{cat} is 19.7(±0.8)×10^{-3} s^{-1}. With

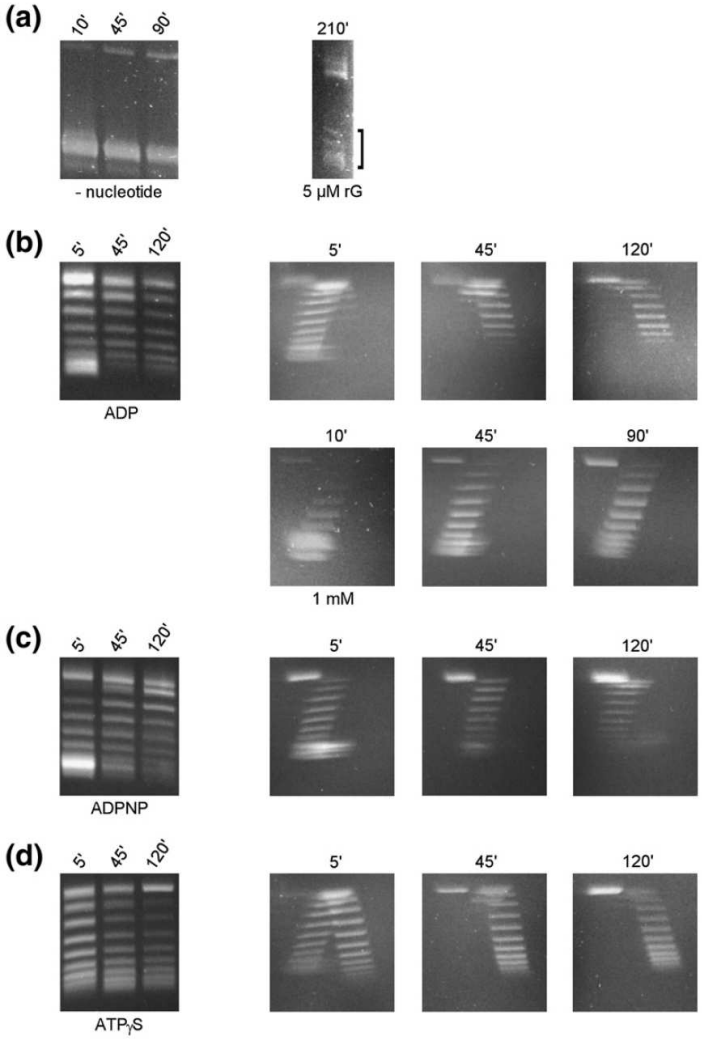

Figure 4. Supercoiling activities of reverse gyrase with different nucleotides. Supercoiling reactions were performed with 1 μM reverse gyrase, 25 ng μl^{-1} pUC18, and 2 mM of the respective nucleotide in 50 mM Tris-HCl (pH 7.5), 0.15 M NaCl, 10 mM $MgCl_2$, 100 μM Zn $(OAc)_2$, 2 mM BME, 10% PEG 8000 at 75 °C. The left panel shows a 1D gel of the supercoiling reaction stopped after 5, 45, and 120 min, the right panels show the corresponding 2D gels for selected time points. (a) In the absence of nucleotides, neither relaxation nor supercoiling are possible. Even with 5 μM reverse gyrase (rG), corresponding to a 330-fold molar excess, and an extended incubation time (210 min), hardly any relaxation is visible (bracket). (b) ADP allows for relaxation of negatively supercoiled DNA. The upper panels show the supercoiling reaction in the presence of 2 mM ADP. Positively supercoiled species are formed after 45 min to a limited extent. The lower panels show the same reaction in the presence of 1 mM ADP only. Here, only relaxation of negatively supercoiled DNA, but no introduction of positive supercoils is observed. Together with the finding that 2 μM ATP are sufficient for positive supercoiling by reverse gyrase (cp. Figure 3(c)), we conclude that positively supercoiled DNA in the upper panels is a result of a 0.1% ATP contamination in the ADP. (c) ADPNP allows for relaxation of negatively supercoiled DNA. No formation of positively supercoiled species is observed. (d) ATPγS promotes positive supercoiling by reverse gyrase. After 5 min, negatively and positively supercoiled species are present in similar amounts. The final extent of positive supercoiling is somewhat smaller than in the reaction with ATP (cp. Figure 3(a)).

ATPγS, no hydrolysis is observed at 37 °C (data not shown).

The reaction velocities in the steady-state assay correspond to the rate-limiting step in the overall ATPase reaction and need not reflect the chemical step of ATP hydrolysis. We therefore examined the ATP hydrolysis by reverse gyrase under single turnover conditions (Figure 6). The single turnover rate constant k_{hyd} for ATP hydrolysis at 37 °C is $4.7(\pm0.7)\times10^{-3}$ s^{-1} (Figure 6(a)), which is similar to the steady-state assay ATPase rate. Together with the observation that nucleotide binding to reverse gyrase is rapid (data not shown), we can conclude that ATP hydrolysis or an associated conformational change is the rate-limiting step in the reverse gyrase nucleotide cycle at 37 °C. Neither ATPγS (Figure 6(b)) nor ADPNP (data not shown) are hydrolyzed by reverse gyrase at this temperature.

At 75 °C, ATP is hydrolyzed rapidly (within 30 s) by reverse gyrase, and the rate constant k_{hyd} can only be estimated to 0.05–0.15 s^{-1} (Figure 6(c)). This corresponds to a ten to 30-fold acceleration compared to 37 °C, which agrees well with the rule of thumb of a twofold increase in rate constants for a 10 deg.C increase in temperature (~2^4, ~16-fold). In contrast to 37 °C, ATPγS is hydrolyzed at 75 °C, although much more slowly than ATP (Figure 6(d)). ATPγS undergoes significant auto-cleavage at 75 °C, which was taken into account in the analysis of reverse gyrase-catalyzed ATPγS hydrolysis. With $3.8(\pm1.1)\times10^{-3}$ s^{-1}, the rate constant for ATPγS hydrolysis by reverse gyrase at 75 °C is 15–40-fold smaller than the rate constant for ATP hydrolysis at 75 °C, but comparable to the rate constant for ATP hydrolysis at 37 °C ($4.7(\pm0.7)\times10^{-3}$ s^{-1}).

To investigate the effect of DNA substrate on nucleotide hydrolysis by reverse gyrase, the steady-

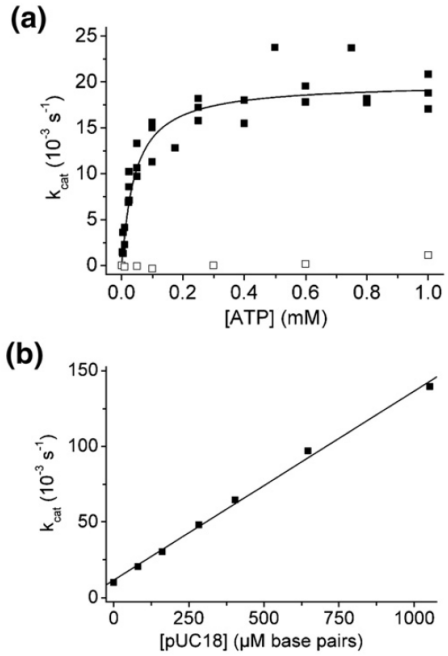

Figure 5. Steady-state ATP hydrolysis. Steady-state ATP hydrolysis assays were performed at 37 °C in 50 mM Tris-HCl (pH 7.5), 0.15 M NaCl, 10 mM $MgCl_2$, 100 μM $Zn(OAc)_2$, 2 mM BME, 0.4 mM phosphoenol pyruvate, 0.2 mM NADH with 1 μM reverse gyrase. Initial velocities v (in μM ATP s^{-1}) were calculated from the absorbance change $\Delta A_{340}/\Delta t$ and converted to k_{cat}. (a) ATP dependence. Reverse gyrase (filled squares) is a Michaelis-Menten enzyme with a $K_{M,ATP}$ of 44(±6) μM and a turnover number k_{cat} of 19.7(±0.8)×10^{-3} s^{-1}. The K106Q mutant (open squares) shows a ~20-fold reduced hydrolysis rate. (b) DNA dependence. As no saturation is observed, Michaelis-Menten parameters could not be determined. At the highest DNA concentration tested, the steady-state rate of wild-type reverse gyrase (140×10^{-3} s^{-1}) is increased sevenfold compared to the rate in the absence of DNA (19.7×10^{-3} s^{-1}).

state ATPase rate was measured in the presence of increasing pUC18 concentrations. At 37 °C, plasmid DNA stimulates the steady-state ATPase rate of reverse gyrase significantly (Figure 5(b)). However, no saturation was observed, and K_M and k_{cat} values could not be determined. The maximum acceleration, observed at 0.4 μM pUC18 (corresponding to 1.1 mM base-pairs), was sevenfold, with a measured rate constant of 140×10^{-3} s^{-1} in the presence, and 19.7×10^{-3} s^{-1} in the absence of DNA. We have identified ATP hydrolysis as the rate-limiting step in the reverse gyrase nucleotide cycle at 37 °C (see above), and steady-state assays generally reflect the rate-limiting step of the overall reaction that is monitored. The effect of DNA on the steady-state ATPase rate thus implies that DNA accelerates ATP hydrolysis. To corroborate this finding, we measured the ATP hydrolysis rate in a single turnover ATPase assay in the presence of DNA at 37 °C (Figure 5(a)). The rate constant $k_{hyd,DNA}$ is 12.9(±4.4)×10^{-3} s^{-1}, corresponding to a ~threefold stimulation by DNA. Hence, DNA substrate stimulates ATP hydrolysis by reverse gyrase at 37 °C, a temperature far too low for positive supercoiling to occur. At 37 °C, ATPγS is not hydrolyzed by reverse gyrase in the absence of DNA (see above), and only extremely slowly in the presence of DNA, with a $k_{hyd,DNA}$ of ~0.1×10^{-3} s^{-1} (Figure 6(b)).

Our results predict a significant stimulation of ATP hydrolysis by DNA substrate at 75 °C, the optimal temperature for efficient positive supercoiling by reverse gyrase. However, ATP hydrolysis is already rapid in the absence of DNA, and in the presence of DNA it becomes too fast to be resolved in hand-mixing experiments. To arrive at an estimate for the stimulation, the reaction at 75 °C in the presence of DNA was stopped after 5 and 10 s, and analyzed for ATP and ADP contents. ATP hydrolysis is indeed much faster in the presence of DNA (Figure 6(c)), and from a comparison of the initial slopes, a ~threefold stimulation can be estimated, putting $k_{hyd,DNA}$ into the range of 0.15–0.45 s^{-1}.

ATPγS is hydrolyzed much more slowly than ATP at 75 °C (15–40-fold), which allowed examination of the effect of DNA on ATPγS hydrolysis at the physiological temperature of reverse gyrase. Notably, reverse gyrase hydrolyzes ATPγS even more efficiently in the presence of DNA, with a rate constant $k_{hyd,DNA}$ of 58.2(±7.7)×10^{-3} s^{-1} (Figure 6(e)). This corresponds to a 15-fold stimulation of ATPγS hydrolysis by DNA at 75 °C, and puts the rate constant close to the one for ATP hydrolysis. In control reactions containing ATPγS and DNA only, cleavage was identical to the background detected with ATPγS only, confirming that the rapid hydrolysis in the presence of DNA is indeed catalyzed by reverse gyrase, and not due to a contamination of the DNA preparation.

Nucleotide hydrolysis and positive supercoiling: a hydrolysis-deficient mutant

To confirm the strict requirement of nucleotide hydrolysis for positive supercoiling by reverse gyrase, we prepared the mutant K106Q, where the catalytic lysine in the GKT motif of the helicase-like domain has been replaced by a glutamine. Such an approach has been used successfully to generate ATPase-deficient variants of P-loop proteins such as adenylate kinase,[20] or DEAD box helicases.[21] In structures of P-loop proteins, this lysine contacts the β and γ-phosphates of the bound nucleotide and most likely stabilizes the developing negative charge upon hydrolysis.[22]

Reverse gyrase K106Q was obtained with similar purity as the wild-type enzyme (Figure 1(a)). Under steady-state conditions at 37 °C, this mutant shows a ~20-fold reduced ATPase activity compared to wild-type, with a k_{cat} of ca. 1×10^{-3} s^{-1} (Figure 5(a)). Binding of adenine nucleotides to the K106Q mutant is reduced by a factor of 10–70. The K_d values of the K106Q/nucleotide complexes determined in

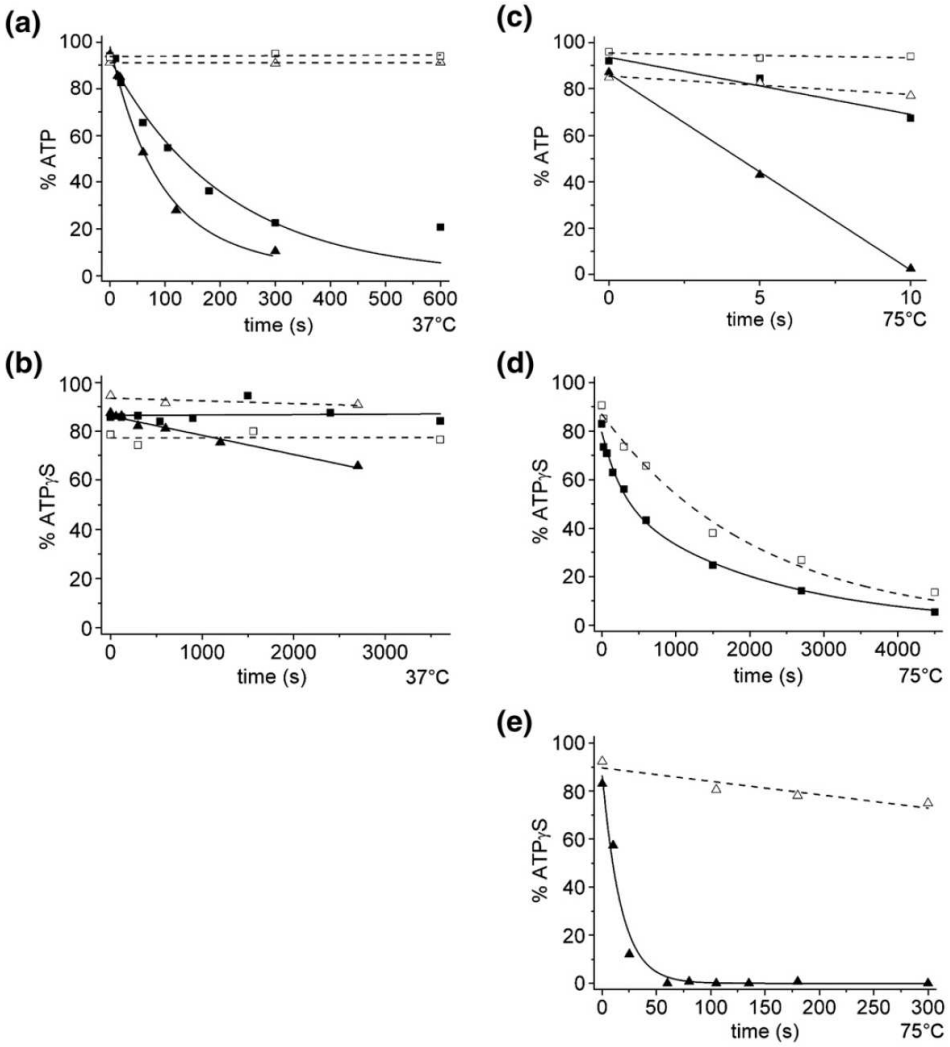

Figure 6. Single turnover nucleotide hydrolysis. All experiments were performed with 20 μM reverse gyrase and 6 μM nucleotide in 50 mM Tris-HCl (pH 7.5), 0.15 M NaCl, 10 mM $MgCl_2$, 100 μM $Zn(OAc)_2$, 2 mM BME. The fraction of ATP or ATPγS is plotted for reactions containing nucleotide only (open squares), nucleotide and DNA (open triangles), nucleotide and reverse gyrase (filled squares), and nucleotide, reverse gyrase, and DNA (filled triangles). Broken lines indicate control reactions without reverse gyrase. (a) ATP hydrolysis at 37 °C. In the absence of DNA, ATP is hydrolyzed by reverse gyrase with a rate constant k_{hyd} of $4.7(\pm0.7)\times10^{-3}$ s^{-1}. In the presence of DNA, hydrolysis is accelerated threefold, and k_{hyd} is $12.9(\pm4.4)\times10^{-3}$ s^{-1}. If no reverse gyrase is present, ATP is stable over the time-course of the experiment. (b) ATPγS hydrolysis at 37 °C. In the absence of DNA, ATPγS is not hydrolyzed by reverse gyrase, whereas in the presence of DNA, slow hydrolysis with a rate constant k_{hyd} of $\sim0.1\times10^{-3}$ s^{-1} is observed. In the absence of reverse gyrase, ATPγS is not hydrolyzed over the time-course of the experiment. (c) ATP hydrolysis at 75 °C. ATP is hydrolyzed rapidly already in the absence of DNA with a rate constant of 0.05–0.15 s^{-1}. In the presence of DNA, ATP hydrolysis is accelerated threefold, with a k_{hyd} estimated to 0.15–0.45 s^{-1}. ATP is not hydrolyzed significantly in the absence of reverse gyrase. (d) ATPγS hydrolysis at 75 °C in the absence of DNA. ATPγS is hydrolyzed spontaneously during the time-course of the experiment. The rate constant k_{spont} is $\sim4.8(\pm0.4)\times10^{-4}$ s^{-1}. In the presence of reverse gyrase, hydrolysis is faster. Taking into account the spontaneous hydrolysis, the rate constant k_{hyd} for reverse gyrase-catalyzed ATPγS hydrolysis is $3.8(\pm1.1)\times10^{-3}$ s^{-1}. (e) ATPγS hydrolysis at 75 °C in the presence of DNA. The rate constant k_{hyd} for ATPγS hydrolysis is $58.2(\pm7.7)\times10^{-3}$ s^{-1}, corresponding to a 15-fold acceleration of ATPγS hydrolysis by DNA.

fluorescence equilibrium titrations are 239(±33) μM (ATP), 118(±11) μM (ADP), 178(±60) μM (ATPγS), and 360(±49) μM (ADPNP). A summary of all K_d values for wild-type reverse gyrase and the K106Q mutant can be found in Table 1. The K106Q mutant shows a reduced affinity for all adenine nucleotides. Substitution of lysine 106 by a glutamine eliminates a positive charge that interacts with the β and γ-phosphate, and the weaker interaction with nucleotides is therefore expected. Despite the lower affinities, the K106Q mutant is saturated with nucleotides under standard conditions of 1 μM

enzyme and 2 mM nucleotide in the supercoiling assays.

Next we investigated supercoiling by the K106Q mutant at 75 °C in the absence of nucleotide, and in the presence of ATP, ATPγS, ADP, and ADPNP (Figure 7(a)). In the presence of ATP, limited positive supercoiling by K106Q is observed, albeit much more slowly than with the wild-type reverse gyrase. After 45 min, only a few positively supercoiled species are populated in the presence of the K106Q mutant, while with wild-type reverse gyrase the reaction has already proceeded towards positively supercoiled species after 5 min (see Figure 3(a)). Hence, positive supercoiling by K106Q is at least tenfold slower compared to wild-type reverse gyrase. Notably, positive supercoiling by reverse gyrase K106Q requires stoichiometric amounts of enzyme. Below a protein:DNA ratio of 7, no positive supercoiling was observed (data not shown). Thus, in contrast to the wild-type reverse gyrase, K106Q does not act catalytically. After 45 min incubation of negatively supercoiled plasmid with K106Q in the presence of ATPγS, less negatively supercoiled species than the starting plasmid are detected, but no positively supercoiled species (yet), indicating that ATPγS may still promote positive supercoiling, but at a significantly reduced velocity.

Due to the reduced nucleotide affinity of the K106Q mutant, it is not possible to investigate nucleotide hydrolysis under single turnover conditions. Therefore, we monitored ATP and ATPγS hydrolysis of wild-type reverse gyrase and the K106Q mutant under identical conditions of the supercoiling assay (Figure 7(b)), where the enzyme is saturated with nucleotides. The K106Q mutant still hydrolyzes ATP under these conditions, but the reaction is about tenfold slower than hydrolysis by the wild-type enzyme. Similarly, ATPγS is hydrolyzed much more slowly by K106Q than by the wild-type reverse gyrase. These findings are consistent with the ~tenfold decelerated positive supercoiling by the K106Q mutant and corroborate the conclusions that ATP(γS) hydrolysis is required for positive supercoiling by reverse gyrase, and that K106 plays a major role in reverse gyrase-catalyzed ATP(γS) hydrolysis.

While ADP and ADPNP allow for DNA relaxation by wild-type reverse gyrase, the K106Q mutant does not relax negatively supercoiled plasmid in the presence of these nucleotides. Instead, in two-dimensional gels, the plasmid is found almost completely in the position where nicked DNA is expected. This indicates that DNA cleavage still occurs in the K106Q mutant, but re-ligation is less

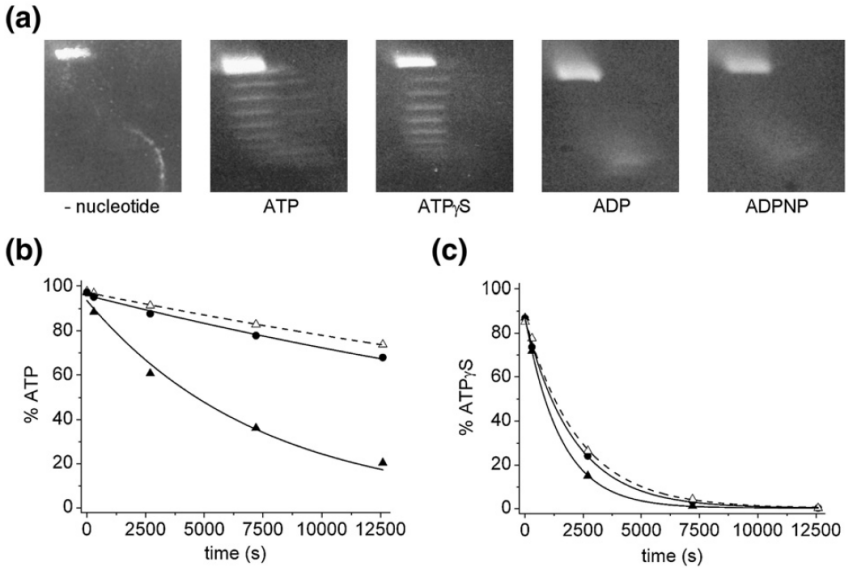

Figure 7. Supercoiling and nucleotide hydrolysis by reverse gyrase and the K106Q mutant. (a) Supercoiling activities of reverse gyrase K106Q with different nucleotides. Supercoiling reactions were performed with 1 μM reverse gyrase K106Q, 25 ng μl ^{1} pUC18, and 2 mM of the respective nucleotide in 50 mM Tris-HCl (pH 7.5), 0.15 M NaCl, 10 mM $MgCl_2$, 100 μM $Zn(OAc)_2$, 2 mM BME, 10% PEG 8000 at 75 °C for 45 min. In the presence of ATP, positive supercoiling is observed, but about tenfold more slowly than with the wild-type enzyme. With ATPγS, only relaxed species are seen, consistent with a much slower positive supercoiling reaction. In the presence of ADP, or ADPNP, or in the absence of nucleotide, the main product is nicked DNA. (b) ATP is hydrolyzed about ten times more slowly by reverse gyrase K106Q compared to the wild-type enzyme. At different time-points of the supercoiling reaction, samples were analyzed for their ATP or ATPγS contents by reversed phase HPLC. Open triangles, control in the absence of reverse gyrase; filled triangles, wild-type reverse gyrase; filled circles, K106Q. (c) Reverse gyrase K106Q hydrolyzes ATPγS more slowly than the wild-type enzyme. At different time-points of the supercoiling reaction, samples were analyzed for their ATP or ATPγS contents by reversed phase HPLC. Open triangles, control in the absence of reverse gyrase; filled triangles, wild-type reverse gyrase; filled circles, K106Q.

efficient than with wild-type reverse gyrase. Moreover, it points towards a lack of coupling between the nucleotide state and the cleavage-ligation activity. In fact, even in the absence of nucleotide, the majority of the plasmid is nicked by the K106Q mutant.

Altogether, we found that *T. maritima* reverse gyrase is a DNA-stimulated ATPase at 37 °C and at 75 °C. At 75 °C, both ATP and ATPγS are readily hydrolyzed by reverse gyrase, and their hydrolysis is accelerated in the presence of DNA. Both nucleotides efficiently promote positive DNA supercoiling. While hydrolysis of the non-hydrolyzable ATP analog ATPγS has been described for a number of enzymes, the efficient conversion of the energy from its hydrolysis into a complex, multi-step enzymatic reaction such as DNA supercoiling is novel.

Discussion

All reverse gyrases characterized to date lack supercoiling activity at low temperatures, with an onset of activity at 35 °C[17] or 50 °C.[18,19] In addition, no ATPase stimulation by DNA has been reported at low temperatures.[19] In this context, our finding that *T. maritima* reverse gyrase is a DNA-stimulated ATPase at 37 °C is quite unexpected. The stimulation of ATP hydrolysis by DNA clearly demonstrates that the hyperthermophilic reverse gyrase is not a "frozen enzyme" at mesophilic temperatures, as at least some of the necessary conformational changes that allow for the communication between different domains in reverse gyrase can take place at 37 °C.

T. maritima reverse gyrase binds ADP with a K_d of 1.6(±0.2) μM at 37 °C. The non-hydrolyzable ATP analogs ATPγS and ADPNP are bound less tightly (K_d 14.3(±1.5) μM, and 43.2(±2.0) μM, respectively). A stronger interaction with ATPγS than with ADPNP has been found in various nucleotide binding proteins, and may reflect the different pK_a values, the higher hydrophobicity of the sulfur, or unidentified structural features of these analogs.[23] While the K_d value for the ATP complex could not be determined in titrations due to significant hydrolysis at 37 °C, a useful measure for ATP affinity is provided by the $K_{M,ATP}$ value of 44 μM from the steady-state ATPase assays. As ATP hydrolysis (or an associated conformational change) is the rate-limiting step, $K_{M,ATP}$ should equal K_d. Hence, ATP binding by reverse gyrase is much weaker than ADP binding, indicating that the additional binding energy from interactions with the γ-phosphate is converted into a conformational change. Moderate affinities for ATP are very common for ATPases and are readily compensated *in vivo* by high cellular concentrations of ATP that provide saturating conditions. Notably, our results imply that ATP binding is significantly strengthened in the presence of DNA: Efficient positive supercoiling occurs with 1 μM reverse gyrase and ATP concentrations as low as 2 μM at 75 °C, demonstrating that ATP is bound to a significant extent under these conditions. Consequently, the K_d value for ATP dissociation from the reverse gyrase/DNA complex must be in the low micromolar range, corresponding to a ~40-fold increase in ATP affinity compared to 37 °C in the absence of DNA. Energy conservation in the thermodynamic cycle describing the formation of the ternary reverse gyrase/DNA/ATP complex in turn predicts an equal stimulatory effect of ATP binding on the DNA affinity of reverse gyrase. As a result, the ATPase reaction and substrate binding (and supercoiling) are tightly coupled.

Relaxation of negative supercoils by reverse gyrase is efficient in the presence of ADP or ADPNP, suggesting that relaxation only requires nucleotide binding (or an associated conformational change), but not hydrolysis. A mutation of K106 in the GKT motif to a glutamine abolishes the relaxation activity in the presence of ADP or ADPNP, even though these nucleotides are still bound. Consequently, ADP or ADPNP binding to reverse gyrase is necessary, but not sufficient for DNA relaxation, suggesting that an associated conformational change has to occur. Interestingly, the main product of reverse gyrase K106Q activity is nicked DNA, both in the absence of nucleotide and in the presence of ADP and ADPNP. Hence, DNA cleavage still occurs in the K106Q mutant, albeit with a different cleavage-ligation equilibrium compared to wild-type reverse gyrase. These observations point towards a critical role of the GKT motif as a nucleotide sensor, and in transmitting this information to the location of strand passage.

In contrast to the relaxation reaction, the introduction of positive supercoils by reverse gyrase strictly depends on ATP hydrolysis. This is corroborated by the behavior of the K106Q mutant, which is impaired in ATP hydrolysis and, at the same time, much less efficient in ATP-driven positive supercoiling than wild-type reverse gyrase. The concomitant effects on ATP hydrolysis and supercoiling again confirm that hydrolysis and positive supercoiling by reverse gyrase are tightly linked.

Interestingly, at 75 °C, positive supercoiling by reverse gyrase is also efficiently promoted by ATPγS. Limited positive supercoiling in the presence of ATPγS has been reported for the *S. acidocaldarius* enzyme,[24] and the reduced efficiency compared to ATP-mediated supercoiling was interpreted as a requirement for ATP hydrolysis for the efficient introduction of positive supercoils.[24] We found that ATPγS not only binds to the nucleotide binding site, but is also efficiently hydrolyzed by *T. maritima* reverse gyrase. As with ATP, ATPγS hydrolysis is significantly stimulated in the presence of DNA. The DNA-stimulated hydrolysis rates are similar for ATP and ATPγS, demonstrating that ATPγS binding and hydrolysis must elicit the same conformational changes in reverse gyrase as ATP, and that the intra-molecular communication between different reverse gyrase domains during positive supercoiling is identical with both nucleotides.

ATPγS has been used as a non-hydrolyzable ATP analog in numerous studies with ATP binding

proteins. It is a poor substrate for phosphatases and most ATPases, which hydrolyze ATPγS three orders of magnitude more slowly than ATP.[25] In contrast, ATPγS is a very good substrate for kinases, in particular protein kinases.[23] Binding and hydrolysis of adenine nucleotides by reverse gyrase is mediated by the N-terminal helicase-like domain, which is related to the helicase superfamily (SF) 2.[26] Interestingly, the eukaryotic translation initiation factor eIF4A, also a member of the helicase SF 2, binds and hydrolyzes ATPγS.[27] The K_M values for ATP and ATPγS are similar, and the k_{cat} values are virtually identical. Most importantly, ATPγS hydrolysis promotes RNA unwinding by eIF4A,[27] demonstrating that all functionally required conformational changes for eIF4A-mediated RNA unwinding can be driven efficiently by both ATP and ATPγS hydrolysis.

Our finding of efficient positive supercoiling by reverse gyrase in the presence of ATPγS provides further support that an ATPγS-mediated conformational cycle can drive a complex molecular machine. As the helicase-like part of reverse gyrase is homologous to SF 2 helicases, it is tempting to speculate that it functions in a similar manner. Helicase structures in the absence of nucleotides and RNA show the two helicase subdomains separated by a cleft, and interactions between them are largely absent.[28–32] The recently determined crystal structures of two SF 2 helicases in complex with single-stranded RNA and ADPNP, the human eIF4A in the exon junction complex,[33] and the *Drosophila* Vasa protein,[34] provide the first detailed picture of the closed helicase conformation. Here, the cleft between the two helicase subdomains is closed, and interactions between residues from both subdomains around the nucleotide and the RNA establish an extensive interface.

Based solely on the crystal structure of the *A. fulgidus* reverse gyrase, a model for conformational changes during positive supercoiling has been put forward by Rodriguez and Stock.[9] Our results on ATP and ATPγS-promoted positive DNA supercoiling by reverse gyrase, in the context of the structural information on SF 2 helicases, provide experimental support for this model and define the requirements for the initial conformational change (Figure 8). As a first step, ATP or ATPγS binds to the cleft in the helicase-like domain, and DNA binds to the helicase-like domain in a similar mode as RNA binds to eIF4A

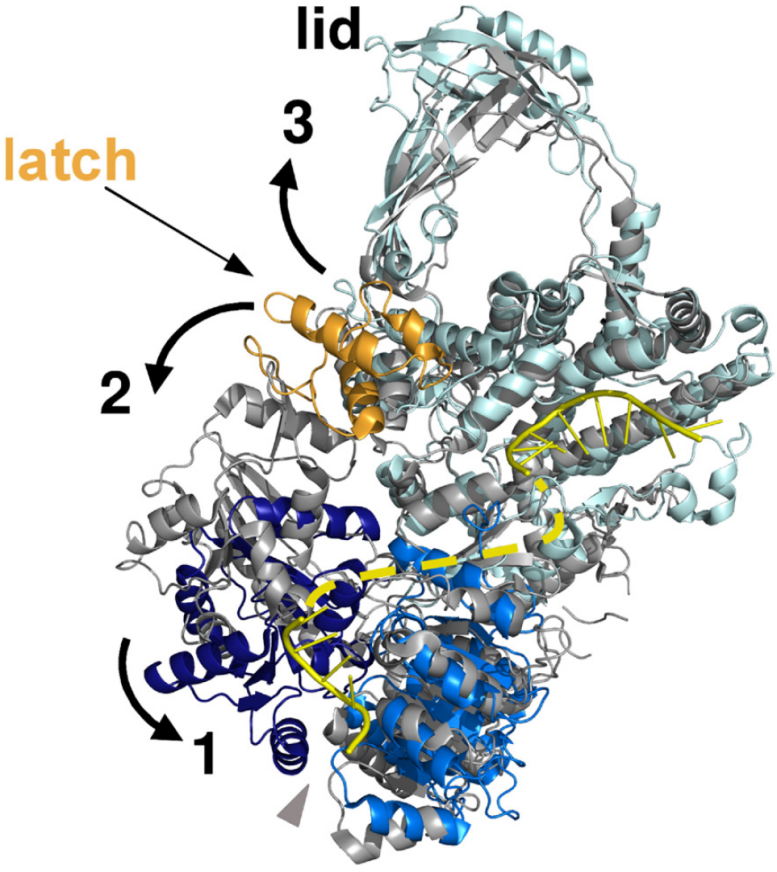

Figure 8. Model for reverse gyrase conformational changes for positive supercoiling. The structure of reverse gyrase from *A. fulgidus* (1GL9,[9] gray) is superimposed with the structures of *E. coli* DNA topoisomerase III in complex with DNA (1I7D,[37] cyan, DNA in yellow) and human eIF4A (2HYI,[33] blue, RNA in yellow). The N-terminal helicase subdomain of eIF4A (light blue) is superposed with the corresponding subdomain of reverse gyrase. The broken yellow line depicts a hypothetical connection between DNA regions bound to the two DNA binding sites. When DNA occupies the binding site in the helicase domain of reverse gyrase, ATP(γS) binding to the cleft between the two helicase subdomains (gray arrow) induces a rotation of the second (dark blue in eIF4A) helicase subdomain by ~32° (arrow 1). This cooperatively induced closure of the cleft between subdomains stabilizes the catalytically competent conformation of the ATPase site. As a consequence of this movement, the latch region (orange) is pulled away from the topoisomerase domain (arrow 2), and the upper part of the topoisomerase domain, the so-called lid region, can swing up (arrow 3) and allow for DNA strand passage. ATP(γS) hydrolysis presumably resets reverse gyrase to the starting conformation, with the lid region fixed by the closed latch, and a cleft between the helicase subdomains. Multiple rounds of these ATP(γS)-driven conformational changes will lead to positive supercoiling of the DNA substrate.

and Vasa. ATP(γS) and DNA binding to the helicase-like domain cooperatively induce a closure of the cleft between its subdomains, thereby stabilizing the catalytically competent conformation of the ATPase site. As a consequence of the movement of the C-terminal helicase-like subdomain, the adjacent so-called latch region[16] is pulled away from the topoisomerase domain, and releases its upper part, the lid (Rodriguez & Stock,[9] Figure 8). Lid opening then allows for DNA strand passage and positive supercoiling. ATP(γS) hydrolysis is required to reset the helicase-like domain to the open conformation, closing the lid, and re-positioning the latch.

The mode of DNA binding to reverse gyrase is unknown. The enzyme has three potential DNA binding sites, one in the helicase-like domain and one close to the conserved catalytic tyrosine for DNA transesterification (Figure 8), as well as two putative zinc fingers. While the specific role of these DNA binding sites in the supercoiling reaction remains elusive, simultaneous interaction of substrate DNA with more than one binding site could provide a crucial link between the helicase-like and the topoisomerase part of reverse gyrase and contribute to inter-domain communication in positive DNA supercoiling.

Supercoiling by reverse gyrase does not occur at 37 °C, most likely because the conformational change within the helicase-like domain is not or only partially transmitted to the topoisomerase domain due to the large activation energy for this coupling process. At 75 °C, the conformational changes induced by ligand binding to the helicase-like domain are transmitted to the topoisomerase domain, and positive supercoiling becomes possible. The similar efficiencies of positive supercoiling with ATP and ATPγS, and the concomitant effects of the K106Q mutation on ATP(γS) hydrolysis and positive supercoiling, underline the notion that nucleotide hydrolysis (or an associated conformational change) is the timer for positive DNA supercoiling by reverse gyrase.

Material and Methods

Cloning, site-directed mutagenesis, protein production and purification

The DNA region coding for the reverse gyrase from *T. maritima* was amplified from genomic DNA. The PCR fragment was ligated into the NcoI/XhoI site of the pET28a vector (Novagen). The reverse gyrase K106Q mutant was constructed *via* site-directed mutagenesis (Quickchange, Stratagene), and the correct sequence was confirmed.

The proteins were produced at 37 °C in *E. coli* BL21 Star (DE3) (Invitrogen) harboring the RIL plasmid (Stratagene), a strain that we specifically constructed for optimal reverse gyrase production. Protein production was induced by adding 50 μM IPTG at an A_{600nm} of 0.5, and cells were harvested after 4 h. All purification steps were performed at room temperature. Cells were disrupted in a Microfluidizer in 50 mM Tris-HCl (pH 7.5), 1 M NaCl, 10 mM $MgCl_2$, 100 μM $Zn(OAc)_2$, 2 mM β-mercaptoethanol (BME), and the crude extract was cleared by centrifugation. After treatment with polyethyleneimine, reverse gyrase was purified on a phenyl Sepharose column equilibrated in 50 mM Tris-HCl (pH 7.5), 1 M NaCl, 0.8 M ammonium sulphate, 10 mM $MgCl_2$, 100 μM $Zn(OAc)_2$, 2 mM BME. It was collected in the flow-through, which was dialyzed against 50 mM Tris-HCl (pH 7.5), 0.1 M NaCl, 4 M urea, 10 mM $MgCl_2$, 100 μM $Zn(OAc)_2$, 2 mM BME, and applied to a SP Sepharose column equilibrated in the same buffer. Reverse gyrase was eluted in a gradient to 1 M NaCl in this buffer, dialyzed against 50 mM Tris-HCl (pH 7.5), 0.1 M NaCl, 4 M urea, 10 mM $MgCl_2$, 100 μM $Zn(OAc)_2$, 2 mM BME, and applied to a blue Sepharose column equilibrated in this buffer. Reverse gyrase eluted from the blue Sepharose at 0.7 M NaCl. Final purification was achieved *via* size-exclusion chromatography on a calibrated S200 column in 50 mM Tris-HCl (pH 7.5), 1 M NaCl, 10 mM $MgCl_2$, 100 μM $Zn(OAc)_2$, 2 mM BME. The pure reverse gyrase was concentrated, shock-frozen in liquid nitrogen, and stored at −80 °C. Protein concentration was determined photometrically using the calculated extinction coefficient at 280 nm of 111,470 M^{-1} cm^{-1}.

Fluorescence equilibrium titrations

Dissociation constants of reverse gyrase/nucleotide complexes at 37 °C were determined in fluorescence equilibrium titrations in a Hitachi F-4500 fluorimeter using the fluorescent ADP analog mantADP.[35] Mant fluorescence was excited at 360 nm (5 nm bandwidth) and detected at 440 nm (10 nm bandwidth).

1 μM mantADP in 50 mM Tris-HCl (pH 7.5), 0.15 M NaCl, 10 mM $MgCl_2$, 100 μM $Zn(OAc)_2$, 2 mM BME was titrated with reverse gyrase until saturation was achieved. The K_d value was determined using the solution of the quadratic equation describing a 1:1 complex formation (equation (1)):

$$F = F_0 + \frac{\Delta F_{max}}{[L]_{tot}} \times \left(\frac{[E]_{tot} + [L]_{tot} + K_d}{2} - \sqrt{\left(\frac{[E]_{tot} + [L]_{tot} + K_d}{2} \right)^2 - [E]_{tot}[L]_{tot}} \right) \quad (1)$$

where F_0 is the fluorescence of free mantADP, ΔF_{max} is the amplitude, $[E]_{tot}$ is the total enzyme concentration, and $[L]_{tot}$ is the total ligand concentration.

The dissociation constants of reverse gyrase/adenine nucleotide complexes were determined in competitive titrations of the mantADP/reverse gyrase complex with ADP, ATPγS, ADPNP, and ATP. The solution of the cubic equation describing the competitive titration was evaluated numerically using the program Scientist (Micromath) to yield the K_d of the respective nucleotide complex.

All nucleotides were purchased from Jena Bioscience and checked for impurities by reversed phase HPLC on a C18 column in 0.1 M sodium phosphate (pH 6.5).

Supercoiling assays and analysis by one and two-dimensional gel electrophoresis

Nucleotide-dependent DNA relaxation and supercoiling by reverse gyrase was studied with negatively supercoiled pUC18 plasmid as a substrate. Assay conditions were 50 mM Tris-HCl (pH 7.5), 0.15 M NaCl, 10 mM

$MgCl_2$, 100 μM $Zn(OAc)_2$, 2 mM BME, 10% (w/v) PEG 8000 and 25 ng μl^{-1} pUC18.

Supercoiling reactions were started by adding 2 mM ATP, ADP, ATPγS, or ADPNP to 1 μM reverse gyrase at 75 °C, and samples taken at different time-points were analyzed on a 1.2% (w/v) agarose gel run at 11 V cm^{-1}. To separate positively and negatively supercoiled species, two-dimensional electrophoresis in 2% agarose gels was performed in the presence of 10 μg ml^{-1} chloroquine in the second dimension.

Steady-state ATPase activity

The steady-state ATPase activity of reverse gyrase was measured in a coupled ATPase assay.[36] ATP hydrolysis was monitored at 37 °C *via* the decrease in A_{340nm} due to oxidation of NADH to NAD^+. Assay conditions were 50 mM Tris-HCl (pH 7.5), 0.15 M NaCl, 10 mM $MgCl_2$, 100 μM $Zn(OAc)_2$, 2 mM BME, 0.4 mM phosphoenol pyruvate and 0.2 mM NADH, 23 μg ml^{-1} lactate dehydrogenase, 37 μg ml^{-1} pyruvate kinase. Concentrations of ATP and DNA were varied to obtain the respective K_M values. Initial velocities v (in μM ATP s^{-1}) were calculated from the absorbance change $\Delta A_{340nm}/\Delta t$ with $\varepsilon_{340,\ NADH} = 6220\ M^{-1}\ cm^{-1}$, and converted to k_{cat}. Data were analyzed according to the Michaelis-Menten equation.

Single turnover ATPase activity

20 μM reverse gyrase was mixed with 6 μM ATP, ADPNP, or ATPγS, in 50 mM Tris-HCl (pH 7.5), 0.15 M NaCl, 10 mM $MgCl_2$, 100 μM $Zn(OAc)_2$, 2 mM BME at 37 °C and 75 °C. If DNA was present, the concentration was 500 ng μl^{-1}. The reaction was quenched by adding 10 μl aliquots to 1 μl of 1 M $HClO_4$ at different time points, neutralized with 13.5 μl of 3 M KOAc, and the ATP/ADP ratio was determined by reversed phase HPLC on a C18 column in 0.1 M sodium phosphate (pH 6.5).

Acknowledgements

This work was supported by the VolkswagenStiftung and the Swiss National Science Foundation. We thank Wolfgang Liebl for kindly providing *T. maritima* genomic DNA, Ramona Heissmann and Andreas Schmidt for excellent technical assistance, and Markus Rudolph for discussions.

References

1. Kikuchi, A. & Asai, K. (1984). Reverse gyrase—a topoisomerase which introduces positive superhelical turns into DNA. *Nature*, **309**, 677–681.
2. Brochier-Armanet, C. & Forterre, P. (2006). Widespread distribution of archaeal reverse gyrase in thermophilic bacteria suggests a complex history of vertical inheritance and lateral gene transfers. *Archaea*, **2**, 83–93.
3. Omelchenko, M. V., Wolf, Y. I., Gaidamakova, E. K., Matrosova, V. Y., Vasilenko, A., Zhai, M. *et al.* (2005). Comparative genomics of *Thermus thermophilus* and *Deinococcus* radiodurans: divergent routes of adaptation to thermophily and radiation resistance. *BMC Evol. Biol.* **5**, 57.
4. Forterre, P. (2002). A hot story from comparative genomics: reverse gyrase is the only hyperthermophile-specific protein. *Trends Genet.* **18**, 236–237.
5. Atomi, H., Matsumi, R. & Imanaka, T. (2004). Reverse gyrase is not a prerequisite for hyperthermophilic life. *J. Bacteriol.* **186**, 4829–4833.
6. Kampmann, M. & Stock, D. (2004). Reverse gyrase has heat-protective DNA chaperone activity independent of supercoiling. *Nucl. Acids Res.* **32**, 3537–3545.
7. Hsieh, T. S. & Plank, J. L. (2006). Reverse gyrase functions as a DNA renaturase: annealing of complementary single-stranded circles and positive supercoiling of a bubble substrate. *J. Biol. Chem.* **281**, 5640–5647.
8. Confalonieri, F., Elie, C., Nadal, M., de La Tour, C., Forterre, P. & Duguet, M. (1993). Reverse gyrase: a helicase-like domain and a type I topoisomerase in the same polypeptide. *Proc. Natl Acad. Sci. USA*, **90**, 4753–4757.
9. Rodriguez, A. C. & Stock, D. (2002). Crystal structure of reverse gyrase: insights into the positive supercoiling of DNA. *EMBO J.* **21**, 418–426.
10. Matoba, K., Mayanagi, K., Nakasu, S., Kikuchi, A. & Morikawa, K. (2002). Three-dimensional electron microscopy of the reverse gyrase from *Sulfolobus tokodaii*. *Biochem. Biophys. Res. Commun.* **297**, 749–755.
11. Declais, A. C., Marsault, J., Confalonieri, F., de La Tour, C. B. & Duguet, M. (2000). Reverse gyrase, the two domains intimately cooperate to promote positive supercoiling. *J. Biol. Chem.* **275**, 19498–19504.
12. Shibata, T., Nakasu, S., Yasui, K. & Kikuchi, A. (1987). Intrinsic DNA-dependent ATPase activity of reverse gyrase. *J. Biol. Chem.* **262**, 10419–10421.
13. Rodriguez, A. C. (2002). Studies of a positive supercoiling machine. Nucleotide hydrolysis and a multifunctional "latch" in the mechanism of reverse gyrase. *J. Biol. Chem.* **277**, 29865–29873.
14. Hsieh, T. S. & Capp, C. (2005). Nucleotide- and stoichiometry-dependent DNA supercoiling by reverse gyrase. *J. Biol. Chem.* **280**, 20467–20475.
15. Jaxel, C., Nadal, M., Mirambeau, G., Forterre, P., Takahashi, M. & Duguet, M. (1989). Reverse gyrase binding to DNA alters the double helix structure and produces single-strand cleavage in the absence of ATP. *EMBO J.* **8**, 3135–3139.
16. Rodriguez, A. C. (2003). Investigating the role of the latch in the positive supercoiling mechanism of reverse gyrase. *Biochemistry*, **42**, 5993–6004.
17. Andera, L., Mikulika, K. & Savelyevab, N. D. (1993). Characterization of a reverse gyrase from the extremely thermophilic hydrogen-oxidizing eubacterium *Calderobacterium hydrogenophilum*. *FEMS Microbiol. Letters*, **110**, 107.
18. Bouthier de la Tour, C., Portemer, C., Kaltoum, H. & Duguet, M. (1998). Reverse gyrase from the hyperthermophilic bacterium *Thermotoga maritima*: properties and gene structure. *J. Bacteriol.* **180**, 274–281.
19. Krah, R., O'Dea, M. H. & Gellert, M. (1997). Reverse gyrase from *Methanopyrus kandleri*. Reconstitution of an active extremozyme from its two recombinant subunits. *J. Biol. Chem.* **272**, 13986–13990.
20. Reinstein, J., Schlichting, I. & Wittinghofer, A. (1990). Structurally and catalytically important residues in the phosphate binding loop of adenylate kinase of *Escherichia coli*. *Biochemistry*, **29**, 7451–7459.
21. Solem, A., Zingler, N. & Pyle, A. M. (2006). A DEAD protein that activates intron self-splicing without unwinding RNA. *Mol. Cell*, **24**, 611–617.

22. Saraste, M., Sibbald, P. R. & Wittinghofer, A. (1990). The P-loop—a common motif in ATP- and GTP-binding proteins. *Trends Biochem. Sci.* **15**, 430–434.
23. Eckstein, F. (1985). Nucleoside phosphorothioates. *Annu. Rev. Biochem.* **54**, 367–402.
24. Forterre, P., Mirambeau, G., Jaxel, C., Nadal, M. & Duguet, M. (1985). High positive supercoiling *in vitro* catalyzed by an ATP and polyethylene glycol-stimulated topoisomerase from *Sulfolobus acidocaldarius*. *EMBO J.* **4**, 2123–2128.
25. Eckstein, F. (1975). Investigation of enzyme mechanisms with nucleoside phosphorothioates. *Angew Chem. Int. Ed. Engl.* **14**, 160–166.
26. Gorbalenya, A. E. & Koonin, E. V. (1993). Helicases: amino acid sequence comparisons and structure-function relationships. *Curr. Opin. Struct. Biol.* **3**, 419–429.
27. Peck, M. L. & Herschlag, D. (2003). Adenosine 5′-O-(3-thio)triphosphate (ATPgammaS) is a substrate for the nucleotide hydrolysis and RNA unwinding activities of eukaryotic translation initiation factor eIF4A. *Rna*, **9**, 1180–1187.
28. Caruthers, J. M., Johnson, E. R. & McKay, D. B. (2000). Crystal structure of yeast initiation factor 4A, a DEAD-box RNA helicase. *Proc. Natl Acad. Sci. USA*, **97**, 13080–13085.
29. Story, R. M., Li, H. & Abelson, J. N. (2001). Crystal structure of a DEAD box protein from the hyperthermophile *Methanococcus jannaschii*. *Proc. Natl Acad. Sci. USA*, **98**, 1465–1470.
30. Cheng, Z., Coller, J., Parker, R. & Song, H. (2005). Crystal structure and functional analysis of DEAD-box protein Dhh1p. *RNA*, **11**, 1258–1270.
31. Shi, H., Cordin, O., Minder, C. M., Linder, P. & Xu, R. M. (2004). Crystal structure of the human ATP-dependent splicing and export factor UAP56. *Proc. Natl Acad. Sci. USA*, **101**, 17628–17633.
32. Yao, N., Hesson, T., Cable, M., Hong, Z., Kwong, A. D., Le, H. V. & Weber, P. C. (1997). Structure of the hepatitis C virus RNA helicase domain. *Nature Struct. Biol.* **4**, 463–467.
33. Andersen, C. B., Ballut, L., Johansen, J. S., Chamieh, H., Nielsen, K. H., Oliveira, C. L. *et al.* (2006). Structure of the exon junction core complex with a trapped DEAD-box ATPase bound to RNA. *Science*, **313**, 1968–1972.
34. Sengoku, T., Nureki, O., Nakamura, A., Kobayashi, S. & Yokoyama, S. (2006). Structural basis for RNA unwinding by the DEAD-box protein Drosophila Vasa. *Cell*, **125**, 287–300.
35. Hiratsuka, T. (1983). New ribose-modified fluorescent analogs of adenine and guanine nucleotides available as substrates for various enzymes. *Biochim. Biophys. Acta*, **742**, 496–508.
36. Adam, H. (1962). Adenosin-5′diphosphat und adenosin-5′monophosphat. In *Methoden der Enzymatischen Analyse*, pp. 573–577. Bergmeyer, H.U. (Hrsg.), Verlag Chemie, Weinheim.
37. Mondragon, A. & DiGate, R. (1999). The structure of *Escherichia coli* DNA topoisomerase III. *Struct. Fold. Des.* **7**, 1373–1383.

Edited by J. E. Ladbury

(Received 15 March 2007; received in revised form 27 April 2007; accepted 10 May 2007)
Available online 18 May 2007

4.3 Appendix

Demonstrated binding of reverse gyrase to pUC18

One of the main findings embodied in the current work is ATPase stimulation of reverse gyrase by pUC18. However, it was not possible to provide saturating conditions of pUC18-stimulated ATP hydrolysis for steady-state ATPase at 37°C. We set out to provide evidence that reverse gyrase efficiently binds to pUC18 using gel mobility shift analysis (GEMSA) with linearised plasmid for better resolution of an eventual band shift. pUC18 was linearised with EcoRI from NEB following the manufacturer's instructions and binding of *T. maritima* reverse gyrase to the linearised plasmid was tested (Figure 9).

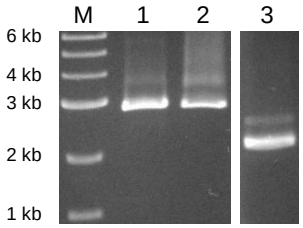

Figure 9. Gel mobility shift analysis (GEMSA) of linearised pUC18 on a 1.2% agarose gel. 10 nM linearised pUC18 in 50 mM Tris/HCl (pH 7.5), 150 mM NaCl, 10 mM $MgCl_2$, 100 µM $Zn(OAc)_2$, 2 mM β-ME, 10% (w/v) PEG 8000 was incubated with 0.5 µM (1), 1 µM (2) or no reverse gyrase wild type (3) at 37°C for 10 minutes. (M) DNA marker. The presence of reverse gyrase reduces the migration velocity of linearised pUC18.

Clearly, reverse gyrase from *T. maritima* binds to linearised pUC18 plasmid. Maximally 130 reverse gyrase molecules could bind to the 2686 bp large pUC18, calculating with a length of 34 Å for 10 bp double helical DNA[38] and ~ 70 Å diameter for reverse gyrase[9]. However, neither the exact number of enzyme molecules bound to pUC18 nor possible interaction between single reverse gyrase molecules can be determined with GEMSA. Experiments with short single- and double-stranded DNA stretches may reveal more details on DNA binding by reverse gyrase.

Effect of Temperature on Reverse Gyrase ATP hydrolysis Rates: Arrhenius Plot

The data in the presented publication shows that *T. maritima* reverse gyrase hydrolyses ATP already at 37°C, whereas ATP-dependent positive supercoiling is not observed at temperatures lower than 65°C (Chapter 3.3). To further our understanding of the single steps during the catalytic cycle of reverse gyrase, it was interesting to investigate the temperature dependency of ATP hydrolysis. Arrhenius plots are used to determine activation energies for chemical reactions and to analyse changes in rate-limiting steps of multi-step reactions like positive supercoiling. The Arrhenius equation is:

$$k = A \cdot e^{-\frac{E_a}{RT}} \quad (1),$$

where k is the rate constant of the reaction, A is the pre-exponential factor, E_a is the activation energy of the reaction, R is the gas constant (R = 8.314 J · K^{-1} mol^{-1}) and T is the absolute temperature in Kelvin. The Arrhenius equation can be linearised to:

$$\ln(k) = \ln(A) - \frac{E_a}{R} \cdot \frac{1}{T} \qquad (2).$$

Single-turnover ATP hydrolysis by reverse gyrase was recorded between 25-75°C and analysed as described (Figure 10).

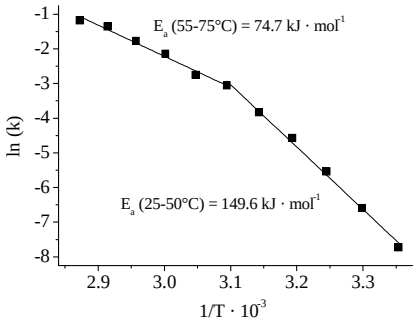

Figure 10. Temperature-dependent ATP hydrolysis by reverse gyrase under single-turnover conditions. Hydrolysis rates were recorded in steps of 5°C form 25-75°C. A time course for the hydrolysis of 6 μM ATP by 20 μM reverse gyrase was each recorded in 50 mM Tris/HCl (pH 7.5), 150 mM NaCl, 10 mM $MgCl_2$, 100 μM $Zn(OAc)_2$, 2 mM β-ME, 10% (w/v) PEG 8000. The resulting exponential rate constants for each temperature were plotted after the linearised form of the Arrhenius equation.

Arrhenius plots are linear in the case of single rate-limited reactions that are thermally activated[39]. Figure 10 shows a two-step Arrhenius plot that may be curved. Curved Arrhenius plots are very rare and their analysis is complex[40-42]. However, the decrease of activation energy for chemical reactions at high temperatures has been interpreted as a change in type of reaction[39]. At low temperatures, enzymatic reactions are therefore controlled by conformational changes with typical high activation energies of about 150 kJ · mol^{-1}. A decrease to about 50 kJ · mol^{-1} is observed at high temperatures and indicates a change to diffusion-controlled reactions[41]. This could also be true for ATP hydrolysis by reverse gyrase. This hyperthermophilic ATPase is already active at temperatures as low as 37°C with an E_a value of 150 kJ · mol^{-1}. However, positive supercoiling by reverse gyrases in general is only possible at temperatures above 50°C. Here, the overall E_a value is decreased to 75 kJ · mol^{-1} in the absence of DNA, indicating a contribution of decreased activation energies to positive supercoiling by reverse gyrase at high temperatures. Thus, inter-domain communication of the helicase-like domain and the topoisomerase domain of reverse gyrase may be energetically hindered at low temperatures. It may be of interest to determine the temperature-dependency of E_a values for the ATPase of reverse gyrase in the presence of DNA substrates.

Supplementary Literature

(38) Watson J. D., Crick F. H., A Structure for Deoxyribose Nucleic Acid, *Nature*, **1953**, *171*, 737-738.

(39) Gutfreund H., Kinetics for the Life Sciences: Receptors, Transmitters, and Catalysts, *Cambridge University Press*, **1995**, *ISBN 052148586X*, 239-241.

(40) Londesborough J., The Causes of Sharply Bent or Discontinuous Arrhenius Plots for Enzyme-Catalysed Reactions, *Eur. J. Biochem.*, **1980**, *105*, 211-215.

(41) Anson M., Temperature dependence and arrhenius activation energy of F-actin velocity generated *in vitro* by skeletal myosin, *J. Mol. Biol.*, **1992**, *224*, 1029-1038.

(42) Truhlar D. G., Kohen A., Convex Arrhenius plots and their interpretation, *Proc. Natl Acad. Sci. USA*, **2001**, *98*, 848-851.

5. Plasmid Relaxation and Supercoiling Promote AMP Generation from ADP and ATP by *T. maritima* Reverse Gyrase

5.1 Introduction

Negatively supercoiled plasmids are relaxed prior to positive supercoiling by the topoisomerase IA reverse gyrase in the presence of ATP or an ATP analogue[1,2]. Relaxation of negatively supercoiled plasmids occurs in the presence of ADP or ADPNP[3,4]. Importantly, both topoisomerase activities of reverse gyrase require high temperatures[5]. We previously described the influence of DNA substrate binding on adenine nucleotide hydrolysis and the influence of adenine nucleotide hydrolysis on topoisomerase activity of reverse gyrase[4,6]. However, no information about the molecular basis for supercoiling is available. Also, the underlying nucleotide cycle and its coordination with DNA binding are not fully understood. For example, the mandatory presence of ADP or ADPNP for plasmid relaxation by reverse gyrase is in contrast to plasmid relaxation by topoisomerase IA from *Escherichia coli*, which relaxes negatively supercoiled plasmids in the absence of nucleotides as reviewed[2]. Binding of ADP to reverse gyrase is suggested to induce conformational changes[6,7]. As a product of ATP hydrolysis, ADP must dissociate from reverse gyrase to reset the enzyme to the energy-generating ATP-bound state.

Surprisingly, we found AMP generation from ADP and ATP in the presence of plasmid DNA. Hypothetically, ADP itself could be converted to AMP to provide activation energy for plasmid relaxation, which *per se* is a downhill reaction. Consequently, ADP hydrolysis may also be considered for the supercoiling activity of reverse gyrase in the presence of ATP, where ADP is generated from ATP. Actually, it is possible to release energy from ATP by direct cleavage to AMP and pyrophosphate, which is normally catalysed by nucleoside triphosphate diphosphohydrolases (NTPDase)[8]. This enzyme class can be found in animal venoms along with ADPases that are specific for ADP hydrolysis[9]. More interestingly, a thermophilic chaperonin with an ATPase/ADPase activity was discovered that might use ADP as an energy source[10]. Similarly, ADP may be hydrolysed by reverse gyrase, which has been proposed to act as a hyperthermophilic DNA chaperone[11] itself.

The current study strongly suggests AMP generation by reverse gyrase in the presence of plasmid DNA and adenine nucleotides. The data shown are preliminary and unpublished, but indicate a feature of *Thermotoga maritima* reverse gyrase that, to our knowledge, so far remained unnoticed.

5.2 Material and Methods

Protein and Plasmid Purification and DNA Substrates

Reverse gyrase wild type and mutants from *T. maritima* and pUC18 were purified as described[4] (Chapter 3.2). A 60-mer ssDNA with the sequence 5'-AAGCCAAGCT TCTAGAGTCA GCCCGTGATA TTCATTACTT CTTATCCTAG GATCCCCGTT-3' and the complementary strand were purchased from Purimex (Grebenstein, Germany). The complementary single strands were annealed to form a 60-mer dsDNA substrate[6].

Western Blotting

Reverse gyrase preparations were tested for contamination with adenylate kinase (AK) in a western blot using the Amersham ECL™ kit (GE Healthcare) and following the manufacturer's instructions. Proteins were separated on a 15% SDS polyacrylamide gel and electro-transferred onto a nitrocellulose filter. Free protein binding sites on the filter were blocked with dry milk solution in PBS buffer (5%). Polyclonal anti-AK antibody was added, and the filter was washed with buffer three times. A polyclonal anti-rabbit antibody bearing horseradish peroxidase was added and the filter was washed again. Added luminol is oxidised in the presence of horseradish peroxidase and starts emitting light, indicating traces of AK. Western blotting was performed by Martin Linden (Klostermeier group).

Fluorescence Equilibrium Titrations

Dissociation constants of adenine nucleotide/reverse gyrase complexes were determined using the fluorescent ADP analogue mantADP as described[4]. Competitive titrations of the mantADP/reverse gyrase complex with adenine nucleotides were carried out in 50 mM Tris/HCl (pH 7.5), 150 mM NaCl, 10 mM $MgCl_2$, 100 µM $Zn(OAc)_2$, 2 mM β-ME at 37°C[4,6]. ATP, ATPγS, ADPCP, ADPNP, ADP, $ADPNH_2$[a], AMPCP[b] and AMP were purchased from Jena Bioscience or Pharma Waldhof. Nucleotide purity was examined with reversed phase HPLC on a C_{18}-column with 100 mM sodium phosphate (pH 6.5) as solvent.

[a] adenosine 5'-O-(3-amino)diphosphate
[b] α,β-methylene-adenosine 5'-diphosphate

Nucleotide Hydrolysis under Single-Turnover Conditions and During DNA Supercoiling

For single turnover conditions, 20 µM reverse gyrase was mixed with 6 µM nucleotide in 50 mM Tris/HCl (pH 7.5), 150 mM NaCl, 10 mM $MgCl_2$, 100 µM $Zn(OAc)_2$, 2 mM β-ME at 37°C or 75°C and 300 nM pUC18, if required. In contrast, nucleotide hydrolysis during supercoiling was determined under multiple turnover conditions in the same buffer with 1 µM reverse gyrase, 2 mM nucleotide, 15 nM pUC18 and 10% PEG 8000. Reactions were stopped with $HClO_4$ and neutralised with KOAc. The ratios of adenine nucleotides and hydrolysis products were determined by reversed phase HPLC as described above (p. 45).

Topoisomerase Reaction

Relaxation and positive supercoiling of negatively supercoiled pUC18 plasmid by reverse gyrase were studied in the presence of various adenine nucleotides. The adenine nucleotide concentration was 2 mM in all cases. Reaction conditions and the analysis of topoisomers are published[4] and described in Chapter 3.2.

5.3 Results

AMP Generation by Reverse Gyrase from ATP/ATPγS in the presence of pUC18

Hydrolysis rates of ATP and ATP analogues were previously determined under single-turnover conditions, as published[4] (Chapter 4). In summary, ATP and ATPγS hydrolysis by reverse gyrase are stimulated by pUC18 at 37°C and 75°C. Positive supercoiling of pUC18 is promoted by adenine nucleotide hydrolysis only at 75°C. Most interestingly, generation of AMP was indicated during ATP hydrolysis by reverse gyrase in the presence of pUC18 at 75°C. Hence, AMP generation was investigated under single-turnover conditions using a fixed nucleotide/enzyme ratio of 0.3 and an enzyme/pUC18 ratio of 67 (Figure 1).

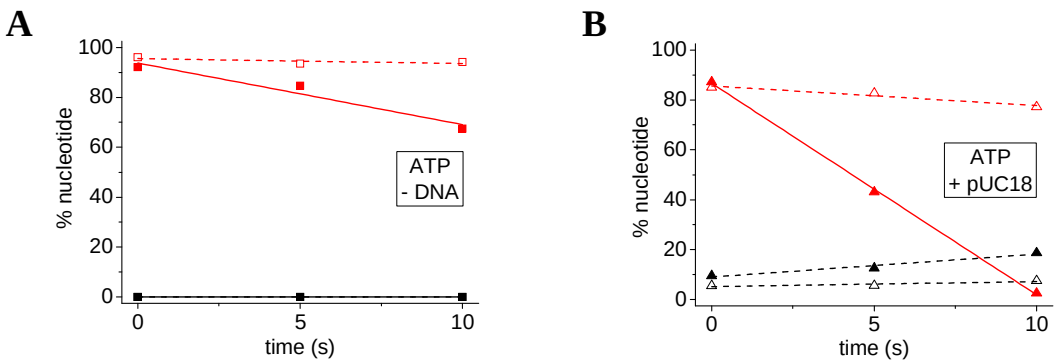

Figure 1. Single-turnover ATP hydrolysis at 75°C. Reaction conditions were 6 µM ATP, 50 mM Tris/HCl (pH 7.5), 150 mM NaCl, 10 mM $MgCl_2$, 100 µM $Zn(OAc)_2$, 2 mM β-ME, 75°C. The nucleotide fraction of ATP (red symbols) and AMP (black symbols) is shown in the presence/absence of 20 µM reverse gyrase (filled/open symbols). (A) Without DNA (squares) no AMP is detected and ATP is hydrolysed with a rate of 0.05-0.15 s^{-1}. (B) AMP is generated in the presence of 300 nM pUC18 (triangles) and reverse gyrase hydrolyses ATP with a rate constant between 0.15-0.45 s^{-1} (data taken from[4]). The fraction of ADP can be calculated: ADP% = 100% - ATP% - AMP%.

After 10 seconds, 20% ATP is hydrolysed to ADP by reverse gyrase in the absence of pUC18 at 75°C. AMP generation is not observed (Figure 1A). In the presence of pUC18, ATP is completely hydrolysed after 10 seconds and converted to 19% AMP and 81% ADP (Figure 1B). The hydrolysis rate can be estimated to 0.15-0.45 s^{-1}. However, the reaction in the presence of pUC18 is too fast to resolve in hand-mixing experiments.

The hydrolysis rate of ATPγS is reduced compared to ATP hydrolysis at 75°C[4]. ATPγS was therefore used to resolve the kinetics of the hydrolysis reaction (Figure 2).

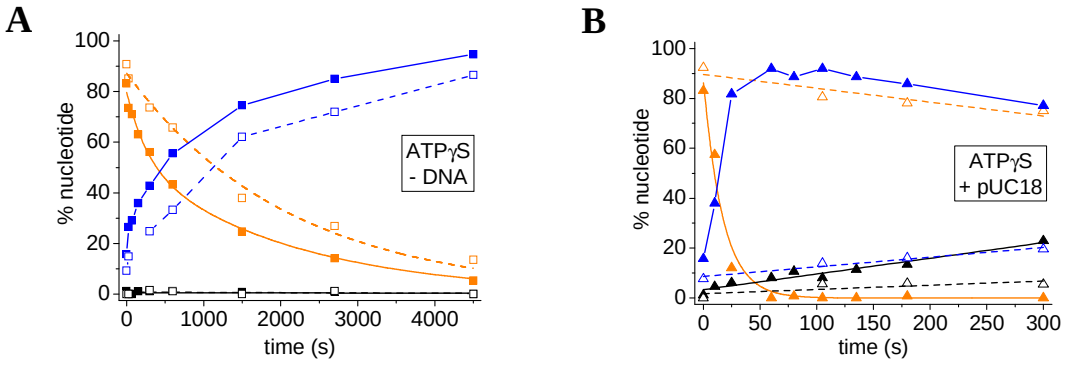

Figure 2. Hydrolysis of ATPγS under single-turnover conditions. Experiments were performed in the presence of 20 µM reverse gyrase (open/filled symbols) with 6 µM ATPγS (orange symbols), 50 mM Tris/HCl (pH 7.5), 150 mM NaCl, 10 mM $MgCl_2$, 100 µM $Zn(OAc)_2$, 2 mM β-ME at 75°C. Samples without enzyme were used as controls (open symbols). The amount of ADP (blue symbols) and AMP (black symbols) after a certain time are also depicted. (A) ATPγS spontaneously hydrolyses to ADP in the absence of DNA (squares) with an exponential decay of 4.8 (±0.4) · 10^{-4} s^{-1}, which is increased to 3.8 (±1.1) x 10^{-3} s^{-1} in the presence of reverse gyrase. Spontaneous ATPγS hydrolysis is taken into account. (B) In the presence of both reverse gyrase and 300 nM pUC18 (triangles), ATPγS is hydrolysed with a rate of 58.2 (±7.7) · 10^{-3} s^{-1}. In this case, 23% AMP is generated during. Hydrolysis rates were previously published[4].

ATPγS spontaneously hydrolyses at 75°C and its concentration decays exponentially with a rate of 4.8 (±0.4) · 10^{-4} s^{-1}. ATPγS hydrolysis is accelerated 8-fold in the presence of reverse gyrase (Figure 2A). The presence of pUC18 further stimulates ATPγS hydrolysis by reverse gyrase 15-fold[4]. The hydrolysis reaction is complete after 80 seconds, where the ADP concentration reaches a maximum at 90% of total nucleotide and subsequently decreases. 20% AMP is generated throughout the observed time course of 300 seconds.

Thus, AMP generation requires the presence of plasmid DNA. Furthermore, the optimal temperature for plasmid supercoiling by reverse gyrase (75°C) may also be important for AMP generation.

We have previously shown that ATP and ATPγS are hydrolysed at 37°C in the presence of pUC18 by reverse gyrase, where no supercoiling activity is observed[4]. The generation of AMP during nucleotide hydrolysis at 37°C was consequently examined (Figure 3).

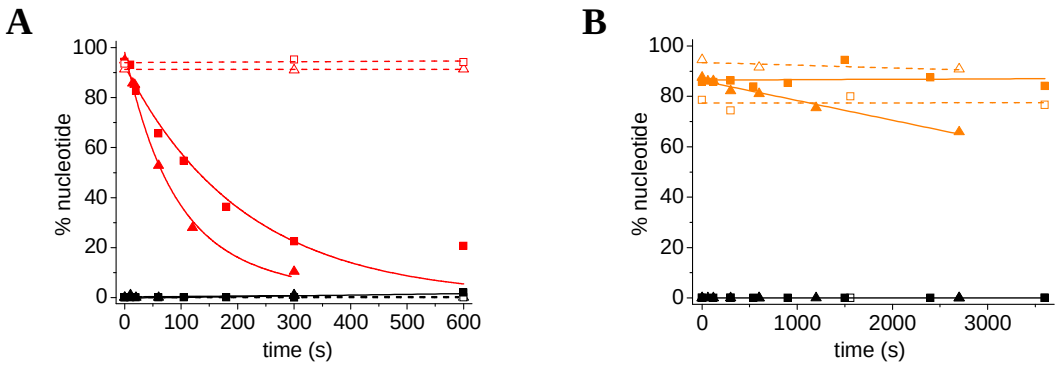

Figure 3. Single-turnover nucleotide hydrolysis at 37°C. Reaction conditions were 20 µM reverse gyrase (filled symbols), 50 mM Tris/HCl (pH 7.5), 150 mM NaCl, 10 mM $MgCl_2$, 100 µM $Zn(OAc)_2$, 2 mM β-ME. Reactions were started with 6 µM ATP (red symbols) or ATPγS (orange symbols). Reference samples contained no enzyme (open symbols) and/or no DNA (triangles). The nucleotide fraction of AMP is shown (black symbols). Depiction of ADP was omitted for clarity. (A) The presence of 300 nM pUC18 (squares) stimulates reverse gyrase ATP hydrolysis with a rate of 12.9 (±4.4) · 10^{-3} s^{-1} compared to a rate of 4.7 (±0.7) · 10^{-3} s^{-1} without DNA as published[4]. (B) ATPγS is slowly hydrolysed with a rate of ~0.1 · 10^{-3} s^{-1} and only in the presence of pUC18. AMP was not generated in these experiments.

AMP could not be detected during either ATP or ATPγS hydrolysis by reverse gyrase at 37°C in the presence of pUC18. This is in contrast to the results obtained at 75°C. Seemingly, AMP is only generated under conditions suitable for plasmid supercoiling (Chapter 3.3). In summary, the results presented here indicate a correlation of AMP generation in the presence of pUC18 with topoisomerase activity of reverse gyrase from *T. maritima*.

Adenylate Kinase Contamination of Reverse Gyrase Preparations

The previous results provide evidence that AMP generation might be coupled to positive plasmid supercoiling by reverse gyrase at 75°C. AMP may also arise from the activity of a contaminant from *E. coli* still present after purification. For example, AK is a ubiquitous enzyme that catalyses the disproportionation of two ADP molecules into AMP and ATP[12]. Contamination of reverse gyrase with *E. coli* AK was tested (Figure 4).

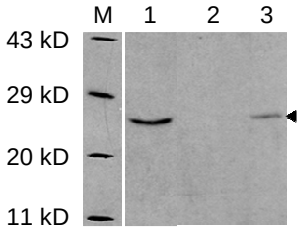

Figure 4. Western blot of a 15% SDS polyacrylamide gel. AK was detected with a polyclonal rabbit anti-AK antibody and visualised with a secondary anti-rabbit antibody fused to horseradish peroxidase using enhanced chemoluminiscence. (M) molecular weight marker, (1) positive control with AK, (2) purified reverse gyrase wild type, (3) flow through after cation exchange chromatography during purification of reverse gyrase wild type. The arrow indicates the position of *E. coli* AK (23.5 kD). Purified reverse gyrase is not contaminated with AK.

A protein sample with AK from *E. coli* was used as reference (Figure 4, lane 1). Purified reverse gyrase wild type (lane 2) does not contain AK. With a pI of 5.5, AK is removed during the purification of reverse gyrase[4] because it does not bind during a cation exchange chromatography step performed at pH 7.5 (lane 3). Thus, previously observed AMP generation is not the result of AK contamination, but is most likely caused by the presence of reverse gyrase.

AMP Generation from ATP by Reverse Gyrase under Multiple-Turnover Conditions Using Various DNA Substrates

The plasmid pUC18 is a substrate for topoisomerase activity by reverse gyrase (Chapter 3). Other DNA substrates could possibly promote AMP generation under conditions suitable for plasmid relaxation and supercoiling by reverse gyrase. ssDNA, dsDNA and pUC18 were compared as substrates for reverse gyrase with respect to AMP generation (Figure 5).

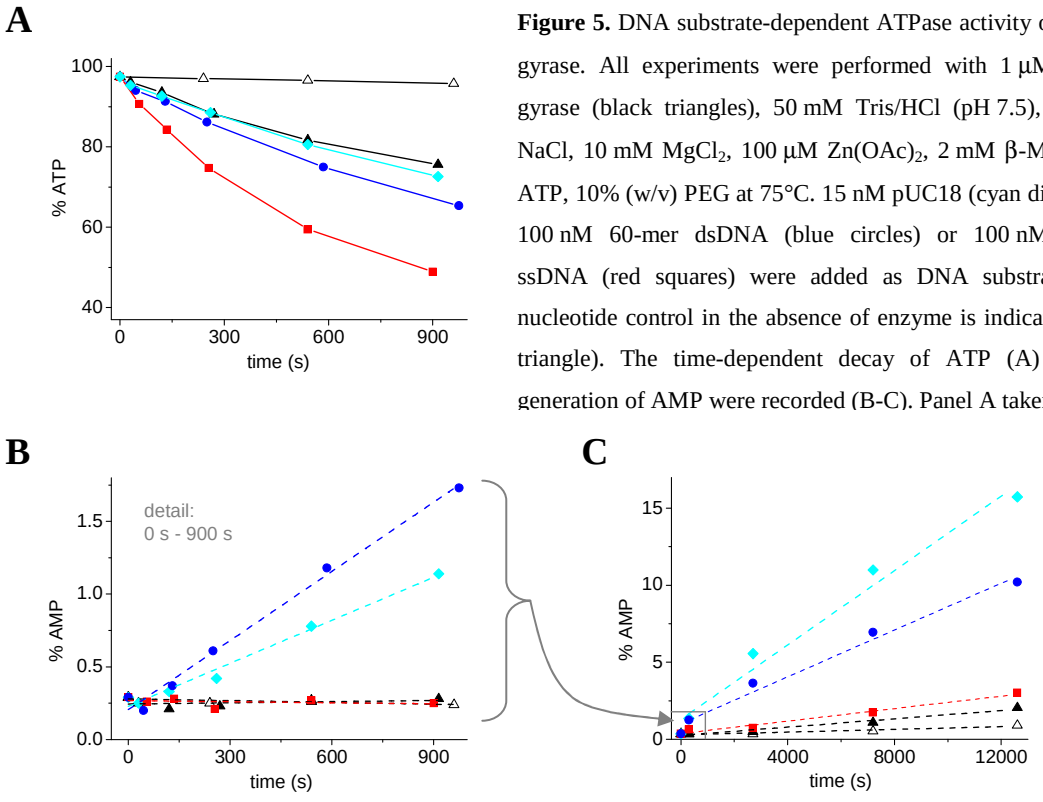

Figure 5. DNA substrate-dependent ATPase activity of reverse gyrase. All experiments were performed with 1 µM reverse gyrase (black triangles), 50 mM Tris/HCl (pH 7.5), 150 mM NaCl, 10 mM $MgCl_2$, 100 µM $Zn(OAc)_2$, 2 mM β-ME, 1 mM ATP, 10% (w/v) PEG at 75°C. 15 nM pUC18 (cyan diamonds), 100 nM 60-mer dsDNA (blue circles) or 100 nM 60-mer ssDNA (red squares) were added as DNA substrates. The nucleotide control in the absence of enzyme is indicated (open triangle). The time-dependent decay of ATP (A) and the generation of AMP were recorded (B-C). Panel A taken from[6].

Reverse gyrase ATPase is only slightly stimulated in the presence of dsDNA or pUC18 but is notably stimulated by ssDNA[6] (Figure 5A). No AMP is generated in the case of ssDNA-stimulated ATP hydrolysis. Most interestingly, both the presence of dsDNA and pUC18 promote the generation of about 1.1-1.7% AMP within 15 minutes (Figure 5B). The appearance of AMP is not very prominent compared to the background. Authentic AMP generation was confirmed over a period of 3.5 h (Figure 5C) where 10% and 16% AMP are generated in the presence of dsDNA or pUC18 by reverse gyrase. Complementary experiments with the isolated helicase-like domain of reverse gyrase reveal AMP generation in the presence of dsDNA and pUC18 (delToro Duany unpublished, data not shown). The helicase-like domain lacks the plasmid supercoiling activity of the wild type enzyme.

In summary, AMP generation is not necessarily linked to positive supercoiling by reverse gyrase. However, the presence of a double stranded DNA substrate and a temperature of 75°C are a prerequisite.

Correlation of AMP Generation from ATP and ATPγS with Plasmid Supercoiling by Reverse Gyrase under Multiple-Turnover Conditions

At the beginning of this section, AMP generation was demonstrated under single-turnover conditions by reverse gyrase from ATP and ATPγS exclusively at 75°C and in the presence of pUC18. However, the adenine nucleotide concentrations under single-turnover conditions are not sufficient to promote plasmid supercoiling by reverse gyrase. For multiple-turnover conditions, the nucleotide/enzyme ratio was changed from 0.3 to 1000 while the enzyme/pUC18 ratio was kept constant at 67. Products of ATP and ATPγS hydrolysis during positive supercoiling activity of reverse gyrase were analysed (Figure 6).

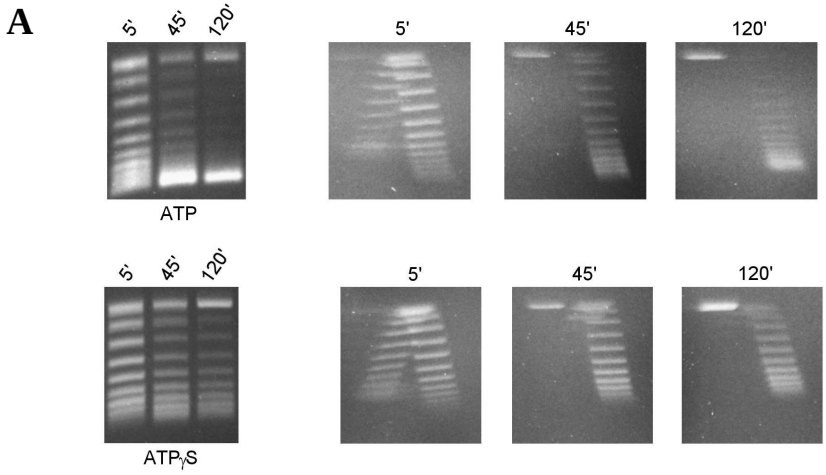

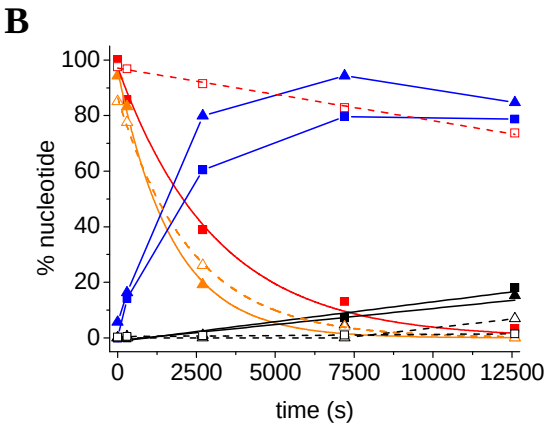

Figure 6. Supercoiling of plasmid DNA by reverse gyrase. Multiple-turnover experiments were performed with 1 µM reverse gyrase, 50 mM Tris/HCl (pH 7.5), 150 mM NaCl, 10 mM $MgCl_2$, 100 µM $Zn(OAc)_2$, 2 mM β-ME, 2 mM nucleotide, 15 nM pUC18, 10% (w/v) PEG at 75°C. (A) Samples taken at different time points were analysed for topoisomer distribution. Positive supercoiling is at least 3-fold faster in the presence of ATP (pictures taken from[4]). (B) Nucleotide analysis of positive supercoiling by reverse gyrase with a hydrolysis rate of 3.2 (±0.3) · 10^{-4} s^{-1} in the presence of ATP (red squares) or 1.6 (±0.4) · 10^{-3} s^{-1} with ATPγS (orange triangles). ATPγS spontaneously hydrolyses at 75°C at a rate of 4.3 (±0.2) · 10^{-4} s^{-1}. The corresponding fractions of ADP (blue symbols) and AMP (black symbols) are depicted. AMP is generated in both series. Controls without enzyme (open symbols) are shown without the ADP fraction for clarity.

ATPγS hydrolysis by reverse gyrase exhibits an exponential decay under multiple-turnover conditions suitable for plasmid supercoiling. The hydrolysis rate for ATPγS is 1.6 (±0.4) · 10^{-3} s^{-1} taking spontaneous ATPγS hydrolysis at 75°C into account. At the same time, ADP is rapidly generated similar to single-turnover hydrolysis (cp. Figure 2B) while AMP is slowly generated (15% after 3.5 h). In the presence of ATP, 18% AMP are generated after 3.5 h. AMP generation at 75°C has not been observed before for ATP hydrolysis under single-turnover conditions due to poor time resolution (cp. Figure 1B). The ATP hydrolysis rate of 3.2 (±0.3) · 10^{-4} s^{-1} is 5-fold reduced compared to ATPγS hydrolysis. This is in contrast to the findings under single-turnover conditions, where ATP is hydrolysed with at least the same rate, indicating less efficient utilisation of ATPγS hydrolysis for positive supercoiling. In fact, more positively supercoiled plasmid is generated by reverse gyrase in the presence of ATP (Figure 6A). The nucleotide hydrolysis profile in Figure 6B suggests that ATP and ATPγS are rapidly hydrolysed to ADP by reverse gyrase, followed by the slower conversion to AMP.

Binding of ADP and ATP Analogues to Reverse Gyrase

To determine nucleotide hydrolysis steps necessary for AMP generation, nucleotide turnover during plasmid relaxation and supercoiling by reverse gyrase was analysed in more detail using non-cleavable ADP and ATP analogues. To ensure saturating conditions for nucleotides during supercoiling experiments, dissociation constants of various nucleotide/reverse gyrase complexes at 37°C were determined in competitive fluorescence equilibrium titrations using mantADP (Table 1).

Table 1. Nucleotide binding to *T. maritima* reverse gyrase wild type at 37°C. Data taken from indicated publications[4,6].

	AMP	ADP	AMPCP	$ADPNH_2$	ATPγS	ADPCP	ADPNP
K_D (μM)	1549 ± 375[6]	1.6 ± 0.2[4]	110 ± 20	480 ± 240	14.3 ± 1.5[4]	74.7 ± 7.3[6]	43.2 ± 2.0[4]

Reverse gyrase binds ADP about 10 to 50-fold more tightly than the ATP analogues ATPγS, ADPCP and APDNP, indicating a negative contribution of the γ-phosphate group to nucleotide binding or possibly of the β-/γ-phosphoester bond. Also, reverse gyrase binds the ADP analogues AMPCP and $ADPNH_2$ 70 to 300-fold less tightly than ADP. Thus, tight binding of ADP to reverse gyrase is at least partially mediated by the α-/β-phosphoester bond or the β-phosphate group. The final hydrolysis product AMP binds an order of magnitude less tightly to reverse gyrase than ADP.

Pathway of AMP Generation by Reverse Gyrase: Directly from ATP or *via* ADP?

Two possible pathways for AMP generation from ATP are imaginable:

$$ATP \rightarrow AMP + PP_i$$
$$ATP \rightarrow ADP + P_i \rightarrow AMP + 2\,P_i$$

ATP may either be directly hydrolysed to AMP and pyrophosphate (PP_i) or undergo stepwise orthophosphate (P_i) cleavage *via* ADP to AMP. An ideal starting point to investigate stepwise ATP hydrolysis is ADP, which promotes plasmid relaxation by reverse gyrase. AMP generation during ATPγS hydrolysis suggests that ADP could be hydrolysed by reverse gyrase. AMP generation during plasmid relaxation by reverse gyrase was investigated (Figure 7).

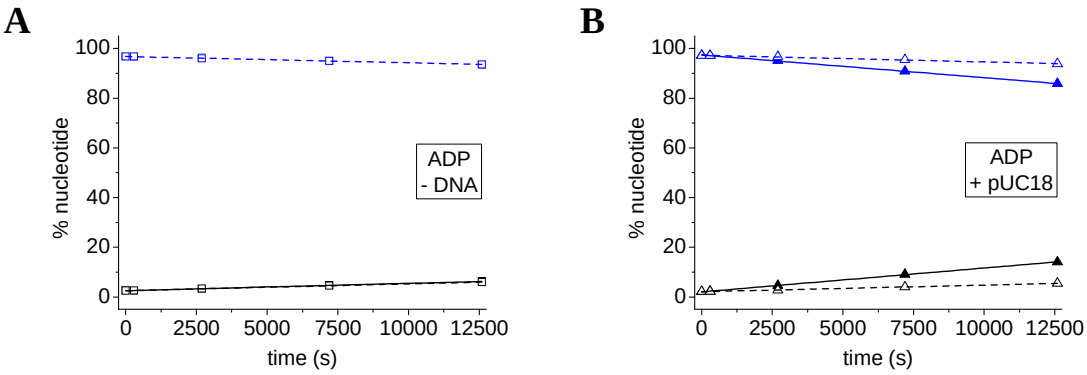

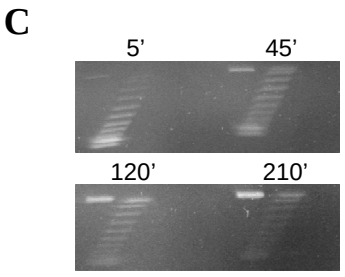

Figure 7. (A-B) ADP and AMP content during plasmid relaxation by reverse gyrase in the presence of ADP (blue symbols). Experiments were performed with 1 μM reverse gyrase (filled symbols), 50 mM Tris/HCl (pH 7.5), 150 mM NaCl, 10 mM $MgCl_2$, 100 μM $Zn(OAc)_2$, 2 mM β-ME, 2 mM ADP, 15 nM pUC18 (triangles), 10% (w/v) PEG at 75°C. Controls without enzyme (open symbols) and the AMP content (black symbols) are indicated. AMP is generated in the presence of pUC18. (C) pUC18 is relaxed by reverse gyrase in the presence of ADP.

No AMP is generated in the absence of plasmid DNA (Figure 7A). ADP is hydrolysed by reverse gyrase in the presence of pUC18. 14% AMP is generated from ADP during plasmid relaxation (Figure 7B-C).

However, which topoisomerase activity of *T. maritima* reverse gyrase is promoted in the presence of the non-cleavable ATP analogue ADPCP is unknown. The methylene group between the β- and γ-phosphate groups of ADPCP prevents stepwise cleavage of single phosphate groups, thus distinction between the two alternative mechanisms for ATP hydrolysis may be possible (Figure 8).

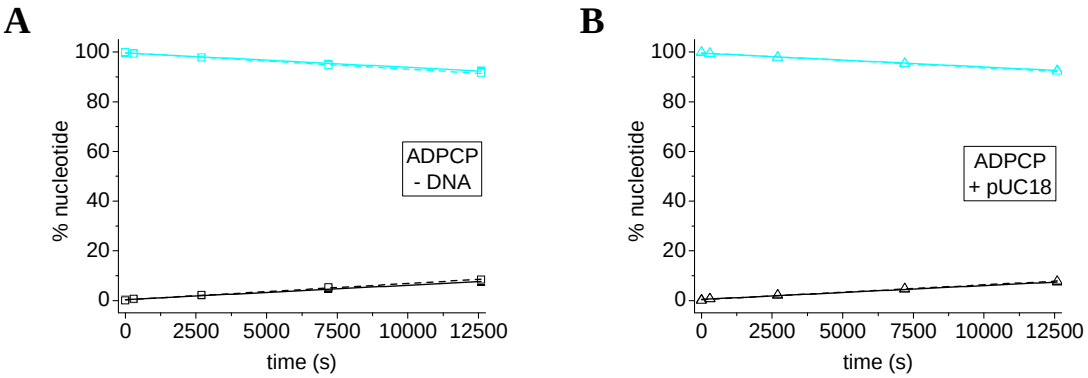

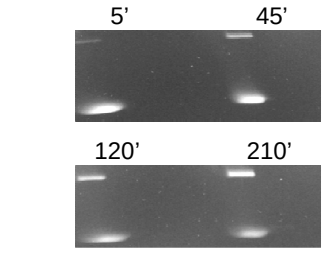

Figure 8. AMP generation by reverse gyrase in the presence of ADPCP (cyan symbols). Conditions were 1 μM reverse gyrase (filled symbols), 50 mM Tris/HCl (pH 7.5), 150 mM NaCl, 10 mM $MgCl_2$, 100 μM $Zn(OAc)_2$, 2 mM β-ME, 2 mM ATP, 15 nM pUC18 (triangles), 10% (w/v) PEG at 75°C. Controls without enzyme (open symbols) and the AMP content (black symbols) are indicated. (A-B) Nucleotide analysis shows AMP generation within the background. (C) No topoisomerase activity of reverse gyrase is detected by agarose gel analysis.

ADPCP is not hydrolysed by reverse gyrase under conditions that allow for supercoiling and no ADP is generated (data not shown). About 10% AMP is generated regardless of the presence of reverse gyrase or pUC18 (Figure 8A-B). Thus, AMP is generated by spontaneous cleavage of methylene-pyrophosphate (pCp) from ADPCP in one step. The

presence of ADPCP neither supports plasmid relaxation nor supercoiling (Figure 8C). Concomitantly, the amount of negatively supercoiled plasmid decreases with time, accompanied by an increase in nicked plasmid. Thus, ADPCP binding to reverse gyrase promotes DNA strand cleavage of the bound plasmid. In summary, plasmid relaxation by reverse gyrase seems to require cleavage of an energy-rich phosphate bond. As ADPNP promotes plasmid relaxation[4], it should consequently lead to AMP generation (Figure 9).

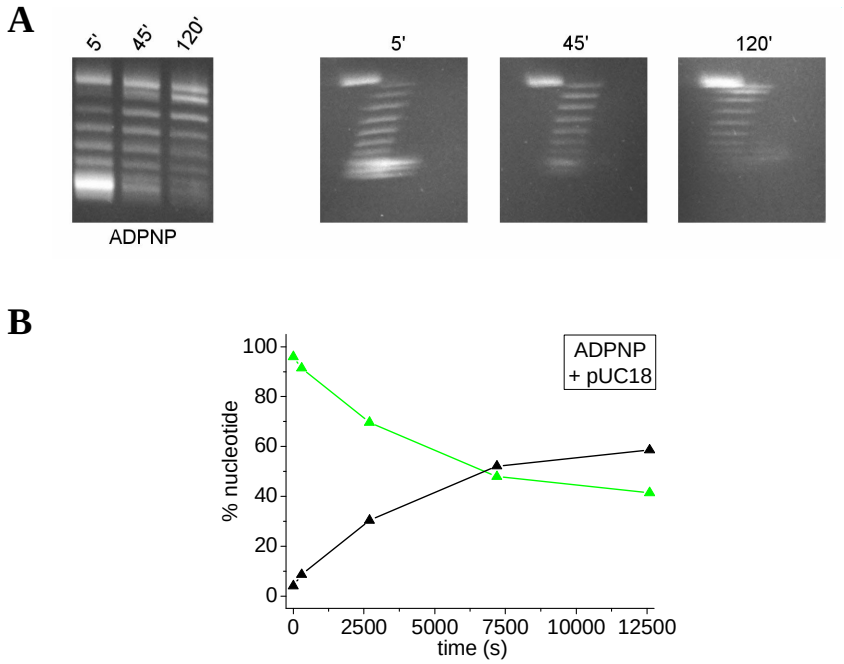

Figure 9. Plasmid relaxation by reverse gyrase in the presence of ADPNP. Experiments were performed with 1 µM reverse gyrase, 50 mM Tris/HCl (pH 7.5), 150 mM NaCl, 10 mM $MgCl_2$, 100 µM $Zn(OAc)_2$, 2 mM β-ME, 2 mM ADPNP, 15 nM pUC18, 10% (w/v) PEG at 75°C. (A) Samples taken at different time points were analysed with one-and two-dimensional gel electrophoresis. ADPNP promotes plasmid relaxation (pictures taken from[4]). (B) AMP is generated exponentially (black curve) during plasmid relaxation while ADPNP is consumed (green curve).

pUC18 is relaxed by reverse gyrase in the presence of ADPNP (Figure 9A), while 60% AMP is generated during 3.5 h (Figure 9B). ADPNP hydrolyses spontaneously at 75°C to 40% AMP within 3.5 h (data not shown). AMP could either be generated stepwise *via* ADP or $ADPNH_2$ or directly by cleavage of imido-pyrophosphate (pNp) from ADPNP. Unfortunately, no clear information about ADPNP hydrolysis steps can be obtained, as ADP and ADPNP are not separated with C_{18}-HPLC under the conditions used. Consequently, $ADPNH_2$ was used to further elucidate nucleotide utilisation and topoisomerase activity by reverse gyrase (Figure 10).

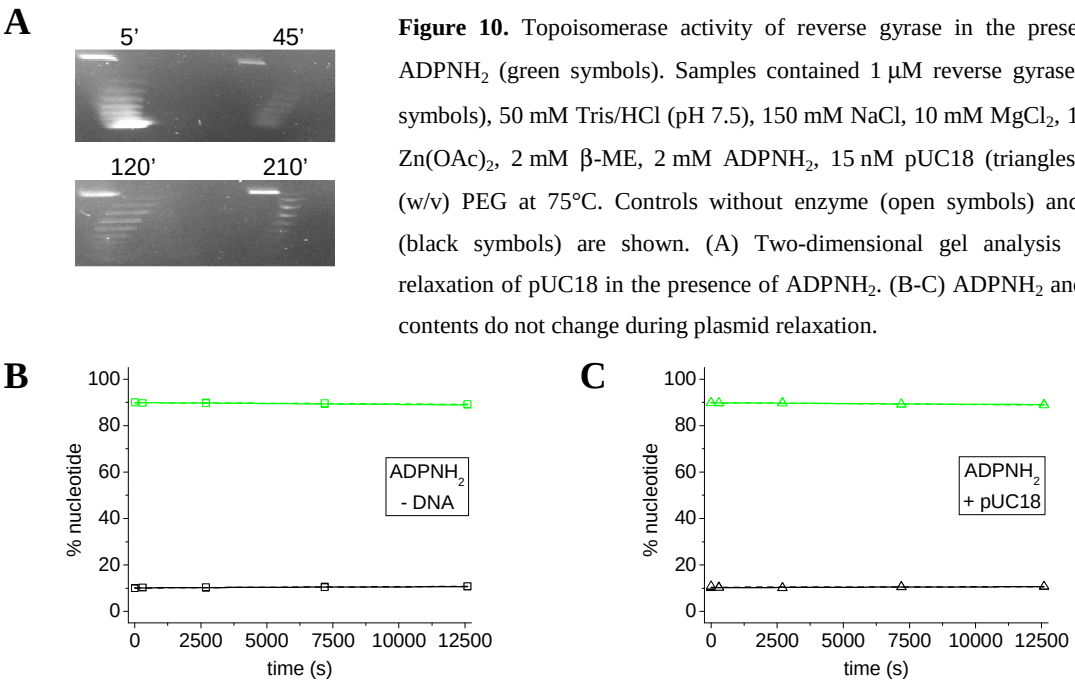

Figure 10. Topoisomerase activity of reverse gyrase in the presence of $ADPNH_2$ (green symbols). Samples contained 1 µM reverse gyrase (filled symbols), 50 mM Tris/HCl (pH 7.5), 150 mM NaCl, 10 mM $MgCl_2$, 100 µM $Zn(OAc)_2$, 2 mM β-ME, 2 mM $ADPNH_2$, 15 nM pUC18 (triangles), 10% (w/v) PEG at 75°C. Controls without enzyme (open symbols) and AMP (black symbols) are shown. (A) Two-dimensional gel analysis reveals relaxation of pUC18 in the presence of $ADPNH_2$. (B-C) $ADPNH_2$ and AMP contents do not change during plasmid relaxation.

Notably, plasmid relaxation by reverse gyrase occurs in the presence of $ADPNH_2$ (Figure 10A), but is remarkably slower than ADP- or ADPNP-promoted relaxation (cp. Figure 7C and 9A). A constant fraction of 10% AMP is present during relaxation and in the absence of DNA and $ADPNH_2$ is not hydrolysed by reverse gyrase during plasmid relaxation (Figure 10B-C). This finding differs from the results obtained in the presence of ADP and ADPNP, where the nucleotides were hydrolysed during plasmid relaxation by reverse gyrase. This discrepancy was consequently examined with a non-hydrolysable ADP analogue. We used AMPCP as an ADP analogue harbouring a methylene bond between the α- and β-phosphate groups (Figure 11).

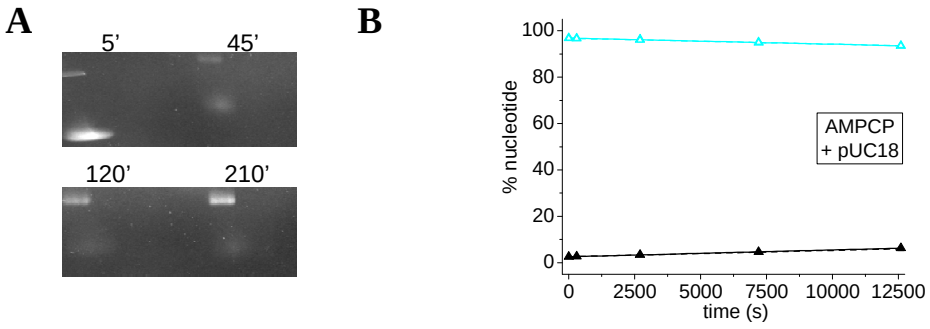

Figure 11. Screen for supercoiling activity of reverse gyrase in the presence of AMPCP. Experiments were performed with 1 µM reverse gyrase in 50 mM Tris/HCl (pH 7.5), 150 mM NaCl, 10 mM $MgCl_2$, 100 µM $Zn(OAc)_2$, 2 mM β-ME, 2 mM AMPCP, 15 nM pUC18, 10% (w/v) PEG at 75°C. (A) Samples taken at different time points were analysed with agarose gel electrophoresis. AMPCP does not promote any topoisomerase activity. (B) Nucleotide fraction of a supercoiling reaction with AMPCP (cyan triangles). Controls without enzyme (open triangles) and the AMP fraction (black triangles) are indicated. AMPCP is not cleaved by reverse gyrase. Control samples without DNA show the same behaviour (data not shown).

AMPCP does not promote topoisomerase activity of reverse gyrase (Figure 11A). AMPCP is neither degraded, nor is AMP generated (Figure 11B). Instead, negatively supercoiled plasmid is increasingly nicked by reverse gyrase. The same behaviour is observed in the presence of ADPCP with respect to nucleotide consumption and plasmid degradation (Figure 8).

In summary, the present chapter provides evidence for the generation of AMP from ATP or ATPγS in the presence of a linear dsDNA substrate and pUC18 plasmid. Positive supercoiling is not required to promote the generation of AMP, and AMP can be generated from ADP and ADPNP during plasmid relaxation by reverse gyrase. However, this is not the case in the presence of AMPCP or ADPCP, where neither nucleotide hydrolysis nor topoisomerase activity by reverse gyrase is observed. Surprisingly, plasmid relaxation is promoted by $ADPNH_2$, while no AMP is generated. This is in contrast to AMP generation observed during positive plasmid supercoiling in the presence of ATP and ATPγS. Finally, AMP generation from ADP and ATP analogues in the presence of double-stranded DNA substrates may be coupled to topoisomerase activity of reverse gyrase. However, the exact prerequisites and need of phosphate bond hydrolysis for topoisomerase activity of reverse gyrase have to be further investigated.

5.4 Discussion

AMP is Generated at 75°C in the Presence of pUC18 and Reverse Gyrase

We set out to elucidate a potential novel feature of reverse gyrase, which might have remained unnoticed since its discovery in 1984: Both ATP and ATPγS hydrolysis by reverse gyrase promote the generation of AMP at 75°C in the presence of plasmid DNA. Temperatures suitable for topoisomerase activity by reverse gyrase may be a requirement for AMP generation, as no AMP is generated at 37°C.

AMP Generation Requires Conditions Sufficient for Plasmid Supercoiling

Interestingly, the helicase-like domain of reverse gyrase promotes AMP generation in the presence of linear dsDNA and pUC18 at 75°C (delToro Duany and Klostermeier, unpublished). The helicase-like domain comprises no topoisomerase activity, demonstrating that plasmid relaxation and/or positive supercoiling are not necessary features for AMP generation. For the full-length enzyme, we found that AMP is not only

generated from ATP and ATPγS during plasmid supercoiling by reverse gyrase, but also in the presence of linear dsDNA. Furthermore, the positive supercoiling activity of reverse gyrase is correlated with the total amount of hydrolysable adenine nucleotide present, and the supercoiling velocity decreases as ATP or ATPγS are consumed. ATPγS is hydrolysed 5-fold more rapidly by reverse gyrase than ATP during plasmid supercoiling at 75°C. However, plasmid DNA is more positively supercoiled in the presence of ATP, and thus, a large fraction of ATPγS must be hydrolysed without being efficiently converted into energy for the supercoiling function. This may indicate that ATP is bound more tightly by reverse gyrase and is simply more protected from heat due to steric effects of the sulphur atom in ATPγS.

Our findings demonstrate that topoisomerase activity of reverse gyrase is correlated to hydrolysis of adenosine tri- and/or diphosphates. Two possibilities for affiliated AMP generation from ATP arise: Firstly, ATP could directly be hydrolysed to AMP by cleavage of PP_i. Secondly, AMP could be generated by reverse gyrase from ATP by consecutive P_i cleavage *via* intermediate ADP generation. In the future, generation of intermediately bound ADP could be examined with pulse chase experiments.

Plasmid Relaxation is Correlated with ADP or ADPNP Hydrolysis by Reverse Gyrase

AMP is generated during plasmid relaxation by reverse gyrase in the presence of ADP- and ADPNP while both nucleotides are hydrolysed. Until now, energy generation from ADP hydrolysis by reverse gyrase has not been considered possible or required for plasmid relaxation[13]. It was of interest to determine whether ADPNP could be converted to AMP *via* intermediate ADP or $ADPNH_2$. Surprisingly, $ADPNH_2$ promotes plasmid relaxation without being hydrolysed to AMP. However, final plasmid relaxation is 3-fold reduced compared to relaxation in the presence of ADP or ADPNP, suggesting that $ADPNH_2$ is insufficient to promote effective plasmid relaxation. Additionally, $ADPNH_2$ binds 300-fold less tightly to reverse gyrase than ADP, indicating that the free amino group of $ADPNH_2$ might interfere with nucleotide binding or reverse gyrase activity.

Non-cleavable AMPCP and ADPCP do not Promote Topoisomerase Activity

ADPCP is neither hydrolysed by reverse gyrase nor promotes any topoisomerase activity. Hypothetically, ADPCP is cleavable between the α- and β-phosphate groups like ADP, which is hydrolysed to AMP and promotes plasmid relaxation by reverse gyrase. The simultaneous absence of both ADPCP hydrolysis and plasmid relaxation suggests stepwise

AMP generation from ATP or ATPγS. This finding indicates that the β- and γ-phosphate groups of ATP and ATPγS are hydrolysed separately during plasmid supercoiling and concomitant AMP generation. However, which phosphate bond cleavage exactly delivers the energy for plasmid relaxation or supercoiling by reverse gyrase is unclear. In future experiments, analogues like AMPNPP or AMPCPP could be used to further investigate nucleotide hydrolysis steps. These analogues can be hydrolysed between the β- and γ-phosphate groups, but not between the α- and β-phosphate groups. Accordingly, we found that the ADP analogue AMPCP is also not hydrolysed by reverse gyrase, and hence, no plasmid relaxation by reverse gyrase is observed. We suggest that AMPNP should be used instead to investigate, if cleavage of single phosphate groups is required for both plasmid relaxation and positive supercoiling by reverse gyrase as shown for ADPNP-promoted plasmid relaxation. Interestingly, nicked pUC18 accumulates in the presence of AMPCP and ADPCP, which are both not hydrolysed by reverse gyrase. Thus, plasmid nicking may reflect a "frozen" conformational state of reverse gyrase in the presence of AMPCP or ADPCP that facilitates DNA cleavage but not DNA religation.

Other Reasons for AMP Generation

The ubiquitous AK from *E coli* generates AMP and ATP from ADP[12], but is removed during reverse gyrase purification. Also, the mesophilic enzyme is not active at 75°C and AMP generation was not observed at 37°C, which argues against a contamination of reverse gyrase with AK as the reason for AMP generation. Furthermore, AMP might also arise from plasmid degradation opposing AMP generation by reverse gyrase. As a topoisomerase type I[2] it cleaves one strand of dsDNA then covalently binds to one single stranded end. The free single stranded end might be subject to degradation at 75°C, generating deoxyribonucleoside monophosphates. However, AMP is not generated in the presence of ssDNA, which already has two free single strand ends. These facts argue against AMP generation from plasmid DNA.

In conclusion, we suggest that reverse gyrase has an ADPase activity. ADP hydrolysis provides about the same amount of energy as γ-phosphate cleavage from ATP[15]. Thus, the utilisation of ADP as an additional energy source might be a general adaption of organisms to thermophilic life. The potential ADPase activity should also be investigated for reverse gyrases from organisms other than *T. maritima*.

5.5 Literature

(1) Kikuchi A., Asai K., Reverse gyrase - a topoisomerase which introduces positive superhelical turns into DNA, *Nature*, **1984**, *309*, 677-681.

(2) Champoux J. J., DNA Topoisomerases: Structure, Function, and Mechanism, *Annu. Rev. Biochem.*, **2001**, *70*, 369-413.

(3) Hsieh T-S., Plank J. L., Reverse Gyrase Functions as a DNA Renaturase, *J. Biol. Chem.*, **2006**, *281*, 5640-5647.

(4) Jungblut S. P., Klostermeier D., Adenosine 5′-O-(3-thio)triphosphate (ATPγS) Promotes Positive Supercoiling of DNA by *T. maritima* Reverse Gyrase, *J. Mol. Biol.*, **2007**, *371*, 197-209.

(5) Forterre P., A Hot Story from comparative genomics: reverse gyrase is the only hyperthermophile-specific protein, *Trends in Genetics*, **2002**, *18*, 236-238.

(6) del Toro Duany Y., Jungblut S. P., Schmidt A. S., Klostermeier D., The reverse gyrase helicase-like domain is a nucleotide-dependent switch that is attenuated by the topoisomerase domain, *Nucleic Acids Research*, **2008**, *36*, 5882-5895.

(7) Rodríguez A. C., Stock D., Crystal structure of reverse gyrase: insights into the positive supercoiling of DNA, *EMBO*, **2002**, *21*, 418-426.

(8) LeBel D., Poirier G. G., Phaneuf S., St.-Jean P., Laliberte J. F., Beaudoin A. R., Characterization and Purification of a Calcium-sensitive ATP Diphosphohydrolase from Pig Pancreas, *J. Biol. Chem.*, **1980**, *255*, 1227-1233.

(9) Valadão Sales P. B., Santoro M. L., Nucleotidase and DNase activities in Brazilian snake venoms, Comp. Biochem. & Physiol., **2008**, 147, 85-95.

(10) Hongo K., Hirai H., Uemura C., Ono S., Tsunemi J., Higurashi T., Mizobata T., Kawata Y., A novel ATP/ADP hydrolysis activity of hyperthermostable group II chaperonin in the presence of cobalt or manganese ion, *FEBS Letters*, **2006**, *580*, 34-40.

(11) Kampmann, M. Stock, D., Reverse gyrase has heat-protective DNA chaperone activity independent of supercoiling, *Nucleic Acids Res.*, **2004**, *32*, 3537-3545.

(12) Noda, L. H., Adenylate Kinase, *Enzymes* (3rd Ed.), **1973**, 279-305.

(13) Shibata T., Nakasug S., Yasuip K., Kikuch A, Intrinsic DNA-dependent ATPase Activity of Reverse Gyrase, *J. Biol. Chem.*, **1987**, *262*, 10419-10421.

(14) Kovalsky O.I., Kozyavkin S.A., Slesarev A.I, Archaebacterial reverse gyrase cleavage-site specificity is similar to that of eubacterial DNA topoisomerases I, *Nucleic Acids Res.*, **1990**, *18*, 2801-2805.

(15) Jencks W.P., Handbook of Biochemistry and Molecular Biology, *CRC Press (Boca Raton, FL)*, **1976**, *3rd edition*.

6. The Reverse Gyrase Helicase-like Domain is a Nucleotide-dependent Switch that is Attenuated by the Topoisomerase Domain

Nucleic Acid Research, 2008

Vol. *36*, 5882-5895

Yoandris del Toro Duany*, Stefan P. Jungblut*, Andreas S. Schmidt and Dagmar Klostermeier (*joint First Authors)

University of Basel, Biozentrum, Department of Biophysical Chemistry, Klingelbergstrasse 70, CH-4056 Basel, Switzerland

Tel: +41 61 267 2381, Fax: +41 61 267 2189, E-mail: dagmar.klostermeier@unibas.ch

6.1 Summary

Reverse gyrase is a hyperthermophilic enzyme with a unique ATP-dependent positive plasmid supercoiling ability. The N-terminal helicase-like domain of reverse gyrase harbours sequence motifs for ATP hydrolysis and the C-terminally fused topoisomerase IA domain contains the catalytically active tyrosine needed for DNA strand cleavage. The isolated domains are both incapable of DNA unwinding or positive supercoiling. However, active reverse gyrase can be reconstituted from the isolated helicase-like and topoisomerase domains, suggesting that functional cooperativity of these two domains is necessary for positive supercoiling. However, the precise role of the helicase-like domain for the positive supercoiling mechanism of reverse gyrase remains unknown.

We characterised the isolated helicase-like domain of reverse gyrase from *Thermotoga maritima* in comparison to the full-length enzyme. The results in this chapter demonstrate that the helicase-like domain of reverse gyrase from *T. maritima* is a fully functional ATPase. The isolated helicase-like domain harbours all determinants for nucleotide binding, ATP hydrolysis and DNA-stimulated ATPase activity of reverse gyrase. These abilities are unaltered in the context of the full-length enzyme in the absence of DNA, suggesting that the conformation of the isolated helicase-like domain is similar in the context of the full-length enzyme. Similarly, we already reported that both ATP and ATPγS hydrolysis facilitate positive supercoiling by reverse gyrase, suggesting that hydrolysis of these nucleotides is sufficient for conformational changes during the nucleotide cycle.

In the presence of ssDNA or dsDNA and pUC18, ATP hydrolysis is vastly accelerated for the helicase-like domain and full-length reverse gyrase. However, the DNA-stimulated ATPase is still 10-fold lower for the full-length enzyme. Hence, we suggest that the helicase-like domain rapidly closes and hydrolyses ATP in the presence of DNA. Conformational changes in the helicase-like domain of the full-length enzyme are much slower, and cooperativity between ATP and DNA binding is reduced. Furthermore, our results confirm earlier qualitative findings that reverse gyrase interacts much more tightly with ssDNA than dsDNA. This was also reported for other type I topoisomerases. Strand cleavage was shown to be favoured in ssDNA regions, and thus, sensing and stabilisation of ssDNA regions may be required for positive supercoiling.

Reverse gyrase contains several potential binding sites for DNA: the helicase-like domain, the latch region, the cleft in the topoisomerase domain near the catalytic tyrosine residue

and two putative zinc finger regions. Characterisation of the potential DNA binding sites has not been carried out for reverse gyrase. We succeeded in an initial quantification of DNA substrate binding to reverse gyrase using the Y851F mutant of the full-length enzyme, where covalent binding of DNA substrates is excluded. Binding affinities for DNA are 10-fold weaker in the isolated helicase-like domain of reverse gyrase. Surprisingly, we found cooperative binding of two full-length reverse gyrase molecules to one ssDNA molecule. This may indicate a functional role of a protein-protein interaction on the same DNA substrate that could be important for positive supercoiling by reverse gyrase. Cooperative binding to ssDNA is less pronounced in the isolated helicase-like domain. More information about DNA affinity was obtained using the reverse gyrase K106Q mutant, lacking ATPase activity. While in the ATP-bound state, ssDNA and dsDNA are similarly bound by the helicase-like domain, but affinity for dsDNA is reduced after ATP hydrolysis in the presence of ADP. In the full-length reverse gyrase, the difference for ssDNA or dsDNA affinity is much smaller in the ADP and ATP state.

Overall, our findings allowed for the proposal of a schematic nucleotide cycle for reverse gyrase and the isolated helicase-like domain and we showed that the helicase-like domain is a nucleotide-dependent switch for DNA affinity.

6.2 Published Article

5882–5895 *Nucleic Acids Research, 2008, Vol. 36, No. 18* *Published online 16 September 2008*
doi:10.1093/nar/gkn587

The reverse gyrase helicase-like domain is a nucleotide-dependent switch that is attenuated by the topoisomerase domain

Yoandris del Toro Duany, Stefan P. Jungblut, Andreas S. Schmidt and Dagmar Klostermeier*

University of Basel, Biozentrum, Biophysical Chemistry, Klingelbergstrasse 70, 4056 Basel, Switzerland

Received July 9, 2008; Revised and Accepted September 1, 2008

ABSTRACT

Reverse gyrase is a topoisomerase that introduces positive supercoils into DNA in an ATP-dependent manner. It is unique to hyperthermophilic archaea and eubacteria, and has been proposed to protect their DNA from damage at high temperatures. Cooperation between its N-terminal helicase-like and the C-terminal topoisomerase domain is required for positive supercoiling, but the precise role of the helicase-like domain is currently unknown. Here, the characterization of the isolated helicase-like domain from *Thermotoga maritima* reverse gyrase is presented. We show that the helicase-like domain contains all determinants for nucleotide binding and ATP hydrolysis. Its intrinsic ATP hydrolysis is significantly stimulated by ssDNA, dsDNA and plasmid DNA. During the nucleotide cycle, the helicase-like domain switches between high- and low-affinity states for dsDNA, while its affinity for ssDNA in the ATP and ADP states is similar. In the context of reverse gyrase, the differences in DNA affinities of the nucleotide states are smaller, and the DNA-stimulated ATPase activity is strongly reduced. This inhibitory effect of the topoisomerase domain decelerates the progression of reverse gyrase through the nucleotide cycle, possibly providing optimal coordination of ATP hydrolysis with the complex reaction of DNA supercoiling.

INTRODUCTION

Reverse gyrase is the only topoisomerase that introduces positive supercoils into DNA at the expense of ATP hydrolysis (1). It is unique to hyperthermophilic archaea and eubacteria. Deletion of the reverse gyrase gene in a hyperthermophilic archaeon leads to growth retardation at higher temperatures, but the organism is still able to survive at 90°C, demonstrating that reverse gyrase is not strictly required for hyperthermophilic life (2,3). The *in vivo* function of reverse gyrase is not clear. A heat-protective DNA chaperone activity (4) and a DNA renaturase activity (5) have been reported, indicating that reverse gyrase protects DNA from damage at high temperatures.

Reverse gyrase consists of an N-terminal helicase-like domain, fused to a C-terminal topoisomerase I domain. While most reverse gyrases are monomeric, a covalent connection between the two domains is not required for positive supercoiling activity. The *Methanopyrus kandleri* reverse gyrase is a dimeric enzyme, with the helicase-like and part of the topoisomerase domain in one subunit, and the remainder of the topoisomerase domain provided by the second subunit (6,7). Furthermore, an active reverse gyrase can be reconstituted by mixing separately produced helicase-like and topoisomerase domains (8; Hilbert,M. and Klostermeier,D., unpublished data). Nevertheless, a functional cooperation of helicase-like and topoisomerase domains is required for positive supercoiling by reverse gyrase (8,9).

The helicase-like domain shares the three-dimensional structure with helicases of the superfamily (SF) 2, namely two tandem RecA-folds (H1, H2) connected by a linker (Figure 1). In reverse gyrase, the subdomain H2 is interrupted by the so-called latch domain (H3) that shows homology to the region of the transcription termination factor Rho that is involved in RNA binding (10). The reverse gyrase helicase-like domain comprises all signature motifs of SF2 helicases, but the sequences of these motifs show large deviations from the consensus (Supplementary Figure S1). These sequence variations may be responsible for the lack of unwinding activity by reverse gyrase or the isolated helicase-like domain (8). Reverse gyrase does not catalyze relaxation in the absence of nucleotides, whereas the topoisomerase domain on its own can relax DNA in

*To whom correspondence should be addressed. Tel: +41 61 267 2381; Fax: +41 61 267 2189; Email: dagmar.klostermeier@unibas.ch

The authors wish it to be known that, in their opinion, the first two authors should be regarded as joint First Authors.

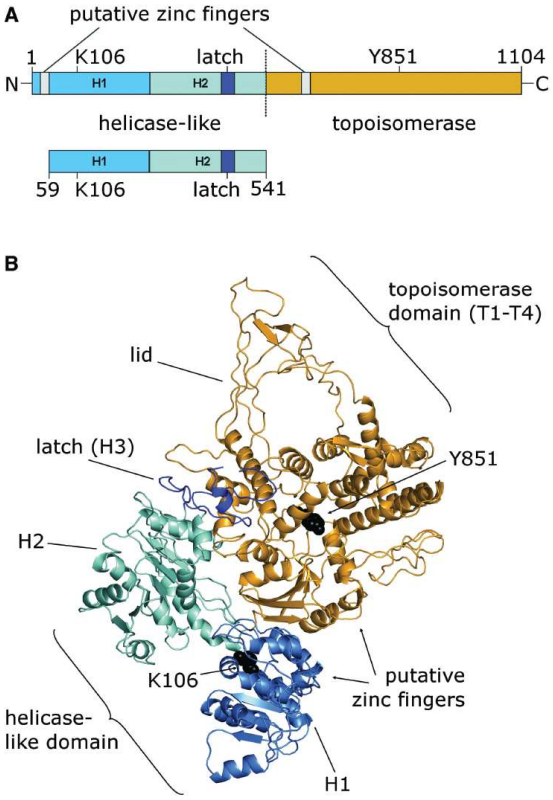

Figure 1. Reverse gyrase and its helicase-like domain. (**A**) Full-length reverse gyrase, consists of an N-terminal helicase-like domain [H1, light blue, H2, cyan, H3 (latch), blue] and a C-terminal topoisomerase domain (orange). The helicase-like domain construct comprises the helicase-like domain (H1 and H2), and the latch-domain H3 that is inserted into H2. The positions of K106 in the Walker A motif and of the catalytic tyrosine, Y851 (black), and the putative zinc fingers (gray) are indicated. (**B**) Structure of *A. fulgidus* reverse gyrase [PDB-ID 1GKU, Ref. (10)], color-coded as in (A). The regions carrying the putative zinc fingers are missing in the electron density.

the absence of nucleotides, but lacks supercoiling activity (8,11). It has been suggested that the latch domain suppresses relaxation in reverse gyrase in the absence of nucleotides (12).

Based on the crystal structure of the reverse gyrase from *Archaeoglobus fulgidus* (10), a mechanism for positive supercoiling has been postulated that is based on a conformational change of the helicase-like domain as the initiating step, leading to a closure of the cleft between the two RecA-like subdomains. This conformational change may then allow for release of the latch domain, and for swinging-up of the 'lid' region in the topoisomerase domain, which is required for strand passage (Figure 1B). We have recently shown that such a conformational change occurs in SF2 helicases in response to the cooperative binding of ATP and nucleic acid substrates (13). Furthermore, we have demonstrated that reverse gyrase can use ATP or ATPγS as the energy source for positive supercoiling, suggesting that both nucleotides can power the conformational cycle (14). This ATPγS-dependent activity has also been observed for the translation factor eIF4A, a member of the SF2 helicase family (15), which further indicates mechanistic similarities of the reverse gyrase helicase-like domain and SF2 helicases. Although the helicase-like domain is a crucial element for ATP-dependent positive supercoiling by reverse gyrase, its role is currently not well understood. We present here the characterization of nucleotide binding, ATP hydrolysis, DNA binding and DNA-stimulation of the ATPase activity for the isolated helicase-like domain of *Thermotoma maritima* reverse gyrase and compare it to the properties of reverse gyrase. The helicase-like domain confers nucleotide-dependent DNA binding to reverse gyrase. The isolated domain is an efficient DNA-stimulated ATPase, but the topoisomerase domain in reverse gyrase exerts a moderating effect onto the ATPase activity, slowing down the nucleotide cycle by a factor of 10. This intra-molecular inhibition suggests that the helicase-like domain is harnessed by reverse gyrase to provide efficient coupling of ATPase activity with the supercoiling reaction.

MATERIALS AND METHODS

Cloning, mutagenesis, protein production and purification

The region encoding the helicase-like domain of reverse gyrase (E59-R541, rGyr_hel) was PCR-amplified from the full-length gene and cloned into pET28a using NcoI and XhoI restriction sites. Site-directed mutagenesis was performed according to the Quikchange protocol (Stratagene, La Jolla, CA, USA).

rGyr_hel was produced at 37°C in *Escherichia coli* Rosetta (DE3) (Invitrogen, Paisley, U.K) in autoinducing medium (16), and cells were harvested after 24 h. All purification steps were performed at room temperature. Cells were disrupted in a Microfluidizer in 50 mM Tris/HCl, pH 7.5, 1 M NaCl, 10 mM $MgCl_2$, 10 μM $Zn(OAc)_2$, 2 mM BME and the crude extract was cleared by centrifugation. The NaCl concentration of the supernatant was adjusted to 0.2 M, and it was applied to a SP sepharose column equilibrated in 50 mM Tris/HCl, pH 7.5, 0.2 M NaCl, 10 mM $MgCl_2$, 10 μM $Zn(OAc)_2$, 2 mM BME. rGyr_hel was eluted in a linear gradient from 0.2–1 M NaCl, dialyzed against 50 mM Tris/HCl, pH 7.5, 0.2 M NaCl, 10 mM $MgCl_2$, 10 μM $Zn(OAc)_2$, 2 mM BME, and applied to a Q sepharose column equilibrated in the same buffer. rGyr_hel was collected in the flowthrough. Final purification was achieved via size-exclusion chromatography on a calibrated S200 column in 50 mM Tris/HCl, pH 7.5, 0.2 M NaCl, 10 mM $MgCl_2$, 10 μM $Zn(OAc)_2$, 2 mM BME. rGyr_hel elutes as a monomer from a calibrated size-exclusion chromatography column (apparent molecular weight: 49.8 kDa, calculated: 56.3 kDa). Protein concentration was determined photometrically using the calculated extinction coefficient at 280 nm of 56 309 $M^{-1} cm^{-1}$. From 1 l of bacterial culture, 4 mg of rGyr_hel with >98% purity (as judged from SDS–PAGE with Coomassie staining) were obtained. The pure protein was concentrated,

5884 Nucleic Acids Research, 2008, Vol. 36, No. 18

shock-frozen in liquid nitrogen, and stored at −80°C. Full-length reverse gyrase was purified as described (14).

Adenine nucleotides and RNA and DNA substrates

Adenine nucleotides were purchased from Pharma Waldhof (Mannheim, Germany) or Jena Bioscience (Jena, Germany), and checked for impurities by reverse-phase HPLC on a C18 column in 0.1 M sodium phosphate, pH 6.5. Oligonucleotides for ssDNA or dsDNA substrates were obtained from Purimex (Grebenstein, Germany). The sequence of the 60-base ssDNA was 5′-(fluorescein)-AAGC CAAGCT TCTAGAGTCA GCCCGTGATA TTCATT ACTT CTTATCCTAG GATCCCCGTT-3′, and the dsDNA substrate was formed by annealing the complementary strand. These substrates contain a preferred cleavage site (17,18) for reverse gyrase; cleavage occurs between the two underlined nucleotides. PolyU-RNA was purchased from Sigma (Hamburg, Germany).

ATPase assays

Steady state ATPase activity was measured in a spectroscopic enzymatic assay that couples ADP production to the oxidation of NADH as described (14). Assay conditions were 50 mM Tris/HCl, pH 7.5, 0.15 M NaCl, 10 mM $MgCl_2$, 100 μM $Zn(OAc)_2$, 2 mM BME, 0.4 mM PEP and 0.2 mM NADH, 23 μg ml^{-1} LDH, 37 μg ml^{-1} PK. ATPase activity at 75°C was determined in 50 mM Tris/HCl, pH 7.5, 0.15 M NaCl, 10 mM $MgCl_2$, 100 μM $Zn(OAc)_2$, 2 mM BME, 10% (w/v) PEG 8000 by mixing 1 μM enzyme, 2 mM ATP and the respective nucleic acid substrate, taking aliquots at different time points, and analyzing the nucleotide composition by reverse-phase HPLC as described (14).

Fluorescence measurements

Dissociation constants of rGyr_hel/nucleotide complexes were determined in fluorescence equilibrium titrations at 37°C using 1 μM of the fluorescent ADP analog mantADP (19) and in competitive titrations of the mantADP/rGyr_hel complex with ADP, ATPγS, ADPNP, ADPCP and ATP, and analyzed as described (14).

Dissociation constants of reverse gyrase/DNA complexes were determined using 5′-fluorescein-labeled DNA and the steady-state anisotropy of fluorescein as a probe for binding. The DNA concentrations were 25 nM for titrations with rGyr_hel, and 10 nM for rGyr_fl, unless stated otherwise. Dissociation constants were obtained by analysis of the data using the solution of a quadratic equation describing a one-site binding model as described (14), or with the Hill equation.

Helicase assay

Helicase activity was tested via the displacement of a 10-mer from a 10/50-mer substrate (2 nM) by 10 μM rGyr_hel in 20 mM HEPES/NaOH, pH 7.5, 70 mM KCl, 1 mM MgOAc, 10% (v/v) glycerol, 2 mM DTT and 1 mg/ml BSA as described for eIF4A (20). The ATP concentration was 2 mM.

RESULTS

Nucleotide binding and ATPase properties of the helicase-like domain

The role of the helicase-like domain for DNA supercoiling by reverse gyrase is currently unknown. A detailed understanding of nucleotide binding and hydrolysis by the helicase-like domain and its interaction with DNA, isolated and in the context of reverse gyrase, is a pre-requisite to delineate its function within reverse gyrase. To this end, we subcloned a DNA fragment coding for amino acids 59–541 of *T. maritima* reverse gyrase (rGyr_hel). This construct comprises the two RecA-like domains H1 and H2, and the so-called latch domain H3, but lacks the N-terminal putative zinc finger (Figure 1). The nucleotide binding properties of rGyr_hel were investigated in fluorescent equilibrium titrations using the fluorescent ADP analog mantADP (Figure 2), which we previously used as a probe for nucleotide binding to reverse gyrase (14). Upon binding to rGyr_hel, the mant fluorescence increases 1.5-fold (Figure 2A). The fluorescence signal returns to the value for free mantADP upon displacement with ADP, confirming that mantADP binds to the ADP binding site and is thus suitable to study nucleotide binding to rGyr_hel. The K_d value of the mantADP/rGyr_hel complex determined from the titration curves is 1.1 ± 0.1 μM. In the displacement titration with ADP (Figure 2B), a K_d value of 2.6 ± 0.8 μM was determined for the ADP complex. The K_d value of the rGyr_hel/AMP complex is three orders of magnitude higher (1600 ± 231 μM), demonstrating that interactions with the β-phosphate provide high affinity binding of adenine nucleotides to rGyr_hel. The ATP analogs ATPγS, ADPNP and ADPCP are bound less tightly than ADP (Figure 2B), with K_d values for the complexes of 10.9 ± 0.8 μM (ATPγS), 20 ± 4.9 μM (ADPNP) and 18 ± 3.8 μM (ADPCP), respectively, indicating that the binding energy from additional interactions with the γ-phosphate is converted into conformational changes. The corresponding K_d values for the full-length reverse gyrase (rGyr_fl) are virtually identical in the case of the mantADP, ADP and AMP complexes, and of the ATP analog ATPγS, and 2- to 4-fold higher for the complexes with the nonhydrolyzable ATP analogs ADPNP and ADPCP (14). The similar K_d values confirm that all determinants for nucleotide binding are contained in the helicase-like domain. A summary of the K_d values for rGyr_fl and rGyr_hel is given in Table 1.

In a steady state ATPase assay, rGyr_hel exhibits a low intrinsic ATPase activity (Figure 3). As with rGyr_fl (14), the rate constant k_{cat} of ATP hydrolysis by rGyr_hel is independent of the protein concentration (<10 μM, data not shown), consistent with a monomer as the active species. The dependence of the ATP hydrolysis rate on ATP concentration follows Michaelis–Menten behavior, with a k_{cat} for ATP hydrolysis of 30 (± 2) × 10^{-3} s^{-1}, and a K_M value for ATP of 77 ± 23 μM. The corresponding values for reverse gyrase are very similar with a k_{cat} of 20 (± 0.8) × 10^{-3} s^{-1} and a K_M of 44 ± 6 μM (14).

These results demonstrate that the nucleotide binding properties and the intrinsic ATPase activity of reverse

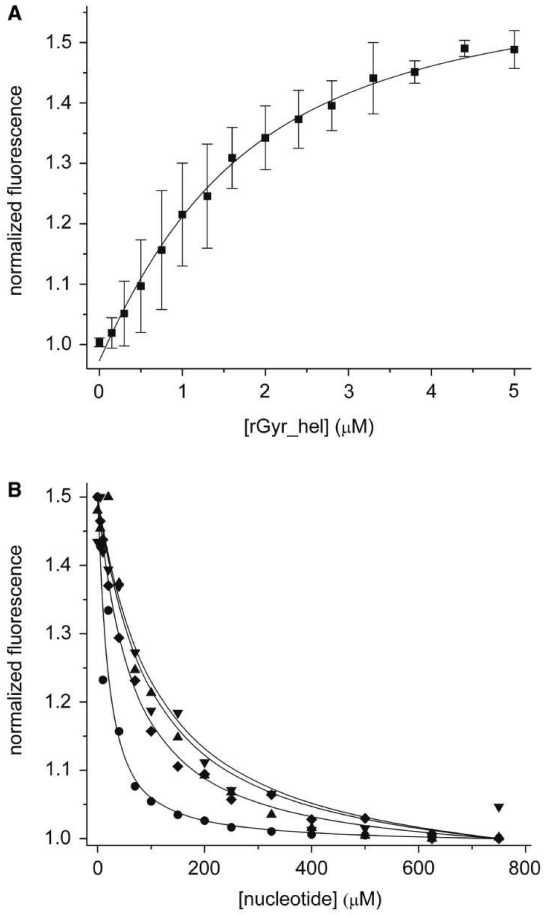

Figure 2. Interaction of rGyr_hel with nucleotides. (**A**) Titration of 1 μM mantADP with rGyr_hel. Description of the binding curve using a one-site binding model yields a K_d of the mantADP/rGyr_hel complex of 1.1 ± 0.1 μM. (**B**) Displacement titrations of the mantADP/rGyr_hel complex with ADP (circles), ADPCP (triangle), ADPNP (inverted triangle), and ATPγS (diamond). The K_d values are summarized in Table 1.

Table 1. Dissociation constants for nucleotide complexes of full-length reverse gyrase and the helicase-like domain

Nucleotide	rGyr_fl K_d (μM)	rGyr_hel K_d (μM)	rGyr_fl K106Q/Y851F K_d (μM)	rGyr_hel K106Q K_d (μM)
mantADP	1.0 ± 0.1[a]	1.1 ± 0.1	22 ± 2	67 ± 5
AMP	1549 ± 375	1600 ± 231	ND	ND
ADP	1.6 ± 0.2[a]	2.6 ± 0.8	36 ± 5	150 ± 85
ATP	ND	ND	98 ± 12	570 ± 300
ATPγS	14.3 ± 1.5[a]	10.9 ± 0.8	ND	ND
ADPNP	43.2 ± 2.0[a]	19.8 ± 4.9	ND	ND
ADPCP	74.7 ± 7.3	17.5 ± 3.8	ND	ND

[a]Data from Ref. (14).

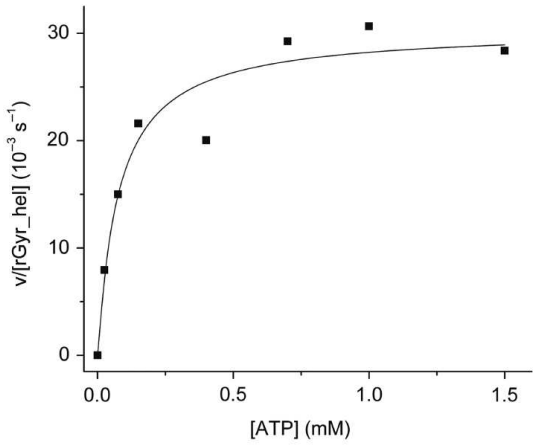

Figure 3. Steady state ATPase activity of rGyr_hel. rGyr_hel is a Michaelis–Menten enzyme with a k_{cat} of 30 $(\pm 2) \times 10^{-3}$ s^{-1}, and a $K_{M,ATP}$ of 77 ± 23 μM.

gyrase are a property of the helicase-like domain and are not significantly affected by the topoisomerase domain.

Stimulation of the rGyr_hel and rGyr_fl ATPase activities by nucleic acids

Reverse gyrases are DNA-stimulated ATPases (21). To investigate the effect of nucleic acid substrates on the ATPase activity of rGyr_hel, steady state ATPase assays were performed in the presence of a 60-base ssDNA substrate, a 60 bp dsDNA, pUC18 plasmid DNA, and polyU-RNA at saturating ATP concentrations (Figure 4A). All substrates led to a significant acceleration of ATP hydrolysis. Saturating concentrations of ssDNA or linear dsDNA increased the k_{cat} by a factor of 40–50, with a slightly higher stimulation by dsDNA. The apparent K_M values are 0.07 ± 0.04 μM for ssDNA (corresponding to 4 μM in terms of bases) and 0.18 ± 0.03 μM for dsDNA (11 μM base pairs), respectively. In the presence of negatively supercoiled pUC18 plasmid, the k_{cat} value increased 22-fold (K_M 0.046 ± 0.006 μM, corresponding to 124 μM base pairs).

Interestingly, polyU-RNA also stimulated the intrinsic ATPase activity of rGyr_hel tremendously (~100-fold). With 25 μM (bases), the apparent K_M value for polyU-RNA was in the same range as for the pUC18 plasmid. PolyU-RNA binding might reflect nonspecific interactions with the negatively charged phosphoribose backbone, and we therefore repeated the steady state ATPase assay in the presence of increasing concentrations of heparin as a model for a negatively charged polymer. Indeed, heparin increased the k_{cat} of rGyr_hel for ATP hydrolysis ~80-fold and thus had a comparable effect to the polyU-RNA. The K_M value for heparin was 0.20 ± 0.05 μM (8 μM monomeric units) and thus also similar to polyU.

To compare ATPase properties of the helicase-like domain with reverse gyrase, the steady state ATPase rates in the presence of ssDNA, dsDNA, pUC18 and

5886 Nucleic Acids Research, 2008, Vol. 36, No. 18

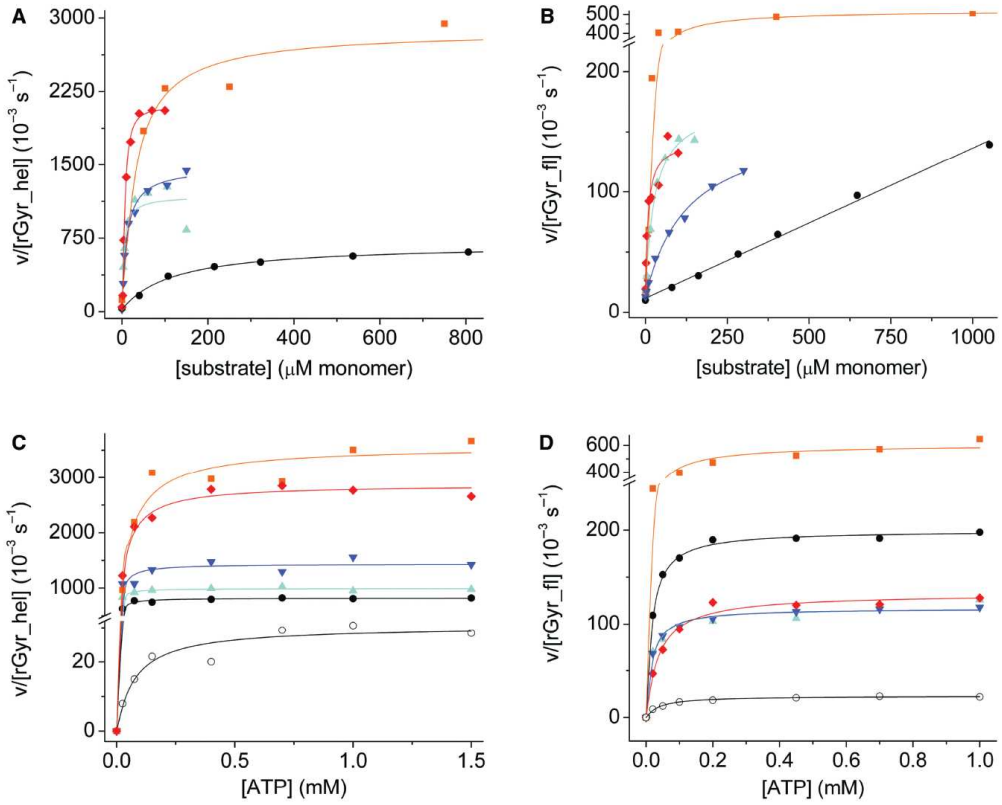

Figure 4. Effect of nucleic acid substrates on the steady state ATPase activity of rGyr_hel and rGyr_fl. (**A** and **B**) The effect of nucleic acid substrates on the ATPase rate at saturating (1 mM) ATP. (**C** and **D**) The ATP-dependence of the ATPase rate at saturating concentrations of nucleic acids. Substrates are indicated as follows: ssDNA (cyan, triangles), dsDNA (blue, inverted triangles), pUC18 (black, circles), polyU-RNA (orange, squares) and heparin (red, diamond). The open symbols in (C and D) indicate data in the absence of DNA. All steady state ATPase parameters are summarized in Tables 2 and 3. (A) Stimulation of the rGyr_hel ATPase by nucleic acids and heparin. The ATPase activity is significantly stimulated by all substrates. (B) Stimulation of the rGyr_fl ATPase by nucleic acids and heparin. The ATPase activity is significantly stimulated by all substrates, but in contrast to rGyr_hel, no saturation is observed with pUC18. (C) Cooperativity between ATP and nucleic acid binding in rGyr_hel. The steady state ATPase activity was measured as a function of ATP concentration in the presence of saturating concentrations of ssDNA (2 μM,), dsDNA (2.5 μM), pUC18 (300 nM), polyU-RNA (1.5 mM monomers) and heparin (40 μM monomers). (D) Cooperativity between ATP and nucleic acid binding in rGyr_fl. The steady state ATPase activity was measured as a function of ATP concentration in the presence of saturating concentrations of ssDNA (2 μM,), dsDNA (5 μM), pUC18 (300 nM), polyU-RNA (0.5 mM monomers) and heparin (60 μM monomers).

polyU-RNA were also determined for rGyr_fl (Figure 4B). As with rGyr_hel, linear ssDNA and dsDNA showed a similar effect on the ATPase rate of rGyr_fl. Importantly, the stimulation of the ATPase activity by ssDNA and dsDNA was only 7- to 8-fold. The ATPase rate of rGyr_fl increases linearly up to a pUC18 concentration of 400 nM (1.1 mM bases), and saturation is not observed (14). In contrast to rGyr_hel, pUC18 only showed a moderate stimulation of the rGyr_fl ATPase rate (7-fold at 400 nM pUC18, compared to 22-fold at saturation for rGyr_hel). As with rGyr_hel, polyU-RNA showed the highest degree of stimulation of the reverse gyrase ATPase activity, with k_{cat} increased 25-fold (K_M 30 μM bases), and heparin showed a 6-fold stimulation (K_M 6 μM monomeric units). These data indicate that interactions with nonspecific substrates are similar for rGyr_hel and rGyr_fl. The k_{cat} values for rGyr_fl and rGyr_hel in the absence and presence of nucleic acids and the apparent K_M values are summarized in Table 2.

Reverse gyrase is an enzyme unique to hyperthermophilic organisms, which thrive at temperatures of 75°C and higher. To investigate if the results from experiments at 37°C reflect the properties of reverse gyrase at its optimum temperature, the ATPase activity was determined at 75°C in the absence of DNA, and in the presence of ssDNA, dsDNA and pUC18 (Figure 5). In the absence of DNA, the ATPase activities of rGyr_fl and rGyr_hel are similar, with initial rates of 0.28 μM s^{-1} (rGyr_hel) and 0.48 μM s^{-1} (rGyr_fl). While we have determined the affinities for DNA substrates at 37°C and could therefore ensure saturating DNA concentrations in ATPase assays, a quantitative comparison of the ATPase stimulation at 75°C is difficult as the corresponding K_d values cannot easily be determined, and the DNA concentrations may not

Table 2. Steady state ATPase parameters for rGyr_hel and rGyr_fl, and the influence of nucleic acid substrates

	Nucleic acid	k_{cat} (10^{-3} s^{-1})	$K_{M,DNA}$ (μM)	K_M (μM base/bp)
rGyr_hel	–	30 ± 2	NA	NA
	ssDNA	1160 ± 188	0.07 ± 0.04	4.2 ± 2.4
	dsDNA	1450 ± 64	0.18 ± 0.03	10.8 ± 1.8
	pUC18	673 ± 21	0.046 ± 0.006	124 ± 16
	polyU-RNA	3264 ± 304	NA	25 ± 10
	Heparin	2420 ± 160	0.20 ± 0.05	8.0 ± 0.04
rGyr_fl	–	20 ± 0.8	NA	NA
	ssDNA	160 ± 6.7	0.45 ± 0.06	27 ± 4
	dsDNA	148 ± 9.1	2.2 ± 0.30	129 ± 18
	pUC18	No saturation for conc. <400 nM		
	polyU-RNA	507 ± 27	NA	30 ± 7
	Heparin	120 ± 10	0.15 ± 0.06	6 ± 2.4

be saturating. In addition, the thermodynamic stability of the 60 bp duplex is limited (T_m = 70°C), and at 75°C more than 50% single strand are expected. Qualitatively, the rGyr_hel ATPase activity at 75°C is stimulated to a similar extent by ssDNA and dsDNA at 75°C, and about 2-fold less by pUC18. Overall, the ATPase activity is increased only 3-fold by DNA substrates, compared to 50-fold at 37°C. The rGyr_fl ATPase is most efficiently stimulated by ssDNA, and to a smaller extent by dsDNA or pUC18. As observed at 37°C, the overall stimulation is smaller for rGyr_fl than for rGyr_hel. Thus, the rGyr_hel and rGyr_fl ATPase activities at 75°C show the same response to DNA as at 37°C.

In summary, the basal ATP hydrolysis rates are very similar for rGyr_hel and rGyr_fl, confirming that all determinants for ATP binding and hydrolysis are confined to the helicase-like domain. The intrinsic ATPase of rGyr_hel is efficiently stimulated by ssDNA, dsDNA and plasmid DNA. All substrates also stimulate the intrinsic ATP hydrolysis of rGyr_fl, but generally to a lesser extent. These data point towards an inhibitory effect of the topoisomerase domain on the ATPase activity of the helicase-like domain in the presence of DNA substrates. The apparent K_M values for DNA are higher for rGyr_fl than for rGyr_hel. This effect seems to be slightly more pronounced for dsDNA, leading to a 5-fold higher apparent K_M for dsDNA over ssDNA for rGyr_fl, compared to an only 2.5-fold difference for rGyr_hel. Both enzymes thus appear to interact more tightly with ssDNA. Interestingly, the apparent K_M values for polyU-RNA and heparin are identical for rGyr_fl and rGyr_hel, indicating similar interactions with nonspecific substrates.

Coupling between DNA and ATP binding to rGyr_hel and rGyr_fl

The interaction of SF2 helicases with ATP and their DNA substrate is cooperative: ATP binding increases the affinity for the DNA substrate, and vice versa (13,22–24). To test whether any of the nucleic acid substrates shows such a cooperative effect on ATP binding to rGyr_hel or rGyr_fl, we determined the effect of DNA on K_M values for ATP by measuring the steady state ATPase rate with increasing

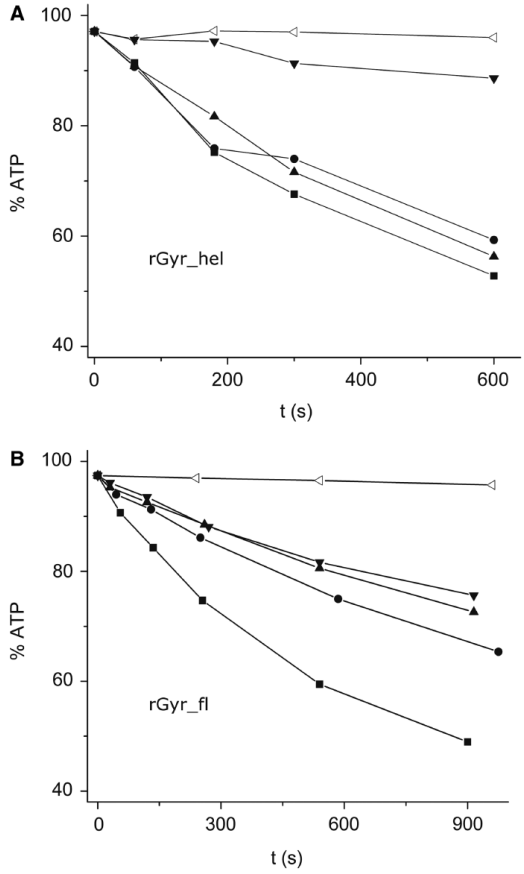

Figure 5. DNA-stimulated ATPase activity at 75°C. ATPase activity of rGyr_hel (**A**) and rGyr_fl (**B**) at 75°C in the absence of enzyme (open triangles), in the presence of 1 μM enzyme without DNA (inverted triangles) and in the presence of ssDNA (100 nM, squares), dsDNA (100 nM, circles), or pUC18 (15 nM, triangles). The ATP concentration was 1 mM.

concentrations of ATP and saturating concentrations of the nucleic acid (Figure 4C and D). In all cases, the k_{cat} values are in good agreement with the values in the DNA-dependent experiments at saturating ATP concentrations (Table 2), confirming that saturation is reached in both series of experiments. In the presence of ssDNA, the apparent $K_{M,ATP}$ value of rGyr_hel is decreased 16-fold, demonstrating cooperative binding of ATP and ssDNA to rGyr_hel. For dsDNA, this cooperativity is lower than for ssDNA, with $K_{M,ATP}$ decreased 7-fold. The effect of pUC18 plasmid is intermediate, with a 10-fold decrease in the apparent $K_{M,ATP}$. Hence, all DNA substrates promote ATP binding to rGyr_hel. PolyU-RNA and heparin only affect the apparent $K_{M,ATP}$ slightly (1.8-fold and 2.5-fold, respectively) and thus do not show significant cooperativity. These data corroborate the notion that the stimulating effect of polyU-RNA and heparin on the ATPase activity of rGyr_hel is due to a nonspecific interaction.

5888 Nucleic Acids Research, 2008, Vol. 36, No. 18

For rGyr_fl, limited cooperativity of DNA and ATP binding was detected (Figure 4D). The reduction of the $K_{M,ATP}$ was 3.8-fold for ssDNA and 2.8-fold for dsDNA. Hence, as for rGyr_hel, the cooperativity with ATP binding is highest for ssDNA. However, the cooperativity of DNA and ATP binding to rGyr_fl is smaller for ssDNA and dsDNA compared to rGyr_hel. For pUC18, it was not possible to perform the experiment under saturating conditions. At 300 nM pUC18, $K_{M,ATP}$ was reduced 2.8-fold. This is similar to the effect of linear dsDNA, whereas for rGyr_hel, pUC18 shows intermediate cooperativity to ssDNA and dsDNA. However, a more pronounced effect of pUC18 on $K_{M,ATP}$ for rGyr_fl at higher plasmid concentrations cannot be excluded. Overall, rGyr_fl shows cooperative interactions with DNA and ATP, but to a lesser extent than rGyr_hel. PolyU-RNA and heparin had a negligible effect on ATP binding (1.4-fold and 1.2-fold, respectively), consistent with a nonspecific interaction. The k_{cat} and $K_{M,ATP}$ values are summarized in Table 3.

Altogether, the interaction of rGyr_hel and rGyr_fl with polyU-RNA or heparin and ATP is noncooperative and most likely reflects a nonspecific interaction. Substantial cooperativity is observed for ssDNA, dsDNA or plasmid DNA and ATP binding to rGyr_hel. rGyr_fl also binds ssDNA or dsDNA and ATP cooperatively, but the effect of the DNA on $K_{M,ATP}$ is only 3- to 4-fold, compared to 7- to 16-fold for rGyr_hel. Again, this points towards a moderating effect of the topoisomerase domain on the helicase-like domain in full-length reverse gyrase.

Table 3. Steady state ATPase parameters for rGyr_hel and rGyr_fl: the influence of nucleic acid substrates on $K_{M,ATP}$

	Nucleic acid (saturating)	k_{cat} (10^{-3} s^{-1})	$K_{M,ATP}$ (μM)
rGyr_hel	–	30 ± 2	77 ± 23
	ssDNA	992 ± 12	4.8 ± 1.0
	dsDNA	1435 ± 57	11 ± 4
	pUC18	818 ± 10	7.4 ± 1.1
	polyU-RNA	3402 ± 79	42 ± 5.5
	Heparin	2869 ± 63	31 ± 4
rGyr_fl	–	20 ± 0.8	44 ± 6
	ssDNA	108 ± 2.1	12 ± 1.5
	dsDNA	117 ± 1.6	16 ± 1.5
	pUC18 (300 nM)	199 ± 1.6	15.6 ± 0.9
	polyU-RNA	565 ± 19	32 ± 5.1
	Heparin	133 ± 7	37 ± 6.7

Influence of the nucleotide state on DNA binding to rGyr_hel

During their nucleotide cycle, SF2 helicases switch between low affinity and high affinity states for their nucleic acid substrate (22,25,26). We therefore investigated the influence of the nucleotide state of rGyr_hel and rGyr_fl on their interaction with DNA. To this end, the affinity of rGyr_hel for nucleic acids was determined in fluorescence anisotropy titrations of a 5′-fluorescein-labeled 60-base ssDNA or a fluorescein-labeled 60 bp dsDNA in the absence of nucleotides, and in the presence of saturating concentrations of ADP, ADPCP, ADPNP and ATPγS (Figure 6, Table 4).

First, we characterized binding of ssDNA to rGyr_hel (Figure 6A). The K_d value for the rGyr_hel/ssDNA complex was 0.20 ± 0.03 μM in the absence of nucleotide, and varied only moderately with the nucleotide state. The non-hydrolyzable ATP analogs ADPNP and ATPγS showed the largest effect on ssDNA binding, with 3-fold (ADPNP) or 6-fold (ATPγS) increased K_d values, respectively, indicating that the affinity for ssDNA is slightly reduced in the ATP state of rGyr_hel. The ADP state of rGyr_hel binds ssDNA 1.5-fold less tightly than the nucleotide-free state, but 2- to 4-fold more tightly than the ATP-state (mimicked by ADPNP and ATPγS). ADPCP has a similar effect on ssDNA binding as ADP, suggesting that ADPCP is not a suitable mimic for ATP.

When the concentration of ssDNA in the titration with rGyr_hel was increased to 2 μM, a sigmoidal binding curve was obtained, indicating that more than one

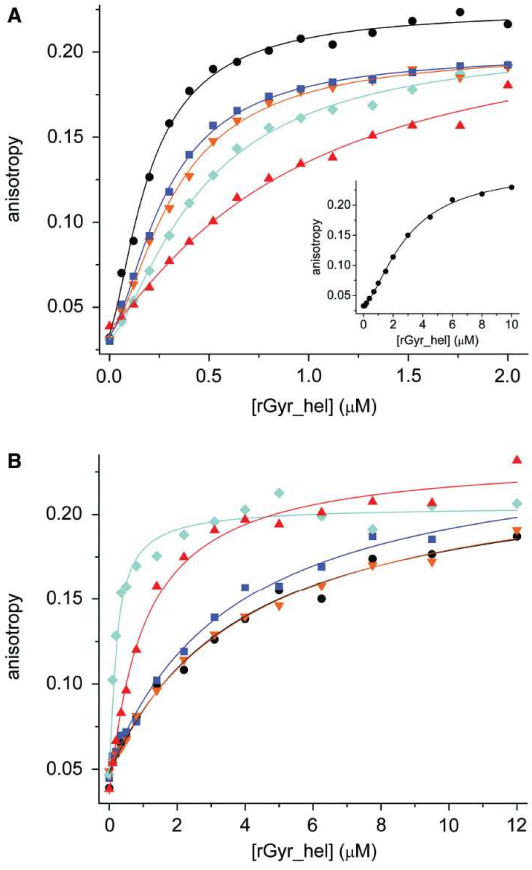

Figure 6. DNA binding and coupling to nucleotide binding (rGyr_hel). Titrations of DNA with rGyr_hel in the absence of nucleotide (black, circles), and in the presence of ADP (100 μM, blue, squares), ADPCP (500 μM, orange, inverted triangles), ATPγS (500 μM, red, triangles) and ADPNP (500 μM, cyan, diamonds). All K_d values and Hill coefficients are summarized in Table 4. (**A**) ssDNA (25 nM). The binding curves are described with the Hill equation. The inset shows the stoichiometric titration of 2 μM ssDNA with rGyr_hel. (**B**) dsDNA (25 nM). The binding curves are described with a one-site binding model.

Table 4. DNA binding properties of different nucleotide states of rGyr_hel

K_d (μM)	nucleotide-free	ADP state		ATP state	
ssDNA					
wt	0.20 ± 0.03[a]	ADP	0.31 ± 0.04[a]	ADPNP	0.60 ± 0.07[a]
	0.20 ± 0.01[b]		0.28 ± 0.01[b]		0.46 ± 0.03[b]
	$n = 1.4 \pm 0.1$		$n = 1.6 \pm 0.1$		$n = 1.4 \pm 0.1$
		ADPCP	0.38 ± 0.05[a]	ATPγS	1.2 ± 0.2[a]
			0.33 ± 0.01[b]		0.92 ± 0.21[b]
			$n = 1.6 \pm 0.1$		$n = 1.2 \pm 0.2$
K106Q	0.18 ± 0.03[a]		0.25 ± 0.03[a]		0.19 ± 0.02[a]
	0.18 ± 0.03[b]		0.24 ± 0.02[b]		0.20 ± 0.02[b]
	$n = 1.3 \pm 0.2$		$n = 1.3 \pm 0.1$		$n = 1.1 \pm 0.1$
dsDNA					
wt	3.9 ± 0.6[a]	ADP	3.7 ± 0.5[a]	ADPNP	0.19 ± 0.03[a]
		ADPCP	4.2 ± 0.3[a]	ATPγS	1.0 ± 0.1[a]
K106Q	3.8 ± 0.6[a]		2.9 ± 0.6[a]		1.7 ± 0.2[a]

[a]One-site.
[b]Hill analysis.

rGyr_hel molecule interacts with each ssDNA (Figure 6A, inset). The data were well-described by the Hill equation, with a Hill coefficient of 1.6 ± 0.1, and a K_d of 2.9 ± 0.1 μM. Analysis of all ssDNA titration curves with the Hill equation gave similar K_d values as the analysis with the one-site binding model (Table 4), and Hill coefficients of 1.2–1.6, indicating that the cooperativity is moderate.

Next, binding of rGyr_hel to dsDNA was characterized (Figure 6B, Table 4). DsDNA was bound 10- to 20-fold less tightly by rGyr_hel than ssDNA, consistent with the observed higher K_M value for dsDNA. The K_d value for dsDNA was ~3.9 μM in the absence of nucleotide, or in the presence of ADP or ADPCP. Only in the presence of ADPNP or ATPγS was a significant change observed: the K_d value of the dsDNA/rGyr_hel complex was decreased 20-fold by ADPNP, or 4-fold by ATPγS. This decrease is consistent with ADPNP and ATPγS mimicking the ATP state. Overall, the ATP state of rGyr_hel thus binds dsDNA 4- to 20-fold more tightly than the ADP state.

Comparison of DNA binding to different nucleotide states (Table 4) reveals that the nucleotide-free form of rGyr_hel shows 20-fold higher affinity for ssDNA over dsDNA. In the ATP state, the affinity for ssDNA remains similar, but the dsDNA affinity increases compared to the nucleotide-free state. Thus, the ATP state exhibits similar affinities for ssDNA and dsDNA. In the ADP state, the affinity for ssDNA is similar to the nucleotide-free or ATP states, but the affinity for dsDNA is reduced compared to the ATP state. As a consequence, ssDNA binding is favored 11- to 13-fold in the ADP state. Hence, during the nucleotide cycle, rGyr_hel does not discriminate between ssDNA and dsDNA prior to ATP hydrolysis, but will preferentially interact with ssDNA after hydrolysis.

Due to thermodynamic coupling, the observed increased affinity of the ATP state for dsDNA requires a reciprocal effect of DNA on ATP binding. Comparison with the steady state ATPase data (Figure 4A and C, Table 3) shows that this coupling is indeed present: the $K_{M,ATP}$ of rGyr_hel is decreased 7-fold in the presence of dsDNA, which is in good agreement with the 4- to 20-fold increased dsDNA affinity in the ATP state of rGyr_hel. The comparison for the ssDNA seems to be inconsistent: the ATP state of rGyr_hel binds ssDNA 3- to 6-fold less tightly than the nucleotide-free form, but $K_{M,ATP}$ is decreased 16-fold when ssDNA is bound. However, the observed differences most likely reflect differences of the ADPNP or ATPγS states compared to the ATP state. This is partly supported by experiments with a hydrolysis-deficient mutant (see below), where ATP binding does not reduce the ssDNA affinity.

Influence of the nucleotide state on DNA binding to rGyr_fl

To test whether the helicase-like domain also acts as a nucleotide-dependent switch with different affinities for dsDNA in the ATP and ADP states in reverse gyrase, we performed DNA binding experiments with rGyr_fl (Figure 7). Quantification of DNA binding to rGyr_fl is complicated by the existence of several potential DNA binding sites that could be located in the helicase-like domain, in the cleft of the topoisomerase domain near the catalytic tyrosine, and possibly at the two putative zinc fingers. To ensure equilibrium conditions, we used the Y851F mutant of reverse gyrase in DNA binding experiments, which is deficient in covalent binding to the DNA.

Again, we first addressed binding of ssDNA to rGyr_fl (Figure 7, Table 5). In a titration of the 60-base ssDNA with rGyr_fl(Y851F), a sigmoidal dependence of the fluorescence anisotropy on the concentration of enzyme was observed (Figure 7A). The binding isotherm was well-described by the Hill equation, with a Hill coefficient of 2.3 (± 0.2) and a K_d of 36 ± 1 nM for nucleotide-free rGyr_fl(Y851F), pointing towards cooperative binding of at least two reverse gyrase molecules to the DNA. To confirm the existence of cooperativity, the titration was repeated at 300 nM of ssDNA, where the sigmoidality became much more prominent (Figure 7A, inset). Description with the Hill equation yielded $K_d = 0.33 \pm 0.02$ μM, and $n = 2.0 \pm 0.14$). In the presence of saturating concentrations of ADP, ADPCP, ADPNP or ATPγS, binding isotherms for ssDNA to rGyr_fl remained sigmoidal (Figure 7A), with Hill coefficients from 1.8 ± 0.10 to 2.1 ± 0.16, again consistent with two reverse gyrase molecules binding to one ssDNA molecule.

Overall, rGyr_fl binds ssDNA 6-fold more tightly than rGyr_hel. In the presence of ADP, the interaction with ssDNA is only slightly affected, and it is virtually unchanged in the presence of nonhydrolyzable ATP analogs. Consequently, the affinity of rGyr_fl for ssDNA is not significantly modulated by the nucleotide state.

Next, the interaction of rGyr_fl(Y851F) with dsDNA was characterized (Figure 7, Table 5). Interestingly, the cooperativity was less pronounced for rGyr_fl binding to dsDNA (Figure 7B). In this case, the binding isotherm could be described by a simple one-site model with a K_d of 490 ± 60 nM. Thus, rGyr_fl interacts 8-fold more tightly with dsDNA than rGyr_hel. dsDNA bound to rGyr_fl was displaced upon addition of an excess of

5890 Nucleic Acids Research, 2008, Vol. 36, No. 18

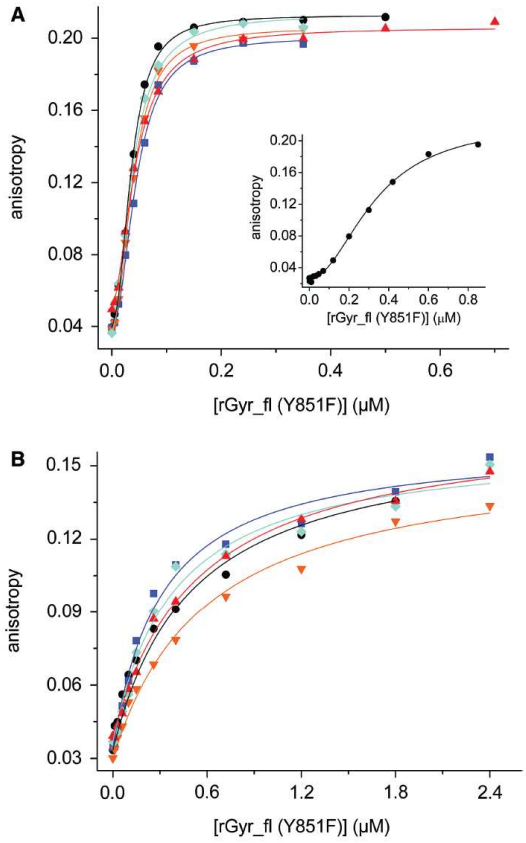

Figure 7. DNA binding and coupling to nucleotide binding (rGyr_fl). Titration of DNA with rGyr_fl in the absence of nucleotide (black, circles), and in the presence of ADP (100 μM, blue, squares), ADPCP (500 μM, orange, inverted triangles), ATPγS (500 μM, red, triangles) and ADPNP (500 μM, cyan, diamonds). All K_d values and Hill coefficients are summarized in Table 5. (**A**) ssDNA (10 nM). The binding curves are described with the Hill equation. The inset shows the stoichiometric titration of 300 nM ssDNA with rGyr_fl. (**B**) dsDNA (10 nM). The binding curves are described with a one-site binding model.

ssDNA (data not shown), demonstrating that both types of nucleic acids interact with the same binding site.

In the presence of nucleotides, the cooperativity of dsDNA binding appeared to increase slightly, as indicated by a slightly improved fit with the Hill equation. Hill coefficients varied between 0.7 and 1.7, consistent with a lower cooperativity compared to ssDNA (or a reduced number of binding sites). However, the experimental data were already reasonably well described with the one-site binding model. The presence of ADP, ADPNP, ADPCP or ATPγS affects the affinity of rGyr_fl for dsDNA <2-fold.

Comparison of DNA binding to different nucleotide states of rGyr_fl (Table 5) shows that the nucleotide-free form binds dsDNA 14-fold less tightly than ssDNA. In the ATP or state, ssDNA or dsDNA binding are not affected. However, the ADP state binds dsDNA 2-fold more tightly than the nucleotide-free and the ATP states. In the nucleotide cycle, both the ATP and the ADP state bind ssDNA more tightly than dsDNA. The preference for ssDNA is slightly reduced after hydrolysis (from 10-fold in the ATP state to 4-fold in the ADP state). The small effect of nucleotides on DNA binding to rGyr_fl is consistent with the small effect of ssDNA and dsDNA on ATP binding according to the steady state ATPase data (Figure 4B and D, Table 3).

In summary, the ATP state of rGyr_hel binds ssDNA and dsDNA with equal affinities, whereas the ADP state interacts preferentially with ssDNA. rGyr_fl binds DNA ~10-fold more tightly than rGyr_hel, but the differences between the nucleotide states are far less pronounced. Both the ATP and the ADP states bind preferentially to ssDNA.

DNA binding to different nucleotide states of a hydrolysis-deficient mutant of rGyr_fl and rGyr_hel

As complexes with the nonhydrolyzable ATP analogs might not perfectly mimic the ATP states, we analyzed the effect of nucleotides on the interaction with DNA using hydrolysis-deficient mutants of rGyr_hel and rGyr_fl. A conserved lysine in the Walker A motif of

Table 5. DNA binding properties of different nucleotide states of rGyr_fl

K_d (μM)	nucleotide-free	ADP state		ATP state	
ssDNA					
Y851F	0.035 ± 0.005[a]	ADP	0.060 ± 0.015[a]	ADPNP	0.041 ± 0.009[a]
	0.036 ± 0.001[b]		0.045 ± 0.002[b]		0.038 ± 0.002[b]
	n = 2.3 ± 0.2		n = 2.1 ± 0.2		n = 2.1 ± 0.2
		ADPCP	0.049 ± 0.012[a]	ATPγS	0.046 ± 0.008
			0.039 ± 0.001[b]		0.041 ± 0.001[b]
			n = 2.1 ± 0.1		n = 1.8 ± 0.1
K106Q/Y851F	0.047 ± 0.005[a]		0.053 ± 0.007[a]		0.037 ± 0.004[a]
	0.044 ± 0.003[b]		0.044 ± 0.002[b]		0.035 ± 0.002[b]
	n = 1.4 ± 0.1		n = 1.5 ± 0.1		n = 1.4 ± 0.1
dsDNA					
Y851F	0.49 ± 0.06[a]	ADP	0.25 ± 0.04[a]	ADPNP	0.33 ± 0.07[a]
		ADPCP	0.59 ± 0.06[a]	ATPγS	0.53 ± 0.07[a]
K106Q/Y851F	0.71 ± 0.11[a]		0.46 ± 0.07[a]		0.49 ± 0.09[a]

[a]one-site.
[b]Hill analysis.

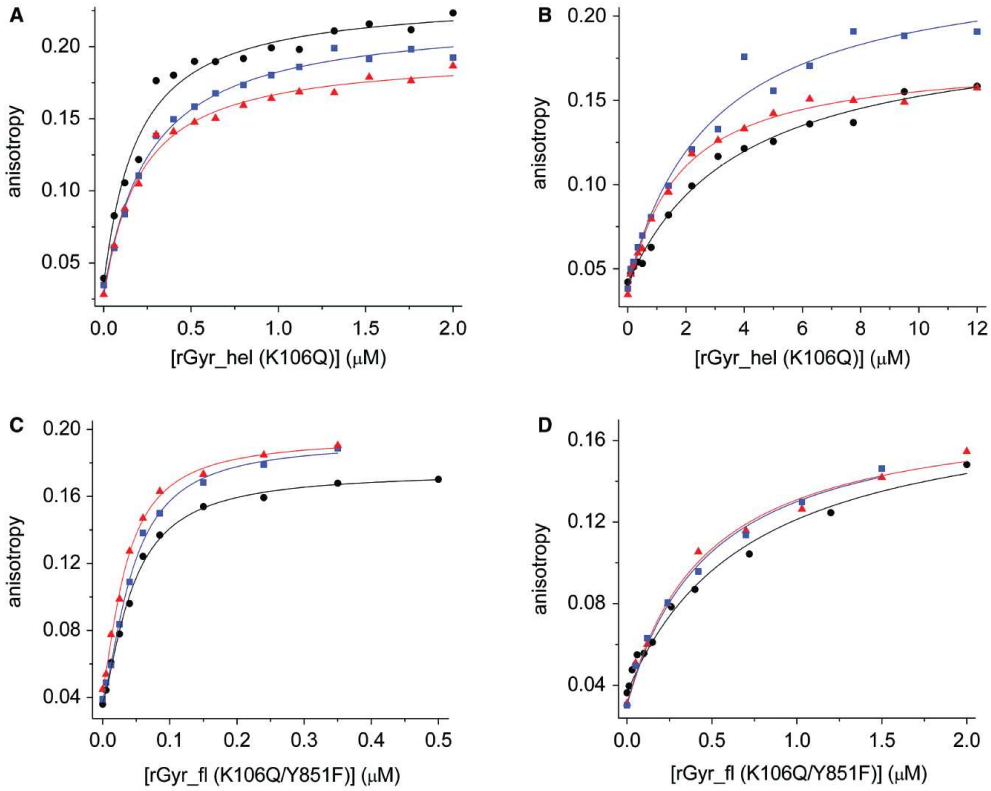

Figure 8. Binding of ssDNA and dsDNA to rGyr_hel(K106Q) and rGyr_fl(K106Q/Y851F). Titrations of ssDNA (**A**, **C**) and dsDNA (**B**, **D**) with rGyr_hel(K106Q) (A, B) or rGyr_fl(K106Q/Y851F) (C, D) in the absence of nucleotide (black, circles), and in the presence of ADP (2 mM, blue, squares) or ATP (4 mM, red, triangles). The DNA concentration was 25 nM in (A and B), and 10 nM in (C and D). The K_d values are summarized in Table 5.

ATPases contacts the β- and γ-phosphates of ATP, and stabilizes negative charges during ATP hydrolysis. In the rGyr_fl(K106Q) mutant, ATP hydrolysis is abolished, but nucleotides are still bound, albeit with reduced affinity (14). The rGyr_fl(K106Q/Y851F) double mutant was created to stably generate ATP and ADP states of reverse gyrase that do not covalently bind to DNA. The absence of ATP hydrolysis was confirmed, and the K_d values of the nucleotide complexes were determined to be $22 \pm 2\,\mu M$ (mantADP), $36 \pm 5\,\mu M$ (ADP) and $98 \pm 12\,\mu M$ (ATP) in equilibrium titrations (Table 1). Overall, nucleotide binding to rGyr_fl(K106Q/Y851F) is reduced ~20-fold compared to wild-type.

The DNA binding properties of this ATP-hydrolysis- and DNA-cleavage-deficient mutant were studied using the 60-base ssDNA and 60 bp dsDNA as a substrate (Figure 8, Table 5). ssDNA was bound independent of the nucleotide state, with K_d values of 44 ± 3 nM (no nucleotide), 44 ± 2 nM (ADP state) and 35 ± 2 nM (ATP state). K_d values for the corresponding dsDNA complexes were higher, consistent with the lower affinity of rGyr_fl for dsDNA. Similar to ssDNA binding, interaction of rGyr_fl(K106Q/Y851F) with dsDNA is independent of the nucleotide state. The K_d values of the dsDNA complexes are $0.71 \pm 0.11\,\mu M$ (no nucleotide), $0.46 \pm 0.07\,\mu M$ (ADP state) and $0.49 \pm 0.09\,\mu M$ (ATP state). Consistent with the wild-type data, the hydrolysis-deficient mutant of rGyr_fl thus shows ~10-fold tighter binding of ssDNA to all nucleotide states.

The data for the wild-type enzyme and nonhydrolyzable ATP analogs (Figure 7, Table 5) support a slightly decreased preference for ssDNA after hydrolysis. The increased preference for ssDNA in the ADP state of rGyr_fl(K106Q/Y851F) results from a 2-fold increased K_d of 0.46 μM for the dsDNA complex, compared to a K_d of 0.25 μM for rGyr_fl(Y851F), and suggests differences between the ADP state of wild-type rGyr_fl and the K106Q/Y851F mutant. Previous work already pointed towards such a difference: Reverse gyrase relaxes negatively supercoiled DNA in the presence of ADP, whereas the K106Q mutant lacks such a relaxation activity (14). Most likely, lysine 106 functions as a nucleotide sensor that triggers an ADP-dependent conformational change that is required for relaxation. If this conformational change is absent in the K106Q mutant, the ADP state will be different, leading to different DNA binding properties.

To compare the DNA binding properties of the nucleotide states of rGyr_hel with rGyr_fl, the corresponding

5892 Nucleic Acids Research, 2008, Vol. 36, No. 18

K106Q mutation in the Walker A motif of rGyr_hel was introduced, and the absence of hydrolysis was confirmed (data not shown). Fluorescence equilibrium titrations revealed a K_d value for the mantADP complex of $67 \pm 5\,\mu M$, and $150 \pm 85\,\mu M$ and $570 \pm 300\,\mu M$ for the ADP and ATP complexes, respectively (Table 1). Thus, the nucleotide affinity of the K106Q mutant of rGyr_hel is ~60-fold reduced compared to the wild-type. This effect is more pronounced than for rGyr_fl (20-fold).

rGyr_hel(K106Q) binds ssDNA 20-fold more tightly than dsDNA ($K_d = 0.18 \pm 0.03$ and $3.8 \pm 0.6\,\mu M$, respectively). In the presence of ADP or ATP, ssDNA binding is not significantly affected, and dsDNA binding is only slightly increased (ADP: 1.3-fold, $K_d = 2.9 \pm 0.6\,\mu M$; ATP: 2.2-fold, $K_d = 1.7 \pm 0.2\,\mu M$). As a consequence, ssDNA interacts more tightly than dsDNA with both nucleotide states (12-fold, ADP state; 9-fold, ATP state), implying a slightly stronger preference for ssDNA after ATP hydrolysis. Similarly, the data from wild-type rGyr_hel suggest a stronger interaction with ssDNA after ATP hydrolysis. However, wild-type rGyr_hel in complex with nonhydrolyzable ATP analogs binds ssDNA and dsDNA with similar affinities, while the ATP state of rGyr_hel(K106Q) interacts 9-fold more tightly with ssDNA. This discrepancy arises from a reduced affinity of the rGyr_hel(K106Q) ATP state for dsDNA compared to the ADPNP or ATPγS state of the wild-type rGyr_hel (Figure 6, Table 4), suggesting structural differences between the ATP state of rGyr_hel(K106Q) and the corresponding complexes of wild-type with nonhydrolyzable analogs.

Altogether, rGyr_hel shows similar affinities for ssDNA and dsDNA in the ATP state, and a 10-fold preference for ssDNA in the ADP state due to a decrease in dsDNA affinity. Thus, the helicase domain switches from a 'high affinity' state with respect to dsDNA to a 'low affinity' state upon ATP hydrolysis, and back to the 'high affinity' state after nucleotide exchange, while the ssDNA affinity remains constant. In rGyr_fl, both nucleotide states show a preference for ssDNA, indicating that the switch to the 'low affinity' state for dsDNA upon ATP hydrolysis is suppressed in the full-length enzyme. Figure 9 summarizes the properties of rGyr_hel and rGyr_fl. The K106Q mutants of rGyr_hel and rGyr_fl show similar DNA preferences, with a 10-fold higher affinity for ssDNA compared to dsDNA in both nucleotide states. These results argue for a critical role of lysine 106 as a nucleotide sensor in the helicase domain, and for inter-domain communication between the helicase-like and the topoisomerase domains.

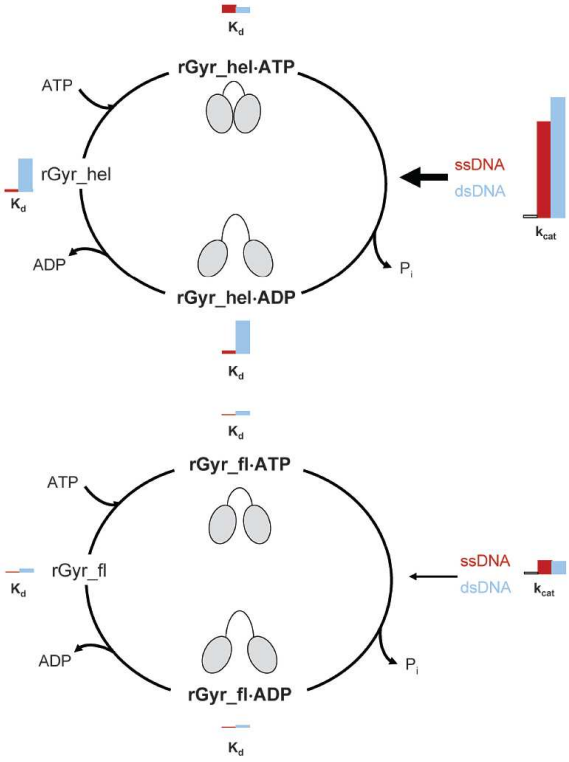

Figure 9. Overview of the nucleotide cycle of rGyr_hel and rGyr_fl. The K_d values of the nucleotide states for ssDNA (red) and dsDNA (blue) are displayed as bars with a size proportional to their value. Analogously, a red bar denotes the k_{cat} value in the presence of ssDNA, a blue bar corresponds to the k_{cat} value in the presence of dsDNA. For reference, an additional bar represents the intrinsic k_{cat} in the absence of DNA. A cartoon indicates possible conformations of the helicase-like domain in the different nucleotide states of rGyr_hel and rGyr_fl. rGyr_hel (upper panel) shows similar affinities for ssDNA and dsDNA in the ATP state, and a preference for ssDNA in the ADP state due to a decrease in dsDNA affinity. This corresponds to a switch from a 'high affinity' state with respect to dsDNA to a 'low affinity' state upon ATP hydrolysis. Both dsDNA and ssDNA efficiently stimulate ATP hydrolysis (arrow). Most likely, the helicase-like domain switches between a closed conformation (cartoon) in the presence of DNA and ATP that hydrolyzes ATP efficiently, and an open conformation in the ADP state, as observed for SF2 helicases. In rGyr_fl (lower panel), both nucleotide states show a preference for ssDNA, indicating that the switch to the 'low affinity' state for dsDNA upon ATP hydrolysis is suppressed in the full-length enzyme. The ATPase stimulation by DNA is 10-fold smaller than in rGyr_hel. Possibly, steric hindrance by the topoisomerase domain prevents a complete closure of the helicase-like domain (cartoon) in the context of full-length reverse gyrase. The progression through the nucleotide cycle with moderate velocity may be required for efficient coupling of ATP hydrolysis and positive supercoiling.

DISCUSSION

The helicase-like domain confers nucleotide-dependent DNA binding to reverse gyrase

We have shown here that the nucleotide binding properties of reverse gyrase are a function of the N-terminal helicase-like domain. Nucleotide affinities and ATP hydrolysis rates are virtually identical for the isolated helicase-like domain and for the full-length enzyme in the absence of nucleic acids. Thus, all determinants for nucleotide binding and hydrolysis are contained within the helicase-like domain, and its characteristics are unaltered in the context of reverse gyrase. The similar ATPase rates suggest that the conformations of the helicase-like domains are similar, indicating that the arrangement of

the catalytic residues in the isolated helicase-like domain and in context of reverse gyrase are the same.

Our results demonstrate that the helicase-like domain mediates nucleotide-dependent interactions of reverse gyrase with ssDNA and dsDNA, and with plasmid DNA. In the ATP state, dsDNA and ssDNA are bound with similar affinities, whereas after ATP hydrolysis, ssDNA is preferentially bound. The DNA substrates influence the rate of switching between these states by stimulating the intrinsic ATPase activity of the helicase-like domain. Thus, the helicase-like domain is a module that confers nucleotide-dependent DNA binding to reverse gyrase. The topoisomerase domain has no influence on nucleotide binding and hydrolysis by the helicase-like domain in the absence of DNA, but modulates the ATPase properties in the presence of DNA. In the context of reverse gyrase, the ATPase activity of the helicase-like domain is still stimulated by the same DNA substrates, but to a much lesser extent. The DNA-stimulated ATPase activity of reverse gyrase is 10-fold lower than that in the isolated domain, demonstrating that the activity of the helicase-like domain is strongly suppressed by the topoisomerase domain.

The nucleic acid-stimulated ATPase activity of SF2 helicases results from a conformational change upon binding of both ligands that leads to a closure of the cleft between the two helicase subdomains. In this closed conformation, the catalytic residues are correctly positioned for efficient ATP hydrolysis. It has been proposed that such a conformational change in the helicase-like domain initiates supercoiling by reverse gyrase (10,14). The observed similar ATPase activities of the helicase-like domain and reverse gyrase suggest a similar open conformation of the helicase in both enzymes (Figure 9). In the presence of DNA, the isolated helicase-like domain adopts a closed conformation that rapidly hydrolyzes ATP. Possibly, in full-length reverse gyrase the topoisomerase domain provides a steric hindrance for the conformational change in the helicase-like domain. This steric hindrance may confine the helicase-like domain to a more open form even in the presence of nucleic acids, and consequently to less efficient ATP hydrolysis by reverse gyrase compared to the isolated helicase-like domain. A restriction of this conformational change by the topoisomerase domain would also readily explain the lower cooperativity between ATP and nucleotide binding in rGyr_fl.

Inter-domain communication in reverse gyrase: DNA binding and ATPase stimulation

The helicase-like domain and reverse gyrase interact more tightly with ssDNA than with dsDNA. This preference for ssDNA is reminiscent of other type I DNA topoisomerases (27). The high affinity of reverse gyrase for ssDNA may allow for sensing of single-stranded regions (5), and lead to stabilization of these regions for strand cleavage and the subsequent strand-passage reaction during catalysis. It has been shown previously that the presence of single-stranded regions in the DNA substrate favors positive supercoiling by reverse gyrase (5). Reverse gyrase contains several potential interaction sites for nucleic acids, located in the helicase-like domain, or in a cleft close to the catalytic tyrosine. In addition, the latch region may contact DNA (10,12), and a transient interaction of the putative zinc fingers with the DNA during supercoiling has been proposed (10). However, nucleic acid binding to these different interaction sites of reverse gyrase has not been characterized in detail. By using the Y851F mutant of reverse gyrase in DNA binding studies, we excluded the covalent binding of DNA *via* the catalytic tyrosine. In general, the DNA affinity of reverse gyrase is about 10-fold higher than that for the helicase-like domain. This increased affinity could either reflect tight DNA binding to the helicase-like domain in reverse gyrase, or point towards simultaneous interactions of DNA with the topoisomerase domain that increase the overall affinity. Clearly, a more detailed analysis of DNA binding to reverse gyrase would be required to further understand the relation between DNA binding to different sites and stimulation of ATP hydrolysis. However, in this context it is important to note that the cooperativity observed for ssDNA binding does not reflect two DNA molecules binding to one molecule of reverse gyrase (as would be possible if one ssDNA molecule interacts with the helicase-like domain and one with the topoisomerase domain). Instead, the data is consistent with the interaction of two reverse gyrase molecules with one ssDNA molecule, pointing towards a possible interaction between reverse gyrase molecules on the same substrate DNA. The fact that this cooperative effect is more pronounced for the full-length enzyme than for the isolated helicase-like domain, and only observed for ssDNA but not for dsDNA, suggests a functional role of this protein–protein interaction during the supercoiling reaction.

Is the ATPase activity of the helicase-like domain modulated to achieve optimal coupling of ATP hydrolysis to positive supercoiling?

Our results demonstrate that the helicase-like domain of reverse gyrase meets most criteria for a bona fide helicase: it has a DNA-dependent ATPase activity, and the nucleotide-state determines its affinity for ssDNA and dsDNA. However, as already reported for other reverse gyrase homologs, we did not detect DNA unwinding activity for the helicase-like domain of *T. maritima* reverse gyrase (data not shown). Altogether, the helicase-like domain of reverse gyrase acts as a nucleotide-dependent switch reminiscent of the nonprocessive DEAD box helicases that constitute a subfamily of SF2 helicases (28).

Helicase domains frequently occur in conjunction with additional domains that mediate substrate specificity or the interaction with protein partners, or regulate helicase activity (29–33). For instance, the DEAD box helicase RIG-I consists of a helicase domain and two N-terminal caspase activation and recruitment domains that connect the helicase function to the caspase signaling pathway, and these additional domains inhibit the RIG-I helicase activity (33). Conversely, the internal helicase domain of dicer inhibits its RNase activity (32), demonstrating that the domains can mutually influence their respective activities. Likewise, the ATPase activity of the helicase-like

domain in the presence of DNA is attenuated in the context of reverse gyrase, and the differences in nucleic acid affinities of the nucleotide states are smaller (Figure 9). A repression of relaxation activity of the topoisomerase domain in the absence of nucleotides by the helicase-like domain, mediated by the latch region (11,12), has been demonstrated earlier. The inhibition of the helicase-like domain we describe here seems to be the reciprocal effect. Deletion of the latch region increases the ATPase activity of reverse gyrase in the presence of ssDNA (11), suggesting a simultaneous role of the latch for the inhibitory effect of the topoisomerase domain on the helicase-like domain. Both effects emphasize the importance of communication between the reverse gyrase domains. The fact that the differences between switching of the helicase-like domain and reverse gyrase are mostly lost in the K106Q mutants suggests a critical contribution of the Walker A motif to inter-domain communication.

As a consequence of the inhibitory effect of the topoisomerase domain on the helicase-like domain in reverse gyrase, the progression through the nucleotide cycle in the presence of DNA is strongly decelerated. DNA supercoiling is a complex multi-step process, and the current model of DNA supercoiling by type IA topoisomerases such as reverse gyrase involves DNA cleavage, strand passage and re-ligation of the cleaved strand. This reaction will most likely require substantial conformational changes in reverse gyrase, and supercoiling is therefore an intrinsically slow process. Thus, a rapid cycling between the nucleotide states may not be necessary or could even be detrimental for supercoiling. Instead, the precise coordination of ATP hydrolysis and supercoiling may require matching rates for both processes, and hence a moderate ATP turnover. The inhibitory effect of the topoisomerase domain on the helicase-like domain emphasizes the role of inter-domain communication for efficient coupling between ATP hydrolysis and positive DNA supercoiling by reverse gyrase.

SUPPLEMENTARY DATA

Supplementary Data are available at NAR Online.

ACKNOWLEDGEMENTS

We thank Manuel Hilbert for performing the unwinding experiment with rGyr_hel and Markus Rudolph for discussions.

FUNDING

VolkswagenStiftung; Swiss National Science Foundation. Funding for open access charge: Swiss National Science Foundation.

Conflict of interest statement. None declared.

REFERENCES

1. Kikuchi,A. and Asai,K. (1984) Reverse gyrase–a topoisomerase which introduces positive superhelical turns into DNA. *Nature*, **309**, 677–681.
2. Forterre,P. (2002) A hot story from comparative genomics: reverse gyrase is the only hyperthermophile-specific protein. *Trends Genet.*, **18**, 236–237.
3. Atomi,H., Matsumi,R. and Imanaka,T. (2004) Reverse gyrase is not a prerequisite for hyperthermophilic life. *J. Bacteriol.*, **186**, 4829–4833.
4. Kampmann,M. and Stock,D. (2004) Reverse gyrase has heat-protective DNA chaperone activity independent of supercoiling. *Nucleic Acids Res.*, **32**, 3537–3545.
5. Hsieh,T.S. and Plank,J.L. (2006) Reverse gyrase functions as a DNA renaturase: annealing of complementary single-stranded circles and positive supercoiling of a bubble substrate. *J. Biol. Chem.*, **281**, 5640–5647.
6. Krah,R., Kozyavkin,S.A., Slesarev,A.I. and Gellert,M. (1996) A two-subunit type I DNA topoisomerase (reverse gyrase) from an extreme hyperthermophile. *Proc. Natl Acad. Sci. USA*, **93**, 106–110.
7. Krah,R., O'Dea,M.H. and Gellert,M. (1997) Reverse gyrase from *Methanopyrus kandleri*. Reconstitution of an active extremozyme from its two recombinant subunits. *J. Biol. Chem.*, **272**, 13986–13990.
8. Declais,A.C., Marsault,J., Confalonieri,F., de La Tour,C.B. and Duguet,M. (2000) Reverse gyrase, the two domains intimately cooperate to promote positive supercoiling. *J. Biol. Chem.*, **275**, 19498–19504.
9. Confalonieri,F., Elie,C., Nadal,M., de La Tour,C., Forterre,P. and Duguet,M. (1993) Reverse gyrase: a helicase-like domain and a type I topoisomerase in the same polypeptide. *Proc. Natl Acad. Sci. USA*, **90**, 4753–4757.
10. Rodriguez,A.C. and Stock,D. (2002) Crystal structure of reverse gyrase: insights into the positive supercoiling of DNA. *EMBO J.*, **21**, 418–426.
11. Rodriguez,A.C. (2002) Studies of a positive supercoiling machine. Nucleotide hydrolysis and a multifunctional "latch" in the mechanism of reverse gyrase. *J. Biol. Chem.*, **277**, 29865–29873.
12. Rodriguez,A.C. (2003) Investigating the role of the latch in the positive supercoiling mechanism of reverse gyrase. *Biochemistry*, **42**, 5993–6004.
13. Theissen,B., Karow,A.R., Kohler,J., Gubaev,A. and Klostermeier,D. (2008) Cooperative binding of ATP and RNA induces a closed conformation in a DEAD box RNA helicase. *Proc. Natl Acad. Sci. USA*, **105**, 548–553.
14. Jungblut,S.P. and Klostermeier,D. (2007) Adenosine 5'-O-(3-thio)-triphosphate (ATPgammaS) promotes positive supercoiling of DNA by *T. maritima* reverse gyrase. *J. Mol. Biol.*, **371**, 197–209.
15. Peck,M.L. and Herschlag,D. (2003) Adenosine 5'-O-(3-thio)triphosphate (ATPgammaS) is a substrate for the nucleotide hydrolysis and RNA unwinding activities of eukaryotic translation initiation factor eIF4A. *RNA*, **9**, 1180–1187.
16. Studier,F.W. (2005) Protein production by auto-induction in high density shaking cultures. *Protein Expr. Purif.*, **41**, 207–234.
17. Kovalsky,O.I., Kozyavkin,S.A. and Slesarev,A.I. (1990) Archaebacterial reverse gyrase cleavage-site specificity is similar to that of eubacterial DNA topoisomerases I. *Nucleic Acids Res.*, **18**, 2801–2805.
18. Jaxel,C., Duguet,M. and Nadal,M. (1999) Analysis of DNA cleavage by reverse gyrase from *Sulfolobus shibatae* B12. *Eur. J. Biochem.*, **260**, 103–111.
19. Hiratsuka,T. (1983) New ribose-modified fluorescent analogs of adenine and guanine nucleotides available as substrates for various enzymes. *Biochim. Biophys. Acta*, **742**, 496–508.
20. Rogers,G.W. Jr, Richter,N.J. and Merrick,W.C. (1999) Biochemical and kinetic characterization of the RNA helicase activity of eukaryotic initiation factor 4A. *J. Biol. Chem.*, **274**, 12236–12244.
21. Shibata,T., Nakasu,S., Yasui,K. and Kikuchi,A. (1987) Intrinsic DNA-dependent ATPase activity of reverse gyrase. *J. Biol. Chem.*, **262**, 10419–10421.
22. Lorsch,J.R. and Herschlag,D. (1998) The DEAD box protein eIF4A. 1. A minimal kinetic and thermodynamic framework reveals coupled binding of RNA and nucleotide. *Biochemistry*, **37**, 2180–2193.

23. Lorsch,J.R. and Herschlag,D. (1998) The DEAD box protein eIF4A. 2. A cycle of nucleotide and RNA-dependent conformational changes. *Biochemistry*, **37**, 2194–2206.
24. Polach,K.J. and Uhlenbeck,O.C. (2002) Cooperative binding of ATP and RNA substrates to the DEAD/H protein DbpA. *Biochemistry*, **41**, 3693–3702.
25. Yang,Q. and Jankowsky,E. (2006) The DEAD-box protein Ded1 unwinds RNA duplexes by a mode distinct from translocating helicases. *Nat. Struct. Mol. Biol.*, **13**, 981–986.
26. Yang,Q. and Jankowsky,E. (2005) ATP- and ADP-dependent modulation of RNA unwinding and strand annealing activities by the DEAD-box protein DED1. *Biochemistry*, **44**, 13591–13601.
27. Kirkegaard,K. and Wang,J.C. (1985) Bacterial DNA topoisomerase I can relax positively supercoiled DNA containing a single-stranded loop. *J. Mol. Biol.*, **185**, 625–637.
28. Pyle,A.M. (2008) Translocation and unwinding mechanisms of RNA and DNA helicases. *Annu. Rev. Biophys.*, **37**, 317–336.
29. Morlang,S., Weglohner,W. and Franceschi,F. (1999) Hera from *Thermus thermophilus*: the first thermostable DEAD-box helicase with an RNase P protein motif. *J. Mol. Biol.*, **294**, 795–805.
30. Rogers,G.W. Jr, Richter,N.J., Lima,W.F. and Merrick,W.C. (2001) Modulation of the helicase activity of eIF4A by eIF4B, eIF4H, and eIF4F. *J. Biol. Chem.*, **276**, 30914–30922.
31. Kossen,K., Karginov,F.V. and Uhlenbeck,O.C. (2002) The carboxy-terminal domain of the DExDH protein YxiN is sufficient to confer specificity for 23S rRNA. *J. Mol. Biol.*, **324**, 625–636.
32. Ma,E., MacRae,I.J., Kirsch,J.F. and Doudna,J.A. (2008) Autoinhibition of human dicer by its internal helicase domain. *J. Mol. Biol.*, **380**, 237–243.
33. Gee,P., Chua,P.K., Gevorkyan,J., Klumpp,K., Najera,I., Swinney,D.C. and Deval,J. (2008) Essential role of the N-terminal domain in the regulation of RIG-I ATPase activity. *J. Biol. Chem.*, **283**, 9488–9496.

6.3 Appendix

Reverse Gyrase Y851F is not Supercoiling Active

The publication presented in this chapter compares DNA binding affinities of the helicase-like domain of reverse gyrase and the full-length enzyme. The Y851F mutant of the full-length reverse gyrase was used to ensure equilibrium conditions during titrations, as it lacks the active tyrosine required for topoisomerase activity. Inactivation of the mutant in terms of positive supercoiling was tested (Figure 10).

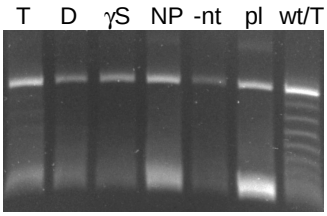

Figure 10. Nucleotide-dependent supercoiling activity of reverse gyrase Y851F analysed with one-dimensional agarose gel electrophoresis. Reaction conditions were 1 µM reverse gyrase Y851F in 50 mM Tris/HCl (pH 7.5), 150 mM NaCl, 10 mM $MgCl_2$, 100 µM $Zn(OAc)_2$, 2 mM β-ME, 2 mM nucleotide, 15 nM pUC18, 10% (w/v) PEG 8000 at 75°C for 120 minutes. ATP (T), ADP (D), ATPγS (γS), ADPNP (NP), without nucleotide (-nt), plasmid alone (pl) and wild type reverse gyrase (wt). Reverse gyrase Y851F neither relaxes nor supercoils pUC18 plasmid.

Reverse gyrase Y851F shows no wild type topoisomerase activity.

ssDNA and dsDNA are Reversibly Bound to Reverse Gyrase Y851F

K_D values for DNA/reverse gyrase complexes were determined in equilibrium titrations with fluorescently labelled ssDNA and dsDNA. Therefore, reversible binding of the DNA constructs by reverse gyrase Y851F is a premise, which was investigated in displacement titrations with unlabelled ssDNA (Figure 11).

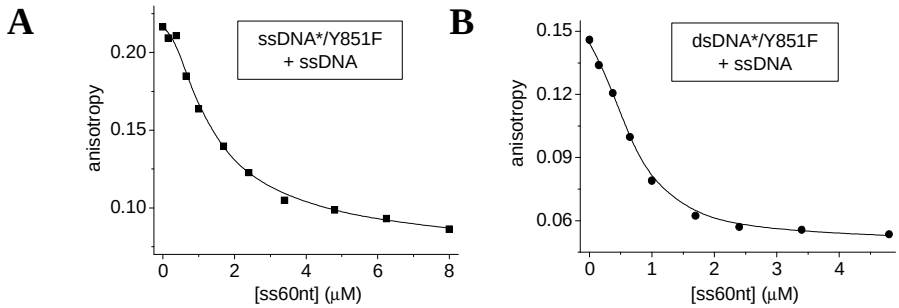

Figure 11: Displacement of 5'-fluoresceine-labelled (*) 60-mer ssDNA and dsDNA in complex with reverse gyrase Y851F with unlabelled ssDNA. Fluorescence anisotropy titrations were carried out in 50 mM Tris/HCl (pH 7.5), 150 mM NaCl, 10 mM $MgCl_2$, 100 µM $Zn(OAc)_2$, 2 mM β-ME at 37°C. Data were fit numerically as previously described[14]. (A) The complexes of 10 nM labelled ssDNA and 0.5 µM enzyme (K_D = 35 ± 5 nM) and (B) 10 nM labelled dsDNA and 2 µM enzyme (K_D = 489 ± 64 nM) were preformed during 3 minutes at 37°C. ssDNA and dsDNA do not form covalent intermediates with reverse gyrase Y851F and can be displaced from the enzyme with ssDNA. The K_D values of the newly formed ssDNA/protein complexes were 69 ± 7 nM (A) and 73 ± 14 nM (B).

Bound labelled ssDNA and dsDNA can be displaced from the complex with reverse gyrase Y851F by unlabelled ssDNA, demonstrating that no covalent intermediate is formed. The K_D values of the complex between unlabelled DNA and the Y851F mutant are identical in both displacement titrations. This indicates formation of an identical complex regardless of whether ssDNA or dsDNA were displaced. dsDNA was not used for displacement titrations due to 14-fold weaker binding compared to ssDNA requiring far higher amounts of dsDNA.

Reverse Gyrase Y851F has wild type ATPase Activity - K106Q/Y851F is Inactive

Reverse gyrase Y851F mutant lacks wild type topoisomerase activity. However, the enzyme should still bear an active ATPase. In contrast, reverse gyrase K106Q/Y851F is also ATPase-inactive. ATPase activity of the mutant enzymes was tested (Figure 12).

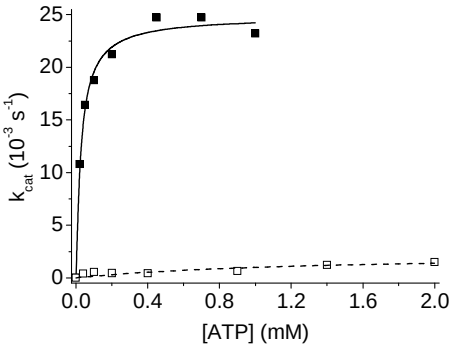

Figure 12. Steady-state ATPase activity of reverse gyrase mutants. 1 µM enzyme was incubated in 50 mM Tris/HCl (pH 7.5), 150 mM NaCl, 10 mM $MgCl_2$, 100 µM $Zn(OAc)_2$, 2 mM β-ME, 0.4 mM phosphoenol pyruvate and 0.2 mM NADH at 37°C with the ATP concentration depicted. Data were processed as reported[14]. The ATPase of reverse gyrase Y851F (filled squares) is fully functional with a k_{cat} of $25 \pm 1 \cdot 10^{-3}$ s^{-1} and a K_M value of 27 ± 3 µM. ATP hydrolysis and binding are vastly reduced for the K106Q/Y851F mutant (open squares) with $k_{cat} = 2.3 \pm 0.1 \cdot 10^{-3}$ s^{-1} and $K_M = 1.3 \pm 1.3$ mM.

The ATPase of reverse gyrase Y851F is fully functional and not influenced by loss of ssDNA cleavage ability. The K_M and k_{cat} values are similar to the data published for the wild type ($k_{cat} = 20 \pm 1 \cdot 10^{-3}$ s^{-1}, $K_M = 44 \pm 6$ µM)[14]. Reverse gyrase K106Q/Y851F has a 10-fold decreased ATP hydrolysis rate and the binding of ATP is 50-fold reduced. Hence, the mutant is ATPase-inactive.

Cooperative Binding Models for ssDNA Binding to Reverse Gyrase

Binding studies with 60-mer ssDNA and reverse gyrase Y851F using fluorescence anisotropy titrations revealed cooperative binding, which was clearly demonstrated by sigmoidal binding curves. Assuming a two-to-one binding event, two binding models are possible (Figure 13).

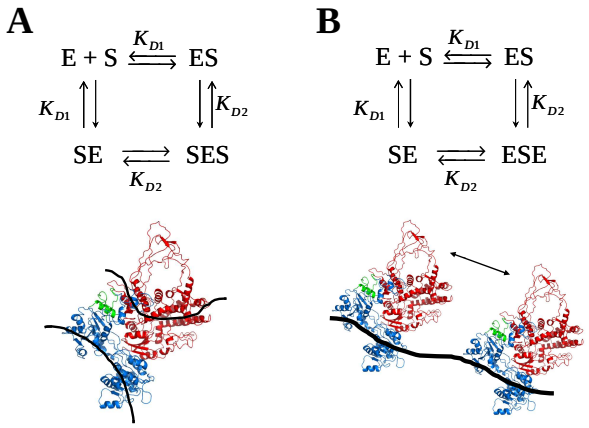

Figure 13. Cooperative binding models for reverse gyrase and ssDNA. The black lines each represent a 60-mer ssDNA stretch. Depictions of reverse gyrase are homology models based on the crystal structure of reverse gyrase from *A. fulgidus*[10] with the sequence of the *T. maritima* enzyme. (A) Stepwise binding of two ssDNA molecules to one reverse gyrase molecule. (B) Opposite case with a possible protein-protein interaction indicated. K_{D2} values are not identical in panel (A) and (B).

The observed cooperativity might either reflect binding of two 60-mer ssDNA stretches to one reverse gyrase molecule or the reverse. The Hill equation was used for the determination of cooperative binding of reverse gyrase to fluorescently labelled ssDNA in anisotropy titrations:

$$r = r_0 + (r_{max} - r_0) * \frac{E^n}{K_D + E^n} \quad (1),$$

where r, r_0 and r_{max} are the observed, starting and maximal fluorescence anisotropy values, K_D is the dissociation constant of the enzyme/DNA complex, E is the enzyme concentration and n is the Hill coefficient. The equation describes cooperative binding of at least n enzymes to one DNA substrate molecule. Binding of two reverse gyrase molecules to one ssDNA is in accordance with the experimental data. In the future, the minimal binding length of DNA for reverse gyrase and the minimal length for cooperative binding may be revealed by shortening of the 60-mer DNA construct.

Ensemble Fluorescence Anisotropy

During fluorescent titrations, the binding of 60-mer ssDNA to reverse gyrase Y851F results in a higher final anisotropy value of about 0.2 compared to 0.15 for the complex with 60-mer dsDNA in the absence and presence of four different adenine nucleotides (see Figure 7). This is surprising because higher anisotropy values indicate reduced complex mobility along with higher complex mass (MW (60-mer ssDNA) = 18’311 g · mol^{-1}; MW (reverse gyrase) = 128’275 g · mol^{-1}). Thus, one-to-one binding of reverse gyrase to ssDNA or dsDNA should give higher final anisotropy values for dsDNA. It is possible, that binding of reverse gyrase to the fluorescently labelled DNA substrates alters the fluorescence properties of the 5’-attached fluoresceine. Further elucidation of the unexpected inverse order of final anisotropy values for reverse gyrase complexes with ssDNA or dsDNA under different nucleotide-bound states was required. We performed

ensemble fluorescence measurements to determine changes in the dye properties upon protein binding *via* changes in fluorescence decay times (Figure 14).

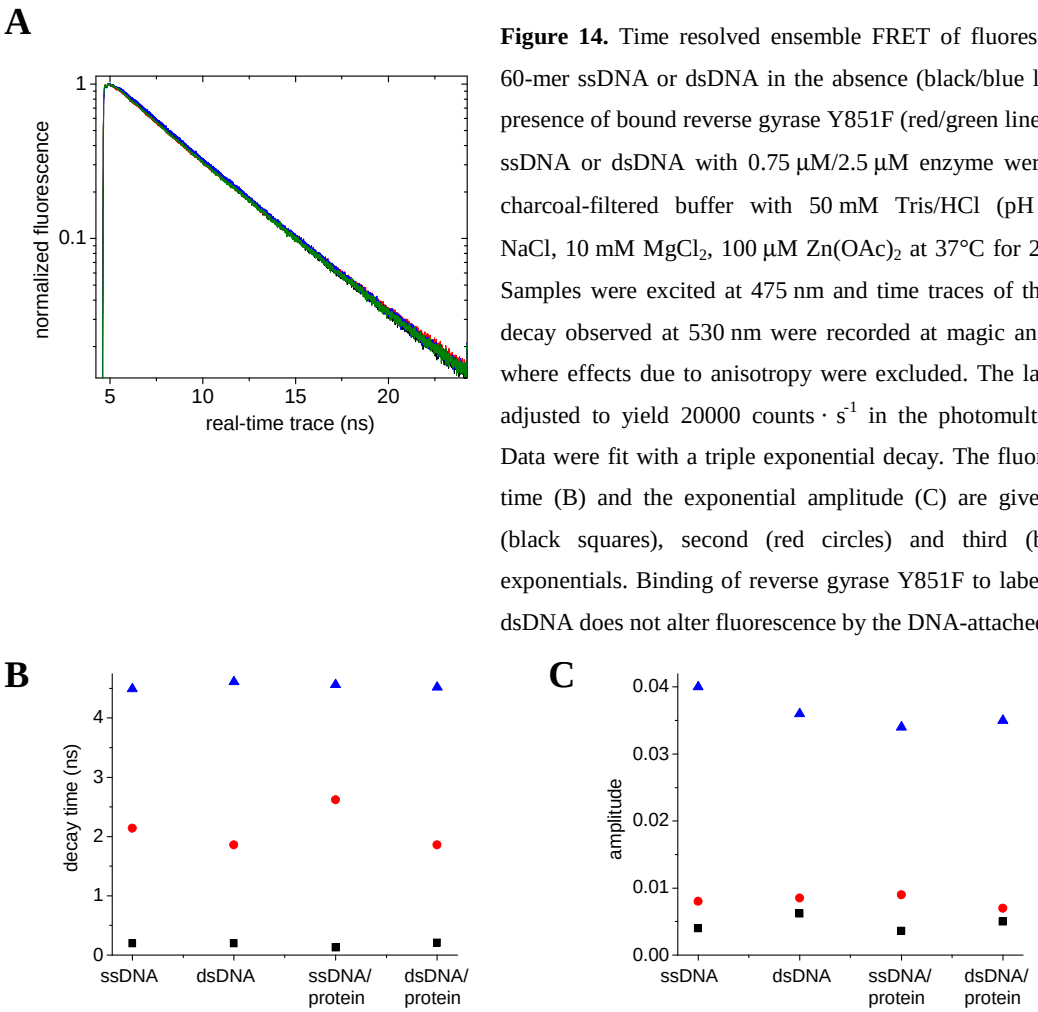

Figure 14. Time resolved ensemble FRET of fluorescently labelled 60-mer ssDNA or dsDNA in the absence (black/blue lines in A) and presence of bound reverse gyrase Y851F (red/green lines in A). 50 nM ssDNA or dsDNA with 0.75 µM/2.5 µM enzyme were measured in charcoal-filtered buffer with 50 mM Tris/HCl (pH 7.5), 150 mM NaCl, 10 mM $MgCl_2$, 100 µM $Zn(OAc)_2$ at 37°C for 20 minutes. (A) Samples were excited at 475 nm and time traces of the fluorescence decay observed at 530 nm were recorded at magic angle conditions, where effects due to anisotropy were excluded. The laser power was adjusted to yield 20000 counts · s^{-1} in the photomultiplier detector. Data were fit with a triple exponential decay. The fluorescence decay time (B) and the exponential amplitude (C) are given for the first (black squares), second (red circles) and third (blue triangles) exponentials. Binding of reverse gyrase Y851F to labelled ssDNA or dsDNA does not alter fluorescence by the DNA-attached fluoresceine.

Fluorescence decays were described by triple exponential equations (Figure 14A). A control measurement with free uranine showed a fluorescence decay that could be fit with a single exponential. Thus, the necessity for three exponentials in the case of the labelled DNA constructs is due to attachment of the dyes to the DNA and not an instrumental error. The results reveal no difference in the fluorescence decay times for all three exponentials of ssDNA and dsDNA in the absence and presence of saturating conditions of reverse gyrase Y851F (Figure 14B and C). This indicates that the difference in the final anisotropy values is not due to an influence of reverse gyrase binding to the fluorescent moiety, but an effect of the complex formation itself. Our findings indicate cooperative binding of two reverse gyrase Y851F molecules to one strand of ssDNA observed before in anisotropy titrations. The combined masses of two enzyme molecules bound to one ssDNA molecule could account for higher final fluorescence anisotropy values compared to one enzyme molecule bound to one dsDNA molecule.

7. Cooperative Binding and Stimulation of ATP Hydrolysis by Reverse Gyrase is Substrate Length-dependent

7.1 Introduction

We have previously tested the plasmid supercoiling and relaxation properties of reverse gyrase[1,2] from *Thermotoga maritima* with respect to the hydrolysis of ATP analogues[3]. Regarding DNA substrates for reverse gyrase, it has been reported that the affinity for single stranded DNA regions (ssDNA) is higher than for double stranded regions (dsDNA)[4]. We consequently tested binding of ssDNA or dsDNA 60-mer substrates to reverse gyrase and found cooperative binding of two reverse gyrase molecules to a 60 nt[a] ssDNA in the presence and absence of different adenine nucleotides in the nanomolar range[5]. ssDNA promotes ATPase activity of reverse gyrase 3-fold more than dsDNA under conditions suitable for plasmid supercoiling[5]. However, reverse gyrase binds 6-15-fold weaker to 60 bp[b] dsDNA and in a non-cooperative way. Cooperative substrate binding and enzyme activity are common features for DNA binding proteins. For example, the eukaryotic DNA-repair enzyme Ku binds with positive cooperativity to dsDNA ends after a double strand break of DNA. If the dsDNA is long enough for more than 2 Ku molecules to bind, cooperativity decreases again[6].

In the case of reverse gyrase, correlation between the coupling of DNA binding and ATPase activity and the DNA substrate-length could also exist, giving more insight into the underlying coupling mechanism of these enzyme features. The previously used 60-mer DNA constructs are about 20 nm in length, calculating with 3.4 nm per 10 bp[8]. Assuming DNA binding to the topoisomerase domain of reverse gyrase with a diameter of about 6 nm for the *Archeoglobus fulgidus* enzyme[7], up to three reverse gyrase molecules could fit on the previously used 60-mer DNA constructs. To investigate the dependence of cooperative binding of ssDNA or dsDNA and stimulatory effects on ATP hydrolysis on substrate length, we systematically shortened the originally used 60-mer substrates. Also, minimal requirement for the binding length of ssDNA and dsDNA substrates for reverse gyrase could be determined in this way.

[a] nt, nucleotide(s)
[b] bp, base pair(s)

7.2 Material and Methods

Protein Purification and DNA Substrates

Reverse gyrase wild type from *T. maritima* and the DNA cleavage-deficient Y851F mutant were purified as described[3] (Chapter 3.2). A 107 bp dsDNA was generated by PCR-amplification of a modified pUC18 plasmid. The plasmid contained a 39 bp stretch with an optimised cleavage site for reverse gyrase[9,10] inserted into the HindIII/BamHI site of pUC18 and was produced by Andreas Schmidt (Klostermeier group). The amplified 107 bp substrate was applied to 2% agarose gel electrophoresis (see Chapter 3.2), excised from the gel after staining with ethidium bromide and purified using the QIAquick Gel Extraction kit (Qiagen) following the manufacturer's instructions. Single stranded oligonucleotides with 20, 40 and 60 nt in length and their complementary strands were synthesised and purified by Purimex (Grebenstein, Germany). The substrates also included the optimised cleavage site for reverse gyrase[9,10]. Sequences of the constructs are listed in Table 1.

Table 1. Sequences of 20 , 40 and 60 nt long ssDNA constructs. A preferential cleavage site for reverse gyrase is depicted in red. dsDNA substrates were generated by annealing with the complementary strands (sequences not shown). The 107 bp dsDNA was produced by PCR amplification of a pUC18 with the inserted preferential cleavage site[9,10].

20-mer	5'-GATA TTCATTACTT CTTATC-3'
40-mer	5'-TCTAGAGTCA GCCCGTGATA TTCATTACTT CTTATCCTAG-3'
60-mer	5'-AAGCCAAGCT TCTAGAGTCA GCCCGTGATA TTCATTACTT CTTATCCTAG GATCCCCGTT-3'
107-mer	5'-CCCAGTCACG ACGTTGTAAA ACGACGGCCA GTGCCAAGCT TCTAGAGTCA GCCCGTGATA TTCATTACTT CTTATCCTAG GATCCCCGGG TACCGAGCTC GAATTCG-3'

Reverse gyrase preferentially cleaves the ssDNA substrates between the two nucleotides highlighted in red (Table 1)[9,10]. For fluorescence anisotropy titrations, the oligonucleotides in the table contained a 5'-fluoresceine moiety. Corresponding dsDNA substrates with 20, 40 and 60 bp were generated by annealing the 5'-fluoresceine-labelled single strands with unlabelled complementary single strands (sequences not shown). The melting temperatures (T_m) for the dsDNA constructs were 42°C, 64°C and 72°C respectively, as calculated with the *OligoCalc* program from the Northwestern University Medical School (Chicago, USA). The unlabelled 107 bp dsDNA was produced by PCR and had a T_m of 80°C.

Fluorescence anisotropy measurements

Dissociation constants of complexes between reverse gyrase and ssDNA or dsDNA constructs were investigated with fluorescence anisotropy titrations in buffer with 50 mM Tris/HCl (pH 7.5), 150 mM NaCl, 10 mM $MgCl_2$, 100 µM $Zn(OAc)_2$, 2 mM β-ME at 37°C. 10 nM of 5'-fluoresceine-labelled ss/dsDNA constructs were titrated with reverse gyrase. The Y851F reverse gyrase mutant was used for all fluorescent titrations to ensure equilibrium conditions. This mutant lacks the active tyrosine and is unable to covalently bind DNA substrates but is still ATPase-active[5] (see Chapter 6.3). Dissociation constants were calculated by fitting a model for one-site binding described by the solution of a quadratic equation to the data, as previously published[3]. Cooperative binding of reverse gyrase to DNA was described with the Hill equation.

Steady-state ATPase activity

Parameters for the steady-state ATPase activity of reverse gyrase were determined in an ATPase assay, coupling ATP hydrolysis and the oxidation of NADH as previously described[3]. Reactions were performed at 37°C with 0.1 µM reverse gyrase wild type in the same buffer described for fluorescence anisotropy titrations additionally containing 0.4 mM phosphoenol pyruvate, 0.2 mM NADH, 23 µg ml^{-1} lactate dehydrogenase and 37 µg ml^{-1} pyruvate kinase. K_M values in the presence of saturating DNA or ATP concentrations were determined in an ATP- or DNA-dependent manner, respectively. Initial reaction velocities v were calculated *via* $\Delta A_{340}/(\Delta t \bullet \varepsilon_{340,NADH})$, with $\varepsilon_{340,NADH}$ = 6220 M^{-1} cm^{-1}. The Michaelis-Menten formalism was used to analyse the data. ATP was purchased from Pharma Waldhof (Düsseldorf, Germany) and checked for impurities by reversed phase HPLC on a C_{18} column in 0.1 M sodium phosphate, pH 6.5.

7.3 Results

Two reverse gyrase Y851F molecules non-covalently bind to the 60-mer ssDNA substrate in a cooperative manner in the absence and presence of various adenine nucleotides. However, no cooperative binding was observed using 60 bp dsDNA as a substrate[5]. Reverse gyrase has an estimated binding surface for 20 bp dsDNA and non-cooperative binding may be revealed with substrates shorter than 60 bp. Binding affinities of 20- and 40-mer ss/dsDNA substrates were determined in comparison with the 60-mer constructs (Figure 1A).

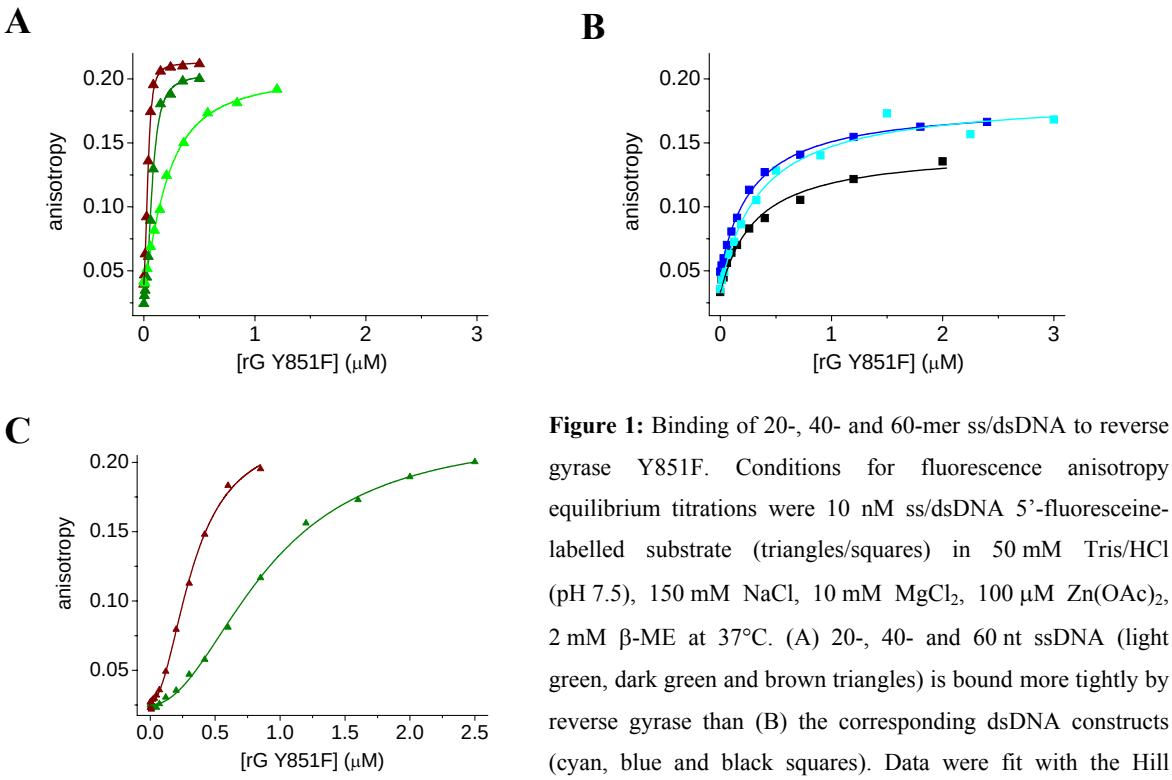

Figure 1: Binding of 20-, 40- and 60-mer ss/dsDNA to reverse gyrase Y851F. Conditions for fluorescence anisotropy equilibrium titrations were 10 nM ss/dsDNA 5'-fluoresceine-labelled substrate (triangles/squares) in 50 mM Tris/HCl (pH 7.5), 150 mM NaCl, 10 mM $MgCl_2$, 100 μM $Zn(OAc)_2$, 2 mM β-ME at 37°C. (A) 20-, 40- and 60 nt ssDNA (light green, dark green and brown triangles) is bound more tightly by reverse gyrase than (B) the corresponding dsDNA constructs (cyan, blue and black squares). Data were fit with the Hill equation, showing cooperative binding of at least two reverse gyrase molecules to one 40- or 60-mer ssDNA (Table 2). No cooperative binding was described by the Hill equation for the 20-mer ssDNA or all dsDNA constructs. Thus, a model describing one-site binding was fit to the corresponding data. (C) Stoichiometric titration of 300 nM 60 nt ssDNA (brown triangles, $K_D = 0.33 \pm 0.02$ μM, $n = 2.0 \pm 0.1$) and 500 nM 40 nt ssDNA (dark green triangles, $K_D = 0.91 \pm 0.03$ μM, $n = 2.0 \pm 0.1$) reveals a sigmoidal binding curve and pronounced cooperative binding of these single-stranded substrates to reverse gyrase.

The data describing the binding curves are summarised in Table 2.

Table 2. ss/dsDNA substrates with different lengths binding to reverse gyrase Y851F at 37°C.

	▲ ssDNA		■ dsDNA
	K_D (nM)	**n**	**K_D (nM)**
20-mer	210 ± 15	1.4 ± 0.1	350 ± 45
40-mer	73 ± 3	2.2 ± 0.2	300 ± 10
60-mer	36 ± 1	2.3 ± 0.2	490 ± 60

The binding affinity of ssDNA constructs to reverse gyrase Y851F increases with substrate length (Figure 1A). dsDNA constructs exhibit the opposite effect, where binding affinity decreases with substrate length (Figure 1B). Thus, the 60 bp duplex binds with the lowest affinity, as opposed to the 60-mer ssDNA binding with the highest affinity. The K_D values between the 60-mer ss/dsDNA constructs span over greater than one order of magnitude. Most interestingly, both the 40- and 60-mer ssDNA are bound in a cooperative manner with Hill coefficients of 2.2 and 2.3, respectively. Notably, binding of ssDNA substrates

results in a higher final anisotropy value of about 0.2 compared to 0.15 for dsDNA constructs, as described earlier (cp. Chapter 6.3).

Because both the type and length of the DNA constructs affect substrate affinity, the various ss/dsDNA substrates might also have an effect on reverse gyrase ATPase activity. Dependency of the steady-state ATPase rates of reverse gyrase wild-type on the DNA substrate was consequently tested (Figure 2).

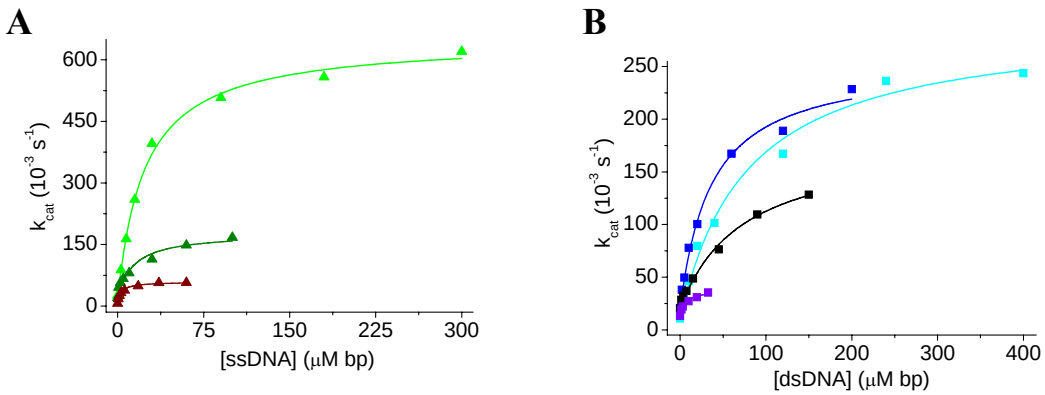

Figure 2: Steady-state ATPase activity of reverse gyrase in dependency of ss/dsDNA substrates of varying lengths. 0.1 µM reverse gyrase wild-type were incubated in 50 mM Tris/HCl (pH 7.5), 150 mM NaCl, 10 mM $MgCl_2$, 100 µM $Zn(OAc)_2$, 2 mM β-ME, 0.4 mM phosphoenol pyruvate and 0.2 mM NADH with 1 mM ATP at 37°C. Initial ATP hydrolysis velocities were calculated *via* the absorbance change at 340 nm over time ($\varepsilon_{340,NADH}$ = 6220 M^{-1} cm^{-1}) and converted to k_{cat} by normalising to the enzyme concentration. Data were analysed with the Michaelis Menten formalism. Reactions had the depicted concentration of (A) 20, 40 and 60 nt ssDNA (light green, dark green and brown triangles) or the corresponding dsDNA constructs (cyan, blue and black squares), as shown in panel (B). For the 107 bp dsDNA (purple squares), 1 µM reverse gyrase was used.

The DNA substrate length influences the ATPase activity of reverse gyrase as follows: the shorter the substrate, the higher are the calculated k_{cat} values. All corresponding values for k_{cat} and $K_{M,DNA}$ are listed in Table 3.

Table 3. Key data for reverse gyrase steady-state ATPase at 37°C in dependency of the ss/dsDNA substrate length.

		k_{cat} (10^{-3} s^{-1})	K_M (µM nt/bp)
▲ **ssDNA**	20-mer	624 ± 14	24 ± 2
	40-mer	157 ± 13	14 ± 4
	60-mer	52 ± 2	3.0 ± 0.4
■ **dsDNA**	20-mer	282 ± 15	78 ± 12
	40-mer	235 ± 10	37 ± 5
	60-mer	160 ± 13	73 ± 13
	107-mer	40 ± 2	5.7 ± 1.6

With about 0.6 s^{-1}, the k_{cat} value for the 20-mer ssDNA is 4-fold and 12-fold higher compared to the ones of the 40-mer and the 60-mer. At the same time, the $K_{M,DNA}$ is 8-fold higher for the 20-mer than the one for the 60-mer. Thus, ATPase stimulation of reverse gyrase and ssDNA substrate binding are inversely correlated. Also, there is a distinct order of dsDNA-stimulated ATP hydrolysis increasing 7-fold from 107 bp to 20 bp substrate. However, no clear pattern is obtained for the $K_{M,DNA}$ values of the dsDNA, which generally lie 2-3-fold above the $K_{M,DNA}$ values for the ssDNA substrates. Accordingly, an overall diminished binding of dsDNA is observed, as confirmed in fluorescence anisotropy titrations (see Table 2).

Next, it was interesting to determine whether DNA substrate binding had an influence on ATP binding, as already shown for the 60-mer ss/dsDNA constructs[5]. In order to examine cooperativity between ATP binding and DNA substrate binding, ATP hydrolysis by reverse gyrase was recorded as a function of the ATP concentration in the presence of different DNA substrates (Figure 3).

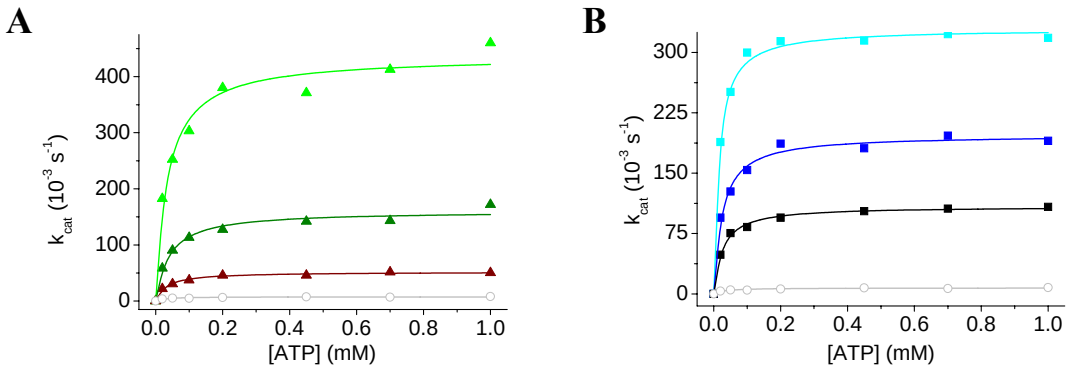

Figure 3: ATP-dependent steady-state ATP hydrolysis by reverse gyrase wild-type in the presence of saturating ss/dsDNA constructs of different length. For conditions and data processing see the legend in Figure 2. For all substrates, 90% saturation was adjusted using (A) 0.5, 2.5 and 7.5 µM of 20-, 40- and 60-mer ssDNA (light green, dark green and brown triangles) or (B) 5, 4 and 20 µM of the corresponding dsDNA constructs (cyan, blue and black squares). The control shown in both panels does not contain any ss/dsDNA (grey circles).

The maximum velocity of ATP hydrolysis is increased from the longest to the shortest substrate with saturating concentrations of both ssDNA and dsDNA substrates present, analogous to the results obtained from DNA-dependent titrations (cp. Figure 2 and Table 3). The corresponding K_M values for ATP binding and the ATP hydrolysis rates in the presence of ss/dsDNA are listed in Table 4.

Table 4. Steady-state ATPase of reverse gyrase wild-type at 37°C in the presence of saturating ss/dsDNA concentrations.

		k_{cat} (10^{-3} s^{-1})	$K_{M,ATP}$ (μM)
no DNA	---	7.5 ± 0.4	28 ± 8
▲ **ssDNA**	20mer	436 ± 16	35 ± 7
	40mer	160 ± 6	40 ± 7
	60mer	52 ± 1	32 ± 4
■ **dsDNA**	20mer	329 ± 4	14 ± 1
	40mer	198 ± 4	24 ± 3
	60mer	109 ± 1	25 ± 2

The k_{cat} values in the presence of ssDNA are increased 7-, 21- and 58-fold from 60-mer down to the 20-mer compared to non-stimulated ATP hydrolysis. The same principle is shown in the case of dsDNA substrates where ATP hydrolysis is stimulated 15-, 26- and 44-fold from 60-mer to 20-mer. Overall, the k_{cat} values in the ATP-dependent titrations are in good agreement with the values determined in DNA-dependent titrations (see Table 3). For both DNA types the following is true: the shorter the substrate, the higher are the maximum velocities of ATP hydrolysis.

Analysing the $K_{M,ATP}$ values in the presence of ssDNA, the binding of ATP is slightly but not significantly decreased compared to the absence of substrate. Most interestingly, cooperative binding of ATP is indicated for dsDNA-stimulated ATP hydrolysis, as the $K_{M,ATP}$ value is reduced to half its value in the presence of the 20-mer. The two other dsDNA substrates do not have any effect on ATP binding.

7.4 Discussion

Preferred binding of reverse gyrase to single stranded DNA regions has been known for quite some time, and has been only qualitatively demonstrated[4]. We previously found that the ATPase activity of reverse gyrase under steady-state conditions is stimulated by 60-mer ss/dsDNA[5]. Interestingly, cooperative binding of at least two reverse gyrase molecules to one 60-mer ssDNA was observed. Moreover, the current chapter quantitatively presents the effect of ss/dsDNA substrate length on steady-state ATPase stimulation of reverse gyrase with respect to binding cooperativity using 20-, 40-, and 60-mer constructs.

For the 40 and 60 nt ssDNA constructs, cooperative binding of two or more reverse gyrase molecules to one substrate molecule was demonstrated along with higher binding affinity. The 20-mer ssDNA and all dsDNA constructs bind up to an order of magnitude weaker and show no cooperative binding, indicating a minimum length for cooperativity between 20 and 40 nt. The fact that ssDNA binding results in significantly higher final anisotropy values than binding to dsDNA substrates also indicates cooperative binding of more than one reverse gyrase molecule and is discussed in Chapter 6.3. In the future, it will be interesting to know if longer ssDNA substrates bind tighter to reverse gyrase and if more reverse gyrase molecules would be capable of binding to it. Unfortunately, the 107-mer used for ATPase stimulation of reverse gyrase was only available as dsDNA. Furthermore, poor availability and purity of the 107 bp dsDNA brought up the use of the artificially synthesised and highly pure 20-, 40- and 60-mer substrates introduced in this chapter.

Regarding ATP hydrolysis by reverse gyrase, a clear dependency on the ssDNA and dsDNA substrate length was demonstrated. Most interestingly, it is evident that the shorter the ssDNA or dsDNA substrate, the higher is the resulting stimulation of the ATPase. There also is a clear inverse correlation for the ssDNA substrates between DNA binding and the stimulation of DNA-dependent ATP hydrolysis. Weak binding of the 20 nt substrate is accompanied by highly effective ATPase stimulation, as seen for other unspecific binding partners for reverse gyrase, such as polyU RNA[5]. Reduced binding of the 20 nt ssDNA is reflected in the 8-fold increased K_M value compared to the 60 nt ssDNA. Notably, the resulting K_M values lie 100-fold above the K_D values obtained in fluorescence anisotropy titrations. This is due to the fact that the K_M value is an implicit measure for substrate affinity, as both ATP hydrolysis and binding to reverse gyrase are included in the coupled enzymatic assay applied. Interestingly, cooperative binding of ATP was shown for the 20 bp dsDNA only. The similar properties compared to the 20 nt ssDNA can also in part be explained by a T_m of 42°C for the 20 bp dsDNA, which is only 5°C above the measuring temperature. In the future, DNA stimulation of reverse gyrase ATPase activity should also be tested under single turnover conditions at 75°C for the ssDNA constructs to confirm the effects observed at 37°C.

Until now, no minimal binding length of ssDNA or dsDNA substrates has been reported for reverse gyrase. Thus, the minimal binding size for ss/dsDNA substrates for reverse gyrase might be below 20 bp. It would be interesting to see what happens with respect to DNA binding and ATPase stimulation at this critical mark. With a diameter of 50-70 Å[7], the maximal binding surface of reverse gyrase is about 15-20 bp wide. On the 2686 bp

large pUC18, about 135-180 reverse gyrase molecules could potentially bind cooperatively and mutually activate the enzyme's plasmid relaxation and positive supercoiling ability. However, the actual working manner of reverse gyrase remains unknown. Reverse gyrase is purified as a monomer and, to the best of our knowledge no cooperation is required for enzyme activity. To further elucidate cooperative binding, more diverse information could be gained from experiments with constructs harbouring combined single and double stranded DNA regions (i.e. 20/40, 20/60, 40/60-mers).

7.5 Literatur

(1) Kikuchi A., Asai K., Reverse gyrase - a topoisomerase which introduces positive superhelical turns into DNA, *Nature*, **1984**, *309*, 677-681.

(2) Champoux J. J., DNA Topoisomerases: Structure, Function, and Mechanism, *Annu. Rev. Biochem.*, **2001**, *70*, 369-413.

(3) Jungblut S. P., Klostermeier D., Adenosine 5′-O-(3-thio)triphosphate (ATPγS) Promotes Positive Supercoiling of DNA by *T. maritima* Reverse Gyrase, *J. Mol. Biol.*, **2007**, *371*, 197-209.

(4) Shibata T., Nakasug S., Yasuip K., Kikuch A, Intrinsic DNA-dependent ATPase Activity of Reverse Gyrase, *J. Biol. Chem.*, **1987**, *262*, 10419-10421.

(5) del Toro Duany Y., Jungblut S. P., Schmidt A. S., Klostermeier D., The reverse gyrase helicase-like domain is a nucleotide-dependent switch that is attenuated by the topoisomerase domain, *Nucleic Acids Research*, **2008**, *36*, 5882-5895.

(6) Ma Y., Lieber M. R., DNA Length-Dependent Cooperative Interactions in the Binding of Ku to DNA, *Biochemistry.*, **2001**, *40*, 9638-9646.

(7) Rodríguez A. C., Stock D., Crystal structure of reverse gyrase: insights into the positive supercoiling of DNA, *EMBO*, **2002**, *21*, 418-426.

(8) Watson J. D., Crick F. H., A Structure for Deoxyribose Nucleic Acid, *Nature*, **1953**, *171*, 737-738.

(9) Kovalsky O.I., Kozyavkin S.A., Slesarev A.I, Archaebacterial reverse gyrase cleavage-site specificity is similar to that of eubacterial DNA topoisomerases I, *Nucleic Acids Res.*, **1990**, *18*, 2801-2805.

(10) Jaxel C., Duguet M., Nadal M., Analysis of DNA cleavage by reverse gyrase from Sulfolobus shibatae B12, *Eur. J. Biochem.*, **1999**, *260*, 103-111.

8. Rationale of Selective Fluorescent Labelling of Reverse Gyrase and Initial smFRET Studies

8.1 Introduction

Structural information about reverse gyrase is as rare as mechanistic details of its intrinsic ATP-dependent positive supercoiling activity[1]. An electron microscopy study of the enzyme indicates a hole of 10-20 Å in diameter that may be suitable for dsDNA binding[2]. This was confirmed in the only available crystal structure from *Archeoglobus fulgidus* reverse gyrase[3]. No structural information exists for the enzyme from *Thermotoga maritima*, the subject of the present thesis.

Single molecular Förster resonance energy transfer (smFRET) is a suitable method to observe predicted conformational changes in reverse gyrases[3] and requires fluorescent donor and acceptor labelling. To investigate the mechanism of positive supercoiling by reverse gyrases in general, preparations for smFRET studies have been carried out using a homology model from *A. fulgidus* reverse gyrase. However, a problem of homology model-based choice of potential labelling sites in proteins remains, namely the surface accessibility in the model must not necessarily be true for the investigated enzyme. Furthermore, the native cysteines present in *T. maritima* reverse gyrase may interfere with fluorescent labelling. It has been reported that these eight cysteines in two putative zinc finger regions in reverse gyrase may play an important role for DNA binding[3,4]. In proteins, Zn^{2+} is bound in structural elements that stabilise tertiary structure and provide various protein functions. Zn^{2+} is coordinated by four cysteines and/or histidines in so called zinc fingers, which are important for DNA binding[5]. An initial mutational study indicates an influence of the N-terminal putative zinc finger on positive supercoiling by reverse gyrase[6]. However, topoisomerase I from *T. maritima* also contains a putative zinc finger region that is able to bind zinc, but is not essential for topoisomerase activity[7]. Also, the crystal structure of the *T. maritima* topoisomerase I reveals no bound zinc ion but shows cystine disulfide bond formation for structural stability of the zinc binding motif[8]. For *T. maritima* reverse gyrase, it remains unknown, if the two putative zinc fingers are capable of binding zinc or are functional during topoisomerase activity. Thus, the first part of the present study concentrates on the investigation of the two putative zinc finger regions of reverse gyrase from *T. maritima* for topoisomerase activity and the reactivity of wild type cysteines with maleimides of fluorescent dyes.

The second part of this chapter aimed at elucidating the molecular mechanism behind the catalytic cycle of reverse gyrase, for which large conformational changes have been proposed[3]. The hypothetical mechanism includes movement of the two subdomains of the helicase-like domain during the adenine nucleotide cycle, which is suggested by findings from authentic helicases[9,10]. Additionally, the latch region inserted in the helicase-like domain of reverse gyrase acts as a trigger upon DNA binding and facilitates opening of the topoisomerase domain[3,11]. For topoisomerase I from *Escherichia coli*, minor conformational changes were observed, when a single protein helix shifts and holds ssDNA bound close to the active site[12]. The crystal structure of *E. coli* topoisomerase III (type IA) in complex with ssDNA reveals conformational changes necessary for binding of the substrate to the groove in the vicinity of the active tyrosine[13]. Further X-ray studies with the same enzyme reveal additional ssDNA-bound conformations during intermediate steps between substrate binding and ssDNA cleavage and suggest consecutive domain movements[14].

For reverse gyrase, inter-domain communication between the helicase-like domain and the topoisomerase domain has also been suggested with respect to an inhibitory influence of the topoisomerase domain on the ATPase cycle[15]. Most likely, conformational changes also mediate coupling of adenine nucleotide binding and hydrolysis[16,17] to DNA binding and strand passage during positive supercoiling[15,16]. Furthermore, cooperative binding of reverse gyrase to ssDNA was found, indicating potential interactions between several reverse gyrase molecules during topoisomerase activity[15]. However, no data that correlates structure and topoisomerase functions exists for any reverse gyrase.

To define the role of conformational changes for topoisomerase function, we set out to observe predicted domain movements[3,4] of reverse gyrase from *Thermotoga maritima* with smFRET.

8.2 Material and Methods

Generation and Purification of Reverse Gyrase Cysteine Mutants

Wild type reverse gyrase was purified as described[17] (Chapter 3.2). Single cysteine mutants (S169C, D173C, F332C, S341C, K440C, D452C, V973C, F993C, Y994C) were generated *via* site-directed mutagenesis (QuikChange, Stratagene). Suitable positions for labelling with donor and acceptor dyes were selected according to labelling efficiencies of single cysteine mutants. Double cysteine mutants were generated *via* stepwise mutagenesis (S169C/F332C, D173C/F332C, D452C/D878C). Cysteine mutants still contain all native cysteines of wild type reverse gyrase. A deletion mutant lacking both putative zinc fingers (ΔM1-H58/ΔR620-I643), named Δzif1/2, and a mutant with altered putative zinc fingers (C11A/C14A-C635A/C638A), abbreviated C_4A_4, were generated correspondingly by Ramona Heissmann (University of Bayreuth). After sequence confirmation, mutants were produced and purified according to the wild type protocol.

Analysis of Topoisomerase Activity

Topoisomerase activity of reverse gyrase wild type and mutants was determined using negatively supercoiled pUC18 plasmid as substrate. Reactions were performed and topoisomer distribution of pUC18 was analysed as described in the literature[17] and Chapter 3.2, unless otherwise stated.

Accessibility of Native Cysteines with DTNB

Cysteine reactivity of wild type reverse gyrase was tested with 5,5'-dithiobis-(2-nitrobenzoic acid) (DTNB) after Ellmann[18]. Upon nucleophilic attack of a deprotonated cysteine on DTNB, 2-nitro-5-thiobenzoate (TNB^{2-}) is released and subsequently detected at 412 nm. The reaction of 1.3 μM reverse gyrase with 21 μM DTNB was carried out in 50 mM Tris/HCl (pH 8.0), 150 mM NaCl, 10 mM $MgCl_2$, 100 μM $Zn(OAc)_2$ at 25°C until saturation of A_{412}. The molar extinction coefficient of TNB^{2-} under these conditions was determined[19] to $\varepsilon_{412,TNB}{}^{2-} = 20'000\ M^{-1}\ cm^{-1}$. The number of accessible cysteines can be calculated from $[TNB^{2-}]/[\text{reverse gyrase}]$, where $[TNB^{2-}] = \Delta A_{412} / \varepsilon_{412,TNB}{}^{2-}$, using cuvettes with a path length of 1 cm after Lambert-Beer.

Zinc Release from Reverse Gyrase with PMB and Detection with PAR

The irreversible reaction of p-(hydroxymercuri)-benzoic acid (PMB) with sulfhydryl groups releases metal ions from zinc fingers. Free Zn^{2+} forms a complex with 4-(2-pyridylazo)-resorcinol (PAR), which absorbs at 500 nm[20,21]. Zinc release from 1 μM reverse gyrase was tested in a PMB-dependent titration in 50 mM Tris/HCl (pH 7.5), 150 mM NaCl, 10 mM $MgCl_2$ at 25°C in the presence of 100 μM PAR until no change in A_{500} was observed. The molar extinction coefficient of the $Zn(PAR)_2$ complex was determined under these conditions (ε_{500} = 100'000 M^{-1} cm^{-1}). The amount of Zn^{2+} released per reverse gyrase molecule is $[Zn(PAR)_2]$/[reverse gyrase]. $[Zn(PAR)_2]$ is calculated after Lambert-Beer.

Fluorescent Labelling of Reverse Gyrase Wild Type and Cysteine Mutants

Single and double cysteine mutants of *T. maritima* reverse gyrase were fluorescently labelled in 50 mM Tris/HCl (pH 7.5), 500 mM NaCl, 10 mM $MgCl_2$, 100 μM $Zn(OAc)_2$, 25 μM tris-(2-carboxyethyl)-phosphine (TCEP). 4-10 μM protein were incubated with the donor dye Alexa488-maleimide (A488, 5-10-fold molar excess) and the acceptor dye tetramethylrhodamine-5-maleimide (TMR, 15-30-fold molar excess) for 3 h at 25°C. Alternatively, the Alexa dye A546 was used as acceptor. The labelling reaction was quenched with β-ME (200-fold excess of acceptor dye), and free dye was removed on Micro Bio-Spin 30 colums (Biorad) by size exclusion chromatography following the manufacturer's instructions. The labelling efficiency was determined from absorbance ratios of the donor (A488: ε_{494} = 72'000 M^{-1} cm^{-1}, corrected for acceptor contributions) and the acceptor (TMR: ε_{555} = 95'000 M^{-1} cm^{-1}, A546: ε_{555} = 93'000 M^{-1} cm^{-1}). The protein concentration was determined from absorbance at 280 nm (ε_{280} = 111'470 M^{-1} cm^{-1}, corrected for dye contributions).

Limited Proteolysis of Reverse Gyrase

Labelled proteins were digested with trypsin to determine positions for donor and acceptor dyes. 1 μM labelled reverse gyrase was incubated with 0.1 μM trypsin in 50 mM Tris/HCl (pH 8.0), 150 mM NaCl, 10 mM $MgCl_2$, 100 μM $Zn(OAc)_2$, 2 mM β-ME at 20°C over night. Protein fragments were analysed with 10% SDS polyacrylamide gel

electrophoresis. N-terminal sequencing of unlabelled fragments after Edman[22] was kindly carried out by Dr. Bernhard Schmidt (University of Göttingen).

Determination of Förster Distances and Quantum Yields

The donor quantum yield of the fluorescent dye A488 bound to the reverse gyrase single cysteine mutants S169C, D173C, F332C, D452C or D878C was determined relative to fluoresceine as a reference[23,24]. The quantum yield Φ of fluoresceine in 0.1 M NaOH is 0.92[24]. For each reverse gyrase double mutant, Förster distances r_0 were calculated after[25]:

$$r_0 = \sqrt[6]{8.785 \cdot 10^{-5} \frac{\kappa^2 \cdot \phi_D}{n^4} \cdot \int F_D(\lambda) \cdot \varepsilon_A(\lambda) \cdot \lambda^4 d\lambda} \quad (1),$$

where κ^2 is the orientation factor, which was set to 2/3 assuming free rotatability of the donor and acceptor dyes. The refractive index n of water is 1.33 and was assumed to be equal for the aqueous solutions in the smFRET experiments. Φ_D is the quantum yield of the donor in the absence of acceptor[23], $F_D(\lambda)$ is the normalised fluorescence spectrum of protein labelled only with donor and $\varepsilon_A(\lambda)$ is the normalised absorbance spectrum of protein labelled only with acceptor.

Single Molecule FRET Experiments

The smFRET experiments were carried out using a self-made confocal microscope (Chapter 1.4). Fluorescence was detected separately for the donor and acceptor dyes. A fluorescence burst was only analysed, if it contained more than 100 photons as the threshold. Corresponding FRET efficiencies (E_{FRET}) were calculated according to[26]:

$$E_{FRET} = \frac{(1+\beta\cdot\gamma\cdot\delta)\cdot\left(I_A - \frac{\alpha+\gamma\cdot\delta}{1+\beta\cdot\gamma\cdot\delta}\cdot I_D\right)}{(1+\beta\cdot\gamma\cdot\delta)\cdot\left(I_A - \frac{\alpha+\gamma\cdot\delta}{1+\beta\cdot\gamma\cdot\delta}\cdot I_D\right) + (\gamma+\gamma\cdot\delta)\cdot(I_D - \beta\cdot I_A)} \quad (2).$$

The measured fluorescence intensities of the donor (I_D) and the acceptor (I_A) were corrected for various effects accounted for in the correction factors α, β, γ and δ explained below. Firstly, crosstalk of donor and acceptor fluorescences was taken into account:

$$\alpha = \frac{I_{D-A}}{I_{D-D}} \quad (3), \qquad \beta = \frac{I_{A-D}}{I_{A-A}} \quad (4).$$

α is the donor crosstalk in the acceptor channel and is expressed as the ratio of fluorescence intensities of donor emission detected in the acceptor channel ($I_{D\text{-}A}$) to donor emission detected in the donor channel ($I_{D\text{-}D}$). The acceptor crosstalk β is described correspondingly.

The detection efficiency for donor and acceptor fluorescences depends on the setup, which is considered along with different quantum yields for donor and acceptor dyes:

$$\frac{C_D}{C_A} = \gamma \cdot \frac{I_D - \beta \cdot I_A}{I_A - \alpha \cdot I_D} \quad (5),$$

where C_D is the number of photons absorbed by the donor without being transferred to the acceptor, in contrast to the number of photons absorbed by the acceptor by direct excitation or transfer from the donor (C_A). Also, the fluorescence intensities of the donor (I_D) and the acceptor (I_A) corrected for crosstalk are included in the correction factor γ. The final correction factor δ takes direct excitation of the acceptor into account:

$$\gamma \cdot \delta = \frac{I_{A-A}}{I_{D-D}} \quad (6).$$

smFRET measurements were performed in 50 mM Tris/HCl (pH 7.5), 150 mM NaCl, 10 mM $MgCl_2$, 100 µM $Zn(OAc)_2$ at 25°C. Fluorescently labelled enzyme (250 pM with respect to the donor concentration) was incubated in the presence and absence of 1 mM ATP, ADP or ADPNP as nucleotide and 15 nM pUC18 or 0.5 µM 60-mer ssDNA or dsDNA as substrate. 5-7 million bursts were collected for every measurement in about 20 minutes. The 60-mer ssDNA (sequence in Chapter 5.2) and the complementary strand were purchased from Purimex (Grebenstein, Germany). The 60-mer dsDNA substrate was formed by annealing the two single strands[15].

Steady-State ATPase Activity of Reverse Gyrase

Steady-state ATP hydrolysis by reverse gyrase wild type and labelled or unlabelled mutants was tested to further characterise the influence of fluorescent labels on the ATPase activity. The coupled enzymatic ATPase assay was performed at 37°C as previously described[17] (Chapter 7.2).

8.3 Results

Native Cysteines of Reverse Gyrase from *T. maritima*

Are native cysteines important for topoisomerase activity of reverse gyrase?

The functional relevance of the putative zinc finger regions of reverse gyrase from *T. maritima* for topoisomerase activity by reverse gyrase is unclear. A deletion mutant lacking both putative zinc finger regions (Δzif1/2) and a second mutant where two cysteines have been changed into alanines in each putative zinc finger (C_4A_4) were tested for positive supercoiling activity (Figure 1).

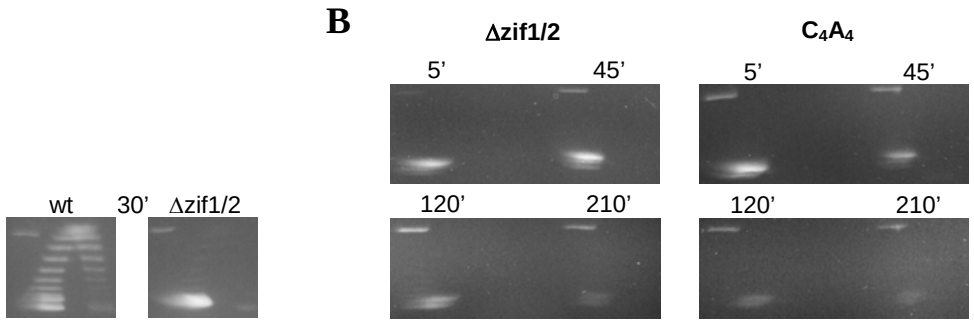

Figure 1. Positive supercoiling activity of reverse gyrase zinc finger mutants analysed with two-dimensional agarose gel electrophoresis. 1 mM reverse gyrase wild type (wt), ΔM1-H58/ΔR620-I643 mutant (Δzif1/2) or C11A/C14A/C635A/C638A mutant (C_4A_4) were incubated in 50 mM Tris/HCl (pH 7.5), 150 mM NaCl, 10 mM $MgCl_2$, 100 µM $Zn(OAc)_2$, 2 mM β-ME, 2 mM ATP, 15 nM pUC18, 10% (w/v) PEG 8000 at 75°C for the time indicated. (A) Δzif1/2 reverse gyrase is inactive. (B) A time course recorded for Δzif1/2 and C_4A_4 shows no supercoiling activity for both reverse gyrase mutants.

Reverse gyrase Δzif1/2 is supercoiling-inactive (Figure 1A). A systematic analysis of Δzif1/2 and C_4A_4 reverse gyrase demonstrates lack of supercoiling activity for both mutants (Figure 1B), and no relaxation is observed in the presence of ADP (data not shown). In summary, intact putative zinc finger regions of *T. maritima* reverse gyrase are required for positive supercoiling. Additionally, the Δzif1/2 and C_4A_4 mutants are less stable compared to the wild type and are purified as aggregates (data not shown). Thus, deletion or mutation of the native cysteines in reverse gyrase is not an alternative in order to avoid fluorescent labelling, as they are required for topoisomerase activity.

Do native cysteines of reverse gyrase interfere with fluorescent labelling?

Six to eight of the native cysteines in reverse gyrase wild type react with DTNB in the absence of zinc[27]. To improve solubility of reverse gyrase, 100 µM $Zn(OAc)_2$ were used as standard supplement at the beginning of the PhD project. The DTNB accessibility of the cysteines in reverse gyrase at 100 µM $Zn(OAc)_2$ and higher was determined to check for potential masking of the native cysteines (Figure 2).

Figure 2. DTNB accessibility of wild type cysteines in reverse gyrase tested in the presence of different zinc concentrations after Ellman[18]. 1.3 µM reverse gyrase were incubated with 21 µM DTNB in 50 mM Tris/HCl (pH 8.0), 150 mM NaCl, 10 mM $MgCl_2$ at 25°C until saturation of A_{412}. The ΔA_{412} values of 0.093, 0.085 and 0.185 correspond to 3.6, 3.3 and 7.1 accessible cysteines in the presence of 100, 250 or 500 µM $Zn(OAc)_2$ (black, green and blue lines) using $\varepsilon_{412,TNB}^{2-}$ = 20'000 M^{-1} cm^{-1}).

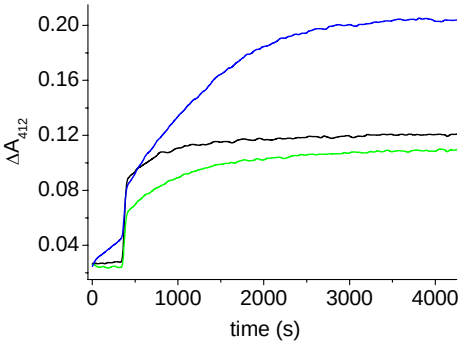

Three to four cysteines of reverse gyrase wild type are DTNB-accessible in the presence of 100 µM and 250 µM zinc. All eight native cysteines react with DTNB in the presence of 0.5 mM zinc, where concomitant protein precipitation was observed (data not shown). Thus, 100 µM $Zn(OAc)_2$ potentially mask all four cysteines contained in one of the two putative zinc fingers rendering it DTNB-inaccessible. The presence of plasmid DNA may also have a masking effect on the two putative zinc fingers as potential DNA binding sites. Subsequently, DTNB reactivity of reverse gyrase was tested in the presence of pUC18 (Figure 3).

Figure 3. Cysteine accessibility of reverse gyrase with DTNB in the presence of pUC18. 0.7 µM reverse gyrase were incubated with 18 µM DTNB in 50 mM Tris/HCl (pH 8.0), 150 mM NaCl, 10 mM $MgCl_2$, 500 µM $Zn(OAc)_2$ at 25°C. Accessibility of 6.4 or 8.6 cysteines in the presence of 30 nM (black line) and 150 nM pUC18 (blue line) is calculated from the ΔA_{412} values of 0.09 and 0.12, correspondingly. ($\varepsilon_{412,TNB}^{2-}$ = 20'000 M^{-1} cm^{-1}).

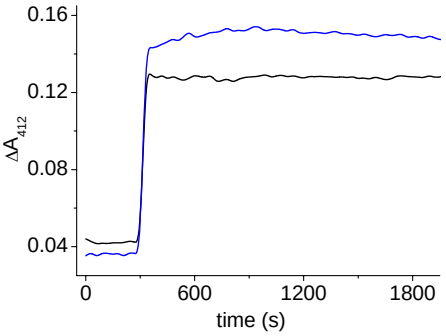

DTNB labels six to eight native cysteines in reverse gyrase in the presence of pUC18. Thus, the two putative zinc-fingers may be in a more accessible conformation in the presence of pUC18 suggesting a role of the putative zinc finger regions of reverse gyrase for DNA binding in general.

How much zinc is bound naturally by wild type reverse gyrase?

It would be now interesting to know, if the putative zinc finger regions of *T. maritima* reverse gyrase are capable of binding zinc. Therefore, zinc release from reverse gyrase wild type and C_4A_4 was tested in the absence of zinc in the buffer (Figure 4).

Figure 4. Zinc release from reverse gyrase wild type and C_4A_4 with PMB. 1 µM enzyme in 50 mM Tris/HCl (pH 7.5), 150 mM NaCl, 10 mM $MgCl_2$ at 25°C were titrated with PMB. Formation of the $Zn(PAR)_2$ complex leads to an absorbance change of 0.05 and 0.02 at 500 nm for reverse gyrase wild type (black) and C_4A_4 (blue) that translates to 0.5 and 0.2 zinc ions released per enzyme ($\varepsilon_{500,Zn(PAR)2}$ = 100'000 M^{-1} cm^{-1}).

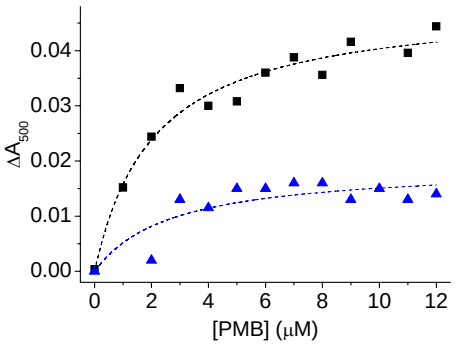

No zinc is released from the reverse gyrase mutant C_4A_4, suggesting that zinc binding by the putative zinc fingers may be disrupted in this mutant. However, only 0.5 zinc ions are released from reverse gyrase wild type, indicating that at the most one zinc ion is bound by one of the putative zinc fingers of reverse gyrase. The DTNB accessibility of four cysteines in wild type reverse gyrase is in agreement with this finding. However, reactivity of DTNB with the native cysteines of *T. maritima* reverse gyrase might not reflect reactivity with maleimides of fluorescent dyes used for labelling. In summary, the cysteines in the putative zinc fingers of reverse gyrase are important for topoisomerase activity and are partially accessible by DTNB. Thus, the conditions for fluorescent labelling have to be chosen accordingly.

Fluorescent labelling of reverse gyrase from *T. maritima*

To investigate the positive supercoiling mechanism of reverse gyrase with smFRET, specific cysteines must be labelled with fluorescent dyes. Although at least four of the eight native cysteines in *T. maritima* reverse gyrase are accessible to DTNB, we set out to find conditions for selective fluorescent labelling of introduced cysteines. Labelling of reverse gyrase wild type and two single cysteine mutants with three fluorescent dyes is shown in Figure 5.

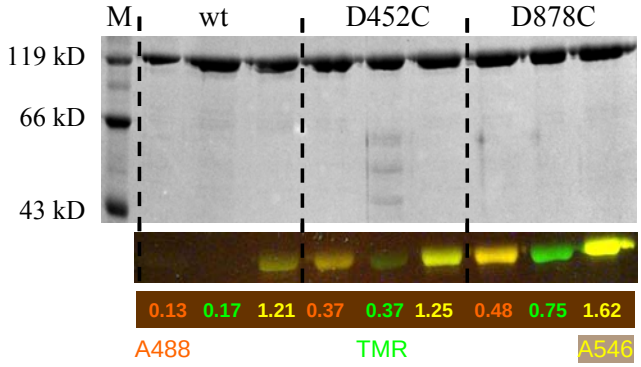

Figure 5. Fluorescent labelling of reverse gyrase wild type and mutants with one additional cysteine at positions D452 or D878. 10% SDS polyacrylamide gel analysis of three labelling reactions with different dyes for each protein. Labelling reactions of 4 µM of reverse gyrase wild (wt) type, D452C or D878C were carried out in 50 mM Tris/HCl (pH 7.5), 500 mM NaCl, 10 mM $MgCl_2$, 100 µM $Zn(OAc)_2$, 1 mM TCEP at 25°C with 100 µM A488, TMR or A546 over night. Free dye was removed with size exclusion chromatography. The gel is shown before (in colors) and after coomassie staining (grey scale) and the position of a molecular size marker (M) is indicated. Labelling efficiencies are given for A488 (orange, donor), TMR (green, acceptor) and A546 (yellow, acceptor). A488 and TMR only label additionally introduced cysteines. A546 also labels native cysteines.

Wild type cysteines of reverse gyrase are only labelled with A546 at high zinc concentrations (100 µM $Zn(OAc)_2$). The cysteine introduced at position D878 of reverse gyrase is more accessible to A488, TMR and A546 compared to position D452. A488 and TMR as fluorescence donor and acceptor is a promising pair for labelling of cysteine mutants of *T. maritima* reverse gyrase, as all native cysteines are unmodified under these conditions. However the low labelling efficiencies for A488 and TMR have to be improved to values closer to 1. To confirm that the fluorescent dyes were covalently attached to the proper position in reverse gyrase, a protease digest with trypsin and subsequent sequencing of the resulting fragments were performed (Figure 6).

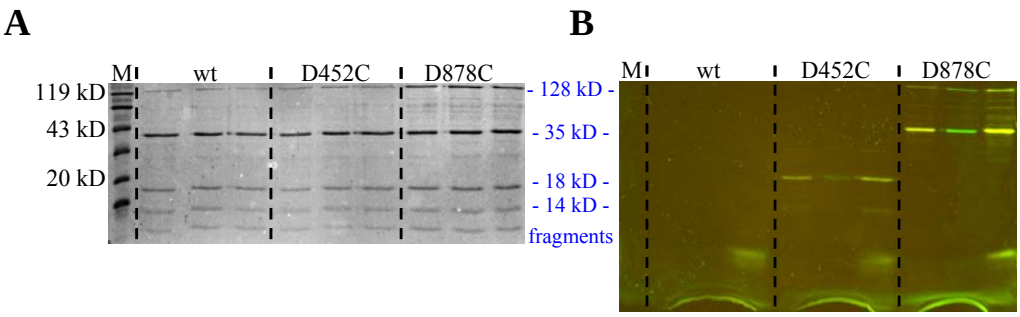

Figure 6. Trypsin digest of reverse gyrase wild type (wt), D452C and D878C after labelling with A488, TMR or A546. Fluorescent labelling was carried out as described in Figure 5. 1 µM labelled protein was digested with 0.1 µM trypsin in 50 mM Tris/HCl (pH 8.0), 150 mM NaCl, 10 mM $MgCl_2$, 100 µM $Zn(OAc)_2$, 2 mM β-ME at 20°C over night and analysed with 10% SDS polyacrylamide gel electrophoresis. The figure shows the gel before (B) and after coomassie staining (A). The position of a molecular size marker (M) is depicted. Fragments of unlabelled protein samples after trypsin digest were N-terminally sequenced after Edman[22]. Three prominent fragments of reverse gyrase

(MW = 128 kD) correspond to the amino acids regions R280 - ~ L404 (14 kD), R370- ~ E533 (18 kD) and R753- ~ R1070 (35 kD). Fraction sizes are depicted in blue. The D452C and D878C mutants are labelled in the 18 kD and 35 kD fragment, respectively.

The serine-protease trypsin hydrolyses protein and peptide chains at the carboxyl side of lysine or arginine. The D452C mutant of reverse gyrase carries a fluorescent dye in an 18 kD fragment containing aspartate 452 and confirms labelling at the correct position. The fluorescent label of the D878C mutant is contained in a 35 kD fragment including aspartate 878. However, labelling of the two putative zinc fingers of reverse gyrase cannot be identified, as fragments including the regions (M1-H58 and R620-I643) were not sequenced and may be completely digest by trypsin.

Cysteine Positions in Reverse Gyrase Mutants Suitable for Fluorescent Labelling

In order to describe conformational changes during topoisomerase activity of reverse gyrase, several regions in the enzyme are of special interest. Single cysteines for fluorescent labelling and subsequent smFRET studies were introduced at either side of the cleft in the helicase-like domain of reverse gyrase and at the predicted lid in the topoisomerase domain (Figure 7).

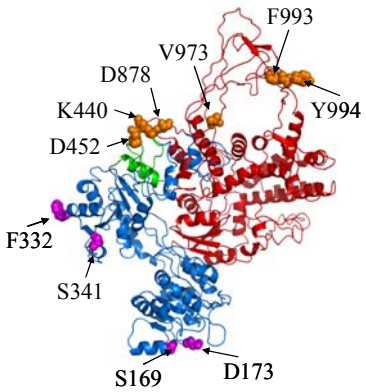

Figure 7. Positions for the introduction of surface-accessible cysteines in functional regions of reverse gyrase. The structure is a homology model of *T. maritima* reverse gyrase based on the X-ray structure of the enzyme from *A. fulgidus*[3]. The positions in magenta are in the N-terminal helicase-like domain (blue) harbouring the ATPase activity of reverse gyrase. Positions on each side of the cleft should approach each other during ATP hydrolysis. The positions in orange lie in the latch region (green) and the C-terminal topoisomerase domain (red) of reverse gyrase. The so called lid is suggested to open between the latch and topoisomerase domains[3].

Single cysteine mutants of reverse gyrase were labelled with A488 and TMR. Only the most promising of these cysteine mutants, judged by labelling efficiency, were selected for the generation of double cysteine mutants. The prospective double cysteine mutants of reverse gyrase that could not be generated with site-directed mutagenesis were not further characterised and are not discussed. The same is true for K440C/D878C reverse gyrase, which was degraded during purification.

Labelling Protocol of Double Cysteine Mutants of *T. maritima* Reverse Gyrase

The positions 169, 173 and 332 in the helicase-like domain, position 452 in the latch and position 878 in the topoisomerase domain (cp. Figure 7) were selected for the generation of the reverse gyrase double mutants S169C/F332C, D173C/F332C and D452C/D878C. The respective Cβ-Cβ distances are 64 Å, 65 Å and 35 Å taken from the crystal structure of reverse gyrase from *A. fulgidus*[3]. The fluorescent dyes A488 and TMR were used as the standard donor and acceptor pair, as they do not label the native cysteines in *T. maritima* reverse gyrase (see Figure 5). The highest labelling efficiencies for the D452C/D878C mutant with A488 and TMR were obtained by reducing the amount of TCEP from 1 mM to 25 μM[28]. The best results were achieved by labelling 10 μM double cysteine mutant with 10-fold excess donor and 30-fold for the acceptor at 25°C for 3h. Finally, free dye was removed with two consecutive size exclusion chromatography steps. The procedure was carried out for the reverse gyrase mutants S169C/F332C, D173C/F332C and D452C/D878C. The final labelling efficiencies for the three double cysteine mutants are given in Table 1.

Table 1. Labelling efficiencies of reverse gyrase S169/F332C, D173C/F332C and D452C/D878C with A488 and TMR.

	labelling efficiency	
reverse gyrase mutant	**A488**	**TMR**
S169C/F332C	1.01	0.77
D173C/F332C	0.45	1.06
D452C/D878C	0.66	0.95

Correction Factors and Förster Distances

For the evaluation of the fluorescence data of the donor and acceptor dyes collected in smFRET experiments, the correction factors and Förster distances of the labelled double mutants of reverse gyrase were determined as described in Chapter 8.2 and are summarised in Table 2.

Table 2. Correction factors, donor quantum yield and Förster distances for reverse gyrase S169/F332C, D173C/F332C and D452C/D878C labelled with A488 (donor) and TMR (acceptor). Data were determined as described in Chapter 8.2.

	α	β	γ	δ	Φ_D	r_0 (Å)
S169C/F332C	0.96	0.019	1.83	0.53	0.14	45
D173C/F332C	0.67	0.020	0.96	0.48	0.25	49.7
D452C/D878C	0.73	0.019	0.92	0.60	0.14	47.8

The correction factors α, β, γ and δ, the quantum yield of the donor in absence of acceptor Φ_D and the Förster distance r_0 for the labelled double mutants were used to determine corrected FRET efficiencies in smFRET measurements individually.

smFRET Measurements

To investigate expected large conformational changes during positive plasmid supercoiling of reverse gyrase[3] and to reveal single steps in the catalytic cycle, saturating substrate conditions of ssDNA, dsDNA and pUC18 in combination with saturating conditions of ATP, ADPNP or ADP were provided. smFRET measurements were performed in a confocal microscope (see Chapter 1.4). Complete substrate and adenine nucleotide series were recorded for the A488- and TMR-labelled cysteine mutants S169C/F332C, D173C/F332C and D452C/D878C. Due to decreased protein stability and setup durability at temperatures above 50°C, the temperature was set to 25°C where no topoisomerase activity but ATP hydrolysis by reverse gyrase is found.

Helicase-like domain

The first smFRET experiments addressed conformational changes within the helicase-like domain using reverse gyrase D173C/F332C (Figure 8).

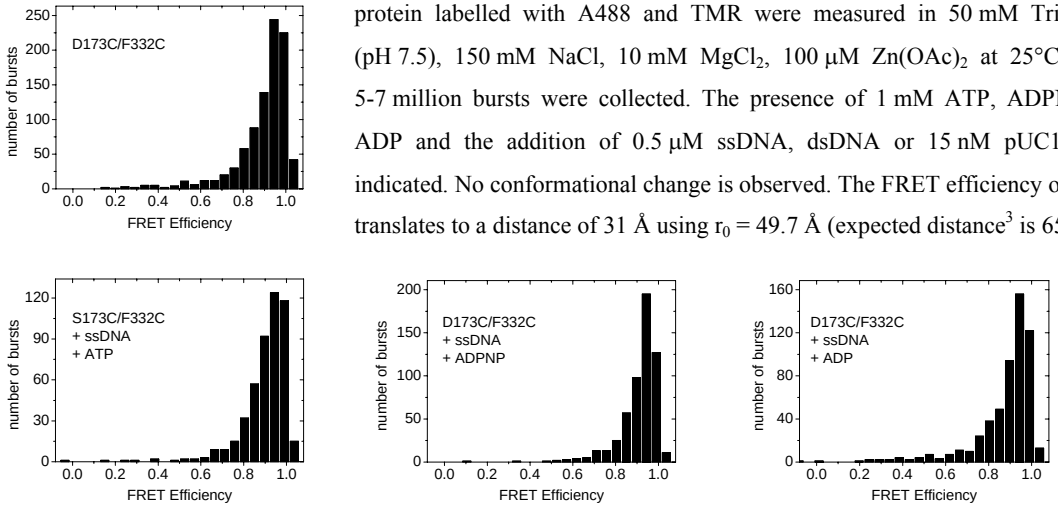

Figure 8. smFRET measurements of D173C/F332C reverse gyrase. 250 pM protein labelled with A488 and TMR were measured in 50 mM Tris/HCl (pH 7.5), 150 mM NaCl, 10 mM $MgCl_2$, 100 µM $Zn(OAc)_2$ at 25°C until 5-7 million bursts were collected. The presence of 1 mM ATP, ADPNP or ADP and the addition of 0.5 µM ssDNA, dsDNA or 15 nM pUC18 are indicated. No conformational change is observed. The FRET efficiency of 0.94 translates to a distance of 31 Å using r_0 = 49.7 Å (expected distance[3] is 65 Å).

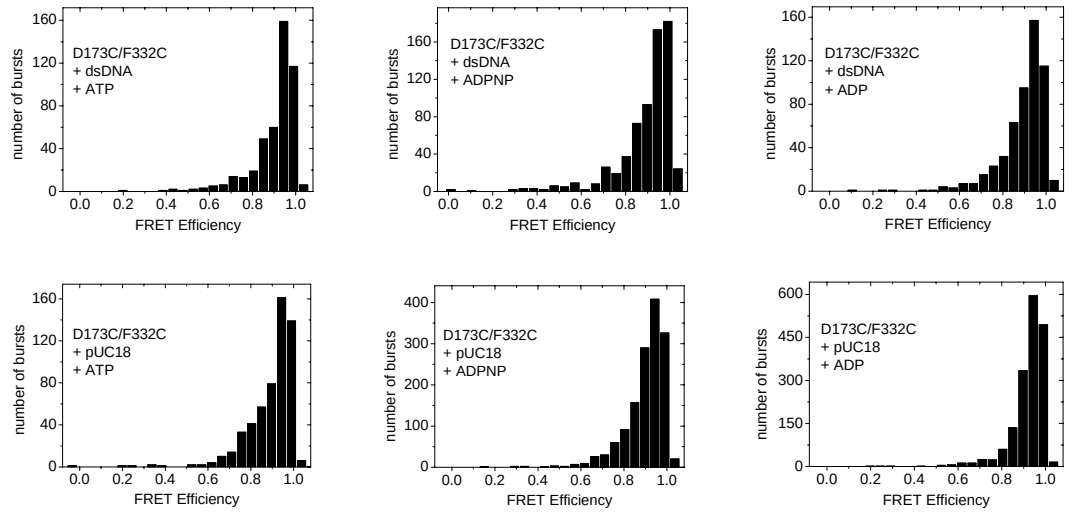

A FRET efficiency of 0.94 is observed for reverse gyrase D173C/F332C regardless of the presence of adenine nucleotides or DNA substrates. Thus, the distance between the positions determined in smFRET is 31 Å. The crystal structure from *A fulgidus* shows an open helicase-like domain with a distance of 65 Å between positions 173 and 332, suggesting a closed conformation of the helicase-like domain of reverse gyrase.

Next, the double mutant S169C/F332C of the helicase-like domain with an expected distance of 64 Å between the mutated positions was used to independently monitor conformational changes in the helicase-like domain (Figure 9).

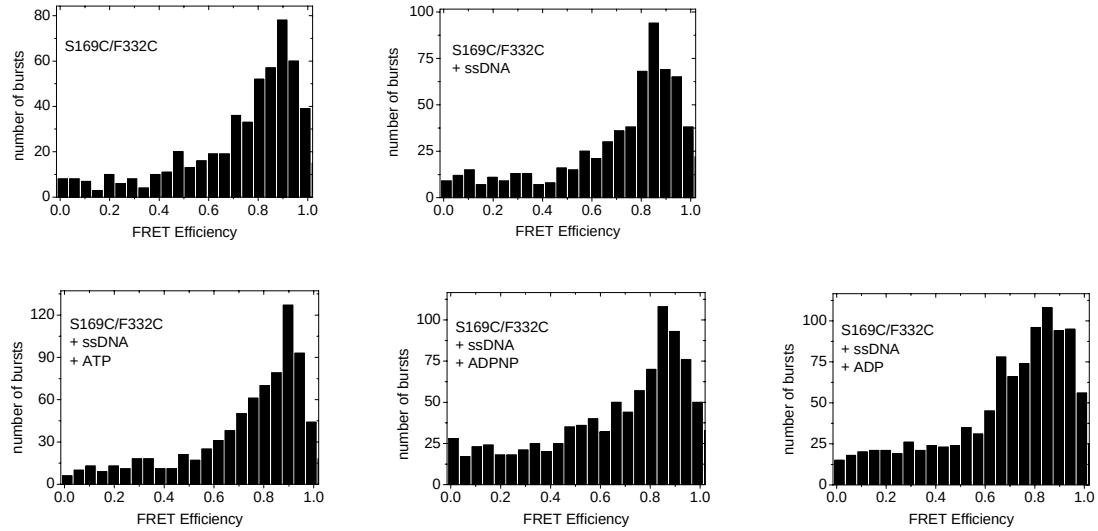

Figure 9. smFRET measurements of S169C/F332C reverse gyrase labelled at 25°C. Measurement conditions for the A488- and TMR- labelled proteins were identical to Figure 8. The series with dsDNA and pUC18 are not shown. Again, no change in FRET efficiencies is observed for all measured series. The calculated distance between positions 169 and 332 lies between 29 and 32 Å, while 64 Å were expected from the structure[3].

For the S169C/F332C mutant, a constant distance of about 30 Å is calculated from E_{FRET} values of about 0.85. Hence, the labelled positions in the helicase-like domain are closer together than suggested from the homology model (64 Å). The results are in agreement with the behaviour of D173C/F332C reverse gyrase.

Topoisomerase domain

Large conformational changes during the supercoiling cycle are also expected upon opening of the latch region and the topoisomerase domain of reverse gyrase[3]. However, no supercoiling activity is present at the measurement temperature of 25°C used for smFRET experiments. Nevertheless, the fluorescently labelled reverse gyrase D452C/D878C was used to investigate the population of distinguishable nucleotide- and DNA-bound states even in the absence of supercoiling activity (Figure 10).

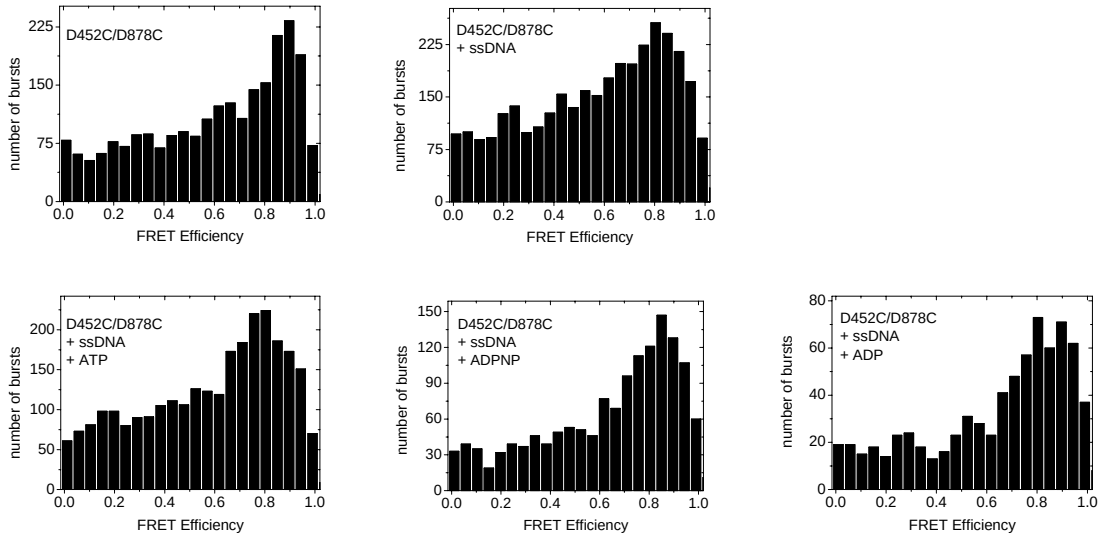

Figure 10. smFRET measurements of D452C/D878C reverse gyrase. Position 452 is situated in the latch region and position 878 is in the topoisomerase domain with an expected distance of 35 Å from the homology model[3]. The protein was labelled with A488 and TMR and measured under conditions described in Figure 8. The series with dsDNA and pUC18 are not shown. No change is observed for any measured series. The calculated distance lies between 33-38 Å.

The distribution of FRET efficiencies is broader in the case of the D452C/D878C mutant compared to the mutants with positions in the helicase-like domain and a lot of fluorescent background is observed. The position of the maximal FRET efficiencies varies only slightly between 0.8 and 0.9, which translates into a distance of 33-38 Å between positions 452 and 878. This finding is in good agreement with the expected distance of 35 Å, as judged from the closed conformation of the latch and topoisomerase domain shown in the crystal structure of reverse gyrase.

Conformational Changes in Reverse Gyrase

At 25°C, no change in FRET efficiencies is detected for reverse gyrase S169C/F332C or D173C/F332C regardless of the presence of adenine nucleotides or DNA substrates. In both cases, the helicase-like domain seems to remain in a closed conformation. Also no opening of the gap between the latch region and the topoisomerase domain could be observed with the D452C/D878C mutant.

Topoisomerase Activity of Labelled and Unlabelled Reverse Gyrase Mutants

The functionality of the double cysteine mutants S169C/F332C, D173C/F332C and D452C/D878C or reverse gyrase was investigated, due to an obvious lack of conformational changes expected during ATP hydrolysis and topoisomerase activity observed during smFRET measurements. Topoisomerase activity of the double mutants labelled with A488 and TMR is shown in Figure 11.

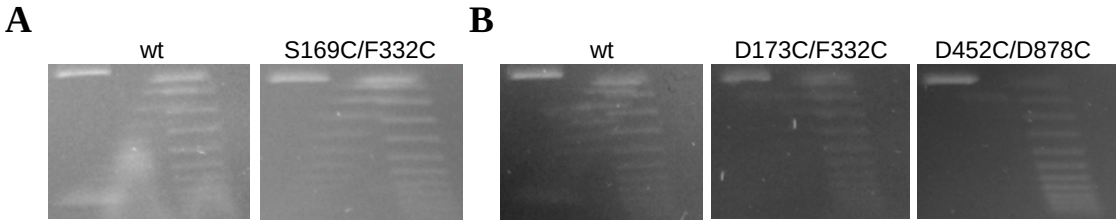

Figure 11. Topoisomerase activity of labelled reverse gyrase analysed on a two-dimensional agarose gel. Experiments were performed in 50 mM Tris/HCl (pH 7.5), 150 mM NaCl, 10 mM $MgCl_2$, 100 µM $Zn(OAc)_2$, 2 mM β-ME, 2 mM ATP, 15 nM pUC18, 10% (w/v) PEG 8000 at 75°C incubating 0.4 µM protein for 45 minutes (A) or 0.25 µM protein for 2 h (B). All labelled mutants of reverse gyrase are active similar to the wild type control (wt).

The double mutants of reverse gyrase labelled with A488 and TMR show wild type activity with respect to plasmid supercoiling, and thus, are suitable for smFRET studies.

Steady-State ATPase Activity of Labelled Reverse Gyrase Mutants

The results obtained with smFRET for reverse gyrase mutants lead to the question of why no conformational change is observed in the presence of various adenine nucleotides and DNA substrates. Supercoiling activity of labelled and unlabelled mutants at 75°C has been confirmed prior to smFRET experiments, indicating that the ATPase function of the helicase-like domain must be intact. However, ATP hydrolysis has not been shown for reverse gyrase cysteine mutants at temperatures insufficient for plasmid supercoiling.

Therefore, we determined the steady-state ATP hydrolysis of unlabelled double cysteine mutants at the standard temperature of 37°C for *T. maritima* reverse gyrase[15,17]. ATP hydrolysis rates and K_M values are summarised in Table 3.

Table 3. Steady-state ATPase parameters of reverse gyrase wild type, S169/F332C, D173C/F332C and D452C/D878C. Data were determined with 1 μM protein in the absence of DNA at 37°C as described[17].

	k_{cat} (10^{-3} s^{-1})	$K_{M,ATP}$ (μM)
wild type	19.7 ± 0.8	44 ± 6
S169C/F332C	10.4 ± 0.3	67 ± 8
D173C/F332C	11.1 ± 0.4	55 ± 8
D452C/D878C	18.7 ± 0.4	39 ± 4

Michaelis-Menten parameters for ATP hydrolysis by reverse gyrase D452C/D878C are similar to the wild type enzyme. Both helicase-like domain mutants (S169C/F332C and D173C/F332C) show reduced k_{cat} values and increased K_M values compared to the wild type but are still functional.

Subsequently it was interesting to determine ATP hydrolysis by the labelled reverse gyrase mutants, as functional ATPase activity suggests underlying conformational changes strongly indicated for the wild type. No ATPase activity in the absence of DNA was detected. Therefore, we compared ATP hydrolysis velocity of the labelled mutants to wild type reverse gyrase in the presence of saturating concentrations of ssDNA at one ATP concentration (Table 4).

Table 4. ssDNA-stimulated steady-state ATPase parameters reverse gyrase S169/F332C, D173C/F332C and D452C/D878C labelled with A488 (donor) and TMR (acceptor). 0.05-0.1 μM enzyme was incubated with 2 mM ATP and 1 μM ssDNA at 37°C under conditions published[17]. The high ATP concentration compared to the standard concentration and the presence of ssDNA were used to ensure stimulation of the ATPase activity[15]. The resulting ATP hydrolysis velocity was normalised to the enzyme concentration. No k_{cat} value can be determined, as the amount of labelled enzyme was too low to record a full ATP-dependent steady-state ATP hydrolysis until saturation.

	v/[enzyme] (10^{-3} s^{-1})
wild type	195
S169C/F332C	22
D173C/F332C	30
D452C/D878C	42

The hydrolysis velocity for the labelled reverse gyrase mutants is 5-10-fold reduced compared to the wild type, which may explain why no conformational change is observed in the helicase-like domain with smFRET. Thus, ATP hydrolysis might simply be too slow at 25°C to observe conformational changes in the helicase-like domain of reverse gyrase with smFRET.

8.4 Discussion

Native Cysteines in Putative Zinc Fingers are Essential for Topoisomerase Activity

Reverse gyrase from *T. maritima* has eight native cysteines in two putative zinc finger regions. A role of these regions for DNA binding has been predicted[3]. Deletion of both putative zinc finger regions (Δzif1/2), as well as removal of two cysteines from each such region (C_4A_4), leads to inactivation of the topoisomerase activity of reverse gyrase. This finding strongly indicates requirement of zinc binding to reverse gyrase for topoisomerase activity, most probably in authentic zinc fingers. Furthermore, reverse gyrase Δzif1/2 and C_4A_4 show no activity in the presence of ADP and ATP, indicating that the different nucleotide-bound states are not sufficient to trigger any topoisomerase activity. However, more detailed mutation studies have to be undertaken to localise essential amino acids in the putative zinc fingers for topoisomerase activity.

In reverse gyrase wild type, approximately one Zn^{2+} can be released per reverse gyrase molecule in the absence of zinc in the buffer. Thus, at least one of the putative zinc fingers reacts with the highly reactive mercury agent PMB releasing Zn^{2+}, which is typically complexed by zinc finger proteins with a very low K_D of about 2 pM[29]. Moreover, four cysteines in reverse gyrase are masked in the presence of high zinc concentrations (100 μM $Zn(OAc)_2$) and not accessible by DTNB. At 10-fold reduced zinc content, all native cysteines of reverse gyrase are exposed, suggesting that zinc is required for potential zinc finger formation in reverse gyrase. The presence of pUC18 also renders the putative zinc fingers accessible to DTNB, indicating conformational changes of these regions in the presence of plasmid compared to the DNA unbound state.

Cysteine Mutants of Reverse Gyrase can be Selectively Labelled

Astonishingly, the native cysteines of *T. maritima* reverse gyrase are also masked from reacting with the fluorescent dyes A488 (donor) and TMR (acceptor) in the presence of 100 μM $Zn(OAc)_2$. This is a prerequisite for specific labelling of cysteines introduced into reverse gyrase wild type background with fluorescent dyes, which is strictly required to investigate conformational changes during positive supercoiling by reverse gyrase with smFRET. Also, the final labelling protocol yielded efficiently labelled double mutants suitable for smFRET measurements.

Clearly, DTNB used to study cysteine accessibility and the maleimides of the fluorescent dyes have different reactivities with respect to the native cysteines of reverse gyrase. Reduced thiol-reactivity of the maleimides may be due to steric effects of the bulky fluorescent dyes compared to DTNB.

The Helicase-like Domain and Topoisomerase Domain have Fixed Conformations

To investigate the positive supercoiling mechanism and predicted concomitant conformational changes[3] of reverse gyrases on the molecular level, the labelled mutants were measure in the presence of ssDNA, dsDNA and pUC18 in combination with ATP, ADPNP or ADP.

Firstly, the cleft in helicase-like domain of *T. maritima* reverse gyrase is in a more closed conformation compared to the homology model with the crystal structure of *A. fulgidus* reverse gyrase, which shows an open conformation[2]. The close proximity of the helicase-like subdomains is confirmed for the isolated helicase-like domain of reverse gyrase with smFRET (Yoandris delToro Duany, Klostermeier group). The findings may point at the known drawback for interpreting crystal structures, which may not necessarily show authentic conformations of proteins. Secondly, the gap between the latch domain and the topoisomerase domain is closed in the homology model, which was also found in smFRET experiments. However, no conformational changes were observed for these regions either. Importantly, although the supercoiling activity of reverse gyrase for unlabelled and labelled mutants was observed at 75°C, no supercoiling activity is expected during smFRET experiments at the measurement temperature of 25°C. But the topoisomerase domain might have adopted different conformations in the presence of different DNA substrates, which was not observed.

Indeed, topoisomerase III from *E. coli* shows conformational changes close to the active site upon ssDNA binding and movement of structural elements interacting with the bound DNA[12,13]. Additionally, the DNA undergoes conformational changes preceding strand cleavage[13,14]. In the future, labelled DNA may be employed as a tool for investigating the supercoiling mechanism of reverse gyrase, revealing potential conformational changes in DNA substrates upon binding. However, there is no experimental proof for an opening of the topoisomerase domain of reverse gyrase for supercoiling activity. Effort is currently being undertaken to crosslink the latch region and the topoisomerase domain to verify an opening requirement for plasmid supercoiling by reverse gyrase. Also, the fluorescent dyes A488 and TMR may act as a crosslink, which is reflected in the relatively small distances of 30-35 Å observed between the labelled positions.

Labelled Cysteine Mutants of Reverse Gyrase are only Partially Active

Lack of conformational changes in the labelled mutants may be confirmed in the finding that the wild type enzyme hydrolyses ATP at 25°C ($k_{cat} = 4.5 \pm 0.2 \cdot 10^{-3}$ s^{-1}, unpublished). And indeed, the unlabelled double cysteine mutants hydrolyse ATP also at 37°C. Thus, the 10-fold reduced ATPase activity determined for the labelled mutants may be due to covalent attachment of the fluorescent dyes or the labelling procedure itself. The question remains why the labelled mutants of reverse gyrase reveal plasmid supercoiling activity at 75°C but show no ATPase activity at 37°C. The labelled cysteines must either still contain a lot of unlabelled and supercoiling-active protein or fluorescent labelling may simply influence the temperature-dependency of the ATPase. We also performed initial smFRET experiments at 75°C with the mutants of the helicase-like domain and the topoisomerase domain. Again, the same FRET efficiencies are obtained and no change is observed. Also, the stability of the labelled protein decreases rapidly at 75°C and the fluorescent background is drastically increased (data not presented).

Finally, the results from smFRET measurements reveal authentic distances measured in the labelled reverse gyrase mutants. Unfortunately, fluorescent double labelling of reverse gyrase S169C/F332C, D173C/F332C and D452C/D878C renders the mutants ATPase-inactive. Furthermore, the use of a homology model for the selection of labelling sites may not reflect suitable positions for observing supercoiling activity of reverse gyrase. The site-specific introduction of cysteines to alternative and more accessible positions in reverse gyrase is currently being undertaken.

8.5 Literature

(1) Shibata T., Nakasu S., Yasui K., Kikuchi A., Intrinsic DNA-dependent ATPase Activity of Reverse Gyrase, *J. Biol. Chem.*, 1987, *262*, 10419-10421.

(2) Matoba K., Mayanagi K., Nakasu S., Kikuchi A., Morikawa K., Three-dimensional electron microscopy of the reverse gyrase from *Sulfolobus tokodaii*, *Biochem. Biophys. Res. Comm.*, **2002**, *297*, 749-755.

(3) Rodríguez A. C., Stock D., Crystal structure of reverse gyrase: insights into the positive supercoiling of DNA, *EMBO*, **2002**, *21*, 418-426.

(4) Rodríguez A. C., Studies of a Positive Supercoiling Machine, *J. Biol. Chem.*, **2002**, *277*, 29865-29873.

(5) Berg J. M., Zinc Finger Proteins, *Curr. Op. Struct. Biol.*, **1993**, *3*, 11-16.

(6) Bouthier de la Tour C., Amrani L., Cossard R., Neuman K. C., Serre M.C., Duguet M., Mutational Analysis of the Helicase-like Domain of Thermotoga maritima Reverse Gyrase, *J. Biol. Chem.*, **2008**, *283*, 27395-27402.

(7) Viard, T., Lamour, V., Duguet, M., Bouthier de la Tour, C., Hyperthermophilic topoisomerase I from *Thermotoga maritima*. A very efficient enzyme that functions independently of zinc binding, *J. Biol. Chem*, **2001**, *276*, 46495-46503.

(8) Hansen G., Harrenga A., Wieland B., Schomburg D., Reinemer P., Crystal Structure of Full Length Topoisomerase I from *Thermotoga maritima*, *J. Mol. Biol.*, **2006**, *358*, 1328-1340.

(9) Gorbalenya A. E., Koonin E. V., Helicases: amino acid sequence comparisons and structure-function relationships, *Curr. Opin. Struct. Biol.*, **1993**, *3*, 419-429.

(10) Theissen B., Karow A. R., Köhler J., Gubaev A., Klostermeier D., Cooperative binding of ATP and RNA induces a closed conformation in a DEAD box RNA helicase, *PNAS*, **2008**, *105*, 548-553.

(11) Rodríguez A. C., Investigating the Role of the Latch in the Positive Supercoiling Mechanism of Reverse Gyrase, *Biochemistry*, **2003**, *42*, 5993-6004.

(12) Perry K., Mondragón A., Structure of a Complex between *E. coli* DNA Topoisomerase I and Single-Stranded DNA, *Structure*, **2003**, *11*, 1349-1358.

(13) Changela A., DiGate R. J., Mondragón A., Crystal structure of a complex of a type IA DNA topoisomerase with a single-stranded DNA molecule, *Nature*, **2001**, *411*, 1077-1081.

(14) Changela A., DiGate R. J., Mondragón A., Structural Studies of *E. coli* Topoisomerase III-DNA Complexes Reveal A Novel Type IA Topoisomerase-DNA Conformational Intermediate, *J. Mol. Biol*, **2007**, *368*, 105-118.

(15) del Toro Duany Y., Jungblut S. P., Schmidt A. S., Klostermeier D., The reverse gyrase helicase-like domain is a nucleotide-dependent switch that is attenuated by the topoisomerase domain, *Nucleic Acids Research*, **2008**, *36*, 5882-5895.

(16) Valenti A., Perugino G., D'Amaro A., Cacace A., Napoli A., Rossi M., Ciaramella M., Dissection of reverse gyrase activities: insight into the evolution of a thermostable molecular machine, *NAR*, **2008**, *36*, 4587-4597.

(17) Jungblut S. P., Klostermeier D., Adenosine 5′-O-(3-thio)triphosphate (ATPγS) Promotes Positive Supercoiling of DNA by *T. maritima* Reverse Gyrase, *J. Mol. Biol.*, **2007**, *371*, 197-209.

(18) Ellmann G. L., Tissue Sulfhydryl Groups, *Arch. Biochem. Biophys.*, **1959**, *82*, 70-77.

(19) Riddles P. W., Blakeley R. L., Zerner B., Ellman's reagent: 5,5'-dithiobis(2-nitrobenzoic acid) - a re-examination, *Anal. Biochem.*, **1979**, *94*, 75-81.

(20) Hunt J. B., Neece S. H., Schachmann H. K., Ginsburg A., Mercurial-promoted Zn2+ Release from *Escherichia coli* Aspartate Transcarbamoylase, *J. Biol. Chem.*, **1984**, *259*, 14793-14803.

(21) Jakob U., Markus E., Bardwell J. C., Redox Switch of Hsp33 Has a Novel Zinc-binding Motif, *J. Biol. Chem.*, **2000**, *275*, 38302-38310.

(22) Edman P., Begg G., A Protein Sequenator, *Eur. J. Biochem.*, **1967**, *1*, 80-91.

(23) Parker C. A., .Rees W. T., Correction of fluorescence spectra and measurement of fluorescence quantum efficiency, *Analyst*, **1960**, *85*, 587-600.

(24) Magde D., Wong R., Seybold P. G., Fluorescence Quantum Yields and Their Relation to Lifetimes of Rhodamine 6G and Fluorescein in Nine Solvents: Improved Absolute Standards for Quantum Yields, *Photochem. Photobiol.*, **2002**, *75*, 327-334.

(25) Förster T., Transfer mechanisms of electronic excitation, *Faraday Soc.*, **1959**, *27*, 7-17.

(26) Theissen B., Karow A. R., Köhler J., Gubaev A., Klostermeier D., Cooperative binding of ATP and RNA induces a closed conformation in a DEAD box RNA helicase, *PNAS*, **2007**, *105*, 548-553.

(27) Jungblut S. P., Diploma Thesis, *University of Bayreuth*, **2005**.

(28) Tyagarajan K., Pretzer E., Wiktorowicz J. E., Thiol-reactive dyes for fluorescence labeling of proteomic samples, *Electrophoresis*, **2003**, *24*, 2348-2358.

(29) Lippard S. J., Berg J. M., Bioorganische Chemie, *Spektrum Akad. Verlag*, **1995**.

9. Summary

The aim of this PhD thesis was to functionally characterise the hyperthermophilic topoisomerase IA reverse gyrase from the eubacterium *Thermotoga maritima* with respect to its unique ATP-dependent positive plasmid supercoiling activity. We set out to apply single molecule FRET to observe conformational changes in the N-terminal helicase-like domain and the C-terminal topoisomerase domain of reverse gyrase during topoisomerase activity.

Initially, the protocol for the purification of *T. maritima* reverse gyrase was improved to yield mg amounts of monomeric enzyme with 95% purity. Requirements for positive plasmid supercoiling by reverse gyrase from *T. maritima* were defined and optimal reaction conditions were established for the rest of the work. However, no universal nucleotide utilisation pattern for topoisomerase activity of reverse gyrases in general exists and various heterogeneous nucleotides-dependent topoisomerase activities have been reported for reverse gyrases from different organisms. Reverse gyrase from *T maritima* exhibits no topoisomerase activity in the absence of nucleotides but relaxes plasmids in an ADP- and ADPNP-dependent manner. Reverse gyrase positively supercoils plasmid DNA in the presence of ATP. Surprisingly, hydrolysis of ATPγS efficiently promotes positive supercoiling to a similar extend as ATP hydrolysis. Mutation of the GKT sequence in the Walker A motif of the helicase-like domain renders reverse gyrase inactive for nucleotide hydrolysis and reveals vastly reduced topoisomerase activity. Most interestingly, we observed AMP generation in the presence of short double-stranded DNA substrates and plasmid DNA. During plasmid relaxation, ADP and ADPNP are converted into AMP. The same is true for ATP and ATPγS during positive supercoiling. Possibly, ATP is hydrolysed to AMP by reverse gyrase *via* intermediately generated ADP and energy may be obtained from ADP cleavage.

Further investigating the function of the reverse gyrase domains, we demonstrated that the helicase-like domain is a DNA-stimulated ATPase that harbours all determinants for adenine nucleotide binding and hydrolysis of reverse gyrase. The full-length enzyme shows highly reduced ATPase compared to the isolated helicase-like domain even in the presence of DNA. Consequently, the coupling of DNA binding to ATP hydrolysis is diminished in full-length reverse gyrase and the effect of DNA binding on $K_{M,ATP}$ is much smaller than for the isolated helicase-like domain. Thus, the helicase-like domain of reverse gyrase is a nucleotide-dependent switch.

Notably, full-length reverse gyrase from *T. maritima* binds DNA much more tightly compared to the helicase-like domain and single-stranded DNA binds in a cooperative manner. Artificial 20-, 40- and 60-mer DNA constructs were used to elucidate cooperative binding of reverse gyrase. We show that the binding affinity increases with substrate length. In contrast, the DNA-dependent ATPase activity of *T. maritima* reverse gyrase decreases with substrate length. Cooperative binding was demonstrated for single-stranded DNA substrates longer than 40 nt and points to possible protein-protein interactions of reverse gyrase that may play a role in the positive supercoiling cycle.

In order to observe conformational changes in reverse gyrase with smFRET during the supercoiling cycle, fluorescent labelling is required. However, labelling of reverse gyrase cysteine mutants for smFRET measurements is quite challenging. Reverse gyrase from *T. maritima* contains eight native cysteines in two putative zinc fingers that have to be intact for positive supercoiling activity. Hence, we improved the conditions accordingly for selective labelling of reverse gyrase cysteine mutants. smFRET measurements indicated that the helicase-like domain might be in a more closed conformation compared to the available crystal structure from *A. fulgidus* reverse gyrase. Furthermore, the gap between the latch region and the topoisomerase domain is suggested to open during the supercoiling cycle, but the calculated FRET distances correspond to the closed conformation observed in the crystal structure.

Conformational changes during the catalytic cycle of reverse gyrase have been predicted for the helicase-like domain and the topoisomerase domain. No conformational changes in the helicase-like domain and the topoisomerase domain are detected with different DNA substrates and adenine nucleotides. Thus, the labelled reverse gyrase mutants may either be inactive under the conditions chosen for smFRET measurements or might have been inactivated by fluorescent labelling. Other positions will be chosen to investigate regions prone to undergo conformational changes during the catalytic cycle without impairing the topoisomerase activity of *T. maritima* reverse gyrase.

10. Acknowledgements

The actual work behind this PhD thesis was carried out from June until December 2005 in the Department of Experimental Physics at the University of Bayreuth and from January 2006 until September 2008 in the Department of Biophysical Chemistry at the Biozentrum of the University of Basel in the laboratories of Prof. Dr. Dagmar Klostermeier.

First of all, I thank Dagmar for giving me the opportunity and the trust to investigate an enzyme so wealthy in properties as reverse gyrase. Dagmar's advice and guidance represent an invaluable contribution to the work at hand. I would also like to thank Prof. Dr. Joachim Seelig for his work as second referee and examiner.

I owe my sincere gratitude to Andreas Schmidt, Dr. Bettina Theissen and Regula Aregger for constant support, discussion, advice and loyalty. Special thanks go to Dr. Michael Hayley, Anne Karow, Regula Aregger, Yoandris del Toro Duany and Martin Lanz for reading and correcting the manuscript of this PhD thesis. I thank Leo Faletti of the workshop for creative technical support. Also, I would like to thank Manuel Hilbert for many useful discussions and Dr. Airat Gubaev for help with the laser setup. Thanks to Ines Hertel, Martin Linden and my entire floor mates for the fruitful working environment. I particularly thank Stefan Langheld, Christophe Bodenreider, Maxime Québatte, Daniela Nebenius and Sandro Scanu for a more than warm welcome and exquisite time in Basel.

I also want to thank the men and women I am happy to call my friends, who inspired me and who allowed me to inspire them. Thank you for your encouragement and criticism. Especially, I appreciate the constant support of Angie, Luci and Simone.

Finally, I thank Marion and Sabrina for their love.

"Acta est fabula, plaudite!"

The play is over, applaud! - *Emperor Augustus*

(Said to have been his last words)

Personally, I conclude with the words "after the game is before the game".